Dissecting Mechanisms of Antimalarials using CRISPR/Cas9 Editing in *Plasmodium falciparum*

SooNee Tan

A dissertation
submitted in partial fulfillment of the
requirements for the degree of

Doctor of Philosophy

University of Washington

2019

Reading Committee:
Pradipsinh K. Rathod, Chair
Dustin Maly
Jesse Zalatan

Program Authorized to Offer Degree:
Chemistry

University of Washington

Abstract

Dissecting Mechanisms of Antimalarials using CRISPR/Cas9 Editing in *Plasmodium falciparum*

SooNee Tan

Chair of the Supervisory Committee:
Pradipsinh K. Rathod
Department of Chemistry

Malaria, caused by *Plasmodium* infections, continues to be a global disease of public health importance with 300 million annual cases and about 500,000 deaths. Continual emergence of resistance to commonly used antimalarials underscores the importance of finding new drug targets and new antimalarial drugs. Previously, the Rathod lab has established systematic approaches to study targets of antimalarials and resistance mechanisms with the use of *in vitro* selection methods and deep sequencing of selected mutants. There are some limitations with these approach as deep sequencing data does not reveal the step-wise mechanism of mutagenesis and mutations observed from the sequencing result might not associate with the resistance phenotype. This thesis has multiple projects aimed to expand the molecular toolbox with genome manipulation using CRISPR/Cas9 technique. It will complement the current tools that we have in performing target identification/validation as well as understanding the mechanism of mutagenesis in malaria parasites.

Ciprofloxacin is an antibacterial known to target bacterial DNA Gyrase. In some instances, ciprofloxacin has been used for malaria prophylaxis but little is known about the mode-of-action of ciprofloxacin in malaria parasites. In the first project, we aim to understand the essentiality of *Plasmodium falciparum* DNA gyrase A subunit (*Pf*GyrA) and its relationship with ciprofloxacin. Based on bioinformatics analyses, *Pf*Gyr A and B subunits are known to contain apicoplast-targeting signals. To test the predicted localization

of this enzyme in the apicoplast and the function of this enzyme at the subcellular level, a CRISPR/Cas9 gene-editing tool was used to disrupt *Pf*GyrA. It is known that isopentenyl pyrophosphate (IPP) rescues malaria parasites from apicoplast-targeting inhibitors and indeed successful growth of *Pf*ΔGyrA required chemical rescue with IPP. *Pf*GyrA disruption was accompanied by loss of the plastid acyl-carrier protein (ACP) immunofluorescnce and the plastid genome. Drug sensitivity assays revealed that a *Pf*ΔGyrA clone, supplemented with IPP was less sensitive to antibacterial compounds (doxycycline and ciprofloxacin) but not the nuclear topoisomerase inhibitor (etoposide). In addition, at high concentrations, ciprofloxacin continued to inhibit IPP-rescued *Pf*ΔGyrA suggesting that this drug has an additional target in *P. falciparum*. We concluded that *Pf*GyrA is an apicoplast enzyme in malaria parasite and it is essential for blood-stage parasites. In the future, untangling the two possible inhibitory functions of ciprofloxacin in malaria parasites may reveal a new and important drug target.

The second project aim involves target validation of a tetrahydroquinolone compound, BMS-388891. Previous publications from the lab showed that resistance to BMS-388891 arises from a single point mutation in either the protein farnesyl transferase (PFT) alpha or beta subunit. Although results indicated that a single point mutation on the *Pf*PFT enzyme led to BMS-3888891 resistant parasites, whole genome sequencing on those mutants have yet to be done. To test that a single mutation is sufficient for parasite acquisition of resistance to BMS-388891, gene alteration with CRISPR/Cas9 tool was utilized to introduce a point mutation (Y837N, Y837S, or Y837C) on the PFT-β-subunit. The CRISPR-modified mutant parasites have shown an increase of 10-20 fold resistance to BMS-388891. This data is the first to formally demonstrate that a single point mutation on the *Pfpft-β-subunit* is sufficient for parasites to confer resistance to BMS-388891 compound. There are very few validated compound to target relationships and CRISPR/Cas9 technique will be a valuable tool in the malaria field.

The third project aim involves the understanding of the mechanism of mutagenesis in malaria parasites. While it is known that amplification and point mutation are the possible

outcomes of resistance selection, the order of the processes is less understood. Recent work by *Guler et. al.* points to a novel step-wise amplification mechanism in the malarial parasite response to DSM1 selection pressure. In these selected parasites, 25-30 kb regions surrounding the *Pfdhodh* locus were amplified. Taking advantage of the highly amplified *Pfdhodh* locus, we were able to introduce *Pfpft-α-subunit* into this region. This sets up future studies for us to dissect the step-wise resistance mechanism in malaria parasites.

Overall, the utilization of CRISPR/Cas9 tool has allowed us to efficiently perform gene knockout, gene alteration and gene translocation. These applications not only enable us to prove for the first time the importance of the *Pf*GyrA enzyme but also to directly confirm the causality of specific point mutations in BMS-388891 resistant parasites. The addition of CRISPR/Cas9 gene-editing to our systematic approach toolbox will ultimately aid in our understanding of how mutagenesis occurs in malaria parasites and allow us to expand our knowledge in the mode-of-action of different antimalarials in *P. falciparum*.

Acknowledgments

This work represents approximately five years of work and during this period I have been fortunate to receive many different forms of support from the University of Washington, colleagues, friends and family.

I would first like to thank the Department of Chemistry for offering me a spot in the doctoral program so that I could develop as a scientist. Specifically, I would like to thank the Department Chair Michael Heinekey for setting up this unique environment in which to learn and grow. I would like to thank all faculty members, especially Jesse Zalatan and Dustin Maly, who have given me both useful feedback and resources with which to perform my experiments.

I would like to give special thanks to my undergraduate and graduate research advisor, Pradipsinh K. Rathod for funding my work. He has been both a scientific and personal inspiration for me from the point that he gave me my first real job as a researcher during my sophomore year in college. Apart from guiding me through research projects, he has encouraged me to participate in various scientific conferences and meetings. All these has contributed not only to my scientific knowledge but also allow me to be more confident in presenting ideas or having discussions with other professionals. Skills (both technical and soft skills) that I have learnt from the Rathod lab is tremendous and have enabled me to grow as a person.

I am also very grateful to work with a group of amazing people in the Rathod lab. I would like to thank all the Rathod lab members for their help and friendship during this journey. Modern biological science cannot be performed alone and every member of the lab has some hand in this work, whether suggesting useful ideas, helping me with a protocol, or simply allowing me to bounce ideas off of them. Specifically, I would like to express gratitude towards my mentor Devaraja Mudeppa. Entering the lab without having any knowledge in Molecular Biology, Dev has been very patient in guiding and mentoring me throughout various projects. Also, I would like to thank John White III for mentoring me in the parasite

culture work. Without work that John has established in the lab (i.e. maintaining the culture room, preparing fresh blood for culture work etc.), these projects would not have progressed smoothly. In addition, I would also like to thank Shiva Kumar for being patient in guiding me through whole genome sequencing analysis as I have no prior computing knowledge. Also, having limited knowledge and skill in chemical synthesis, Sreenkath Kokkonda has been really helpful in mentoring me through synthesis of different compounds and I am really grateful for that.

Furthermore, I cannot easily express all of my gratitude to my friends and classmates who have been there for me over the years. I would never have made it this far without the support network I have around me. They are truly a smart, funny and down to earth group of extremely talented scientists. From help with work in the lab to socialization outside of it, this is truly a special group that I count myself lucky to be a part of.

I would like to thank members of my family who have been a constant source of love, support, and laughter. Although being more than 8000 miles away, my parents have always been supportive of my goals and been there to offer advice and counsel when needed. My siblings have also been an enormous positive presence in my life and I thank them for that. Finally, I would like to thank my fiance, KimSiang Khaw for being there for me every day. Besides holding me through ups and downs in life, he has been very supportive of my work and provided valuable advice in scientific research in general.

List of Abbreviations

ACP	Acyl-carrier protein
ACT	Artemisinin-based combination therapy
BSA	Bovine serum albumin
BSD	Blasticidin S-deaminase
CRISPR/Cas9	Clustered regularly interspaced short palindromic repeats/ CRISPR-associated gene 9
cDNA	Complement deoxyribonucleic acid
CD	Cytosine deaminase
CH_2Cl_2	Methylene chloride
DAPI	4',6-diamidino-2-phenylindole
DHFR-TS	Dihydrofolate reductase-Thymidylate synthase
DMAP	4-Dimethylaminopyridine
DMSO	Dimethyl sulfoxide
DNA	Deoxyribonucleic acid
EC_{50}	Effective concentration of an inhibitor to reduce cellular effect by 50%
EDTA	Ethylenediaminetetraacetic acid
ESI-MS	Electrospray ionization - mass spectrometry
GOI	Gene of interest
HSP70	Heat shock protein 70
hDHFR	Human dihydrofolate reductase
IRS	Indoor residual spraying
ITN	Insecticide-treated mosquito nets
IPP	Isopentenyl pyrophosphate
MeCN	Acetonitrile
nptII	Neomycin phosphotransferase II
NHEJ	Non-homologous end joining
NMR	Nuclear magnetic resonance

pRBCs	Parasitized red blood cells
PAM	Protospacer adjacent motif
PBS	Phosphate buffered saline
PCR	Polymerase chain reaction
PFT	Protein farnesyl transferase
PFTI	PFT inhibitors
PGGT-I	Protein geranylgeranyltransferase-I
qPCR	Quantitative polymerase chain reaction
RBC	Red blood cells
RNA	Ribonucleic acid
RT	Room temperature
sgRNA	Single-guide ribonucleic acid
sfGFP	Super-fluorescent green fluorescent protein
THQ	Tetrahydroquinolones
TK	Thymidine kinase
TLC	Thin-layer chromatography
TsCl	4-Toluenesulfonyl chloride
VCF	Variant calling file
yFCU	Yeast cytosine deaminase combined with uridyl phosphoribosyl transferase
yDHODH	Yeast dihydroorotate dehydrogenase
ZFN	Zinc finger nuclease

Contents

List of Figures

List of Tables

Chapter 1

Introduction

Malaria is a disease caused by parasitic protozoan infections from species of the genus *Plasmodium*. Parasites are transmitted to humans during a blood meal of an infected female *Anopheles* mosquito, which introduces parasites from its saliva into a person's circulatory system. There are five species of parasites that are infectious to humans: *P. falciparum, P. vivax, P. ovale, P. malariae, and P. knowlesi*, with *P. falciparum* being the most virulent [1].

1.1 The disease burden of malaria

Malaria is a serious global disease in which half of the world's population live in areas at risk for malaria transmission. As of year 2017, the World Health Organization (WHO) has estimated 200 million global cases with 500,000 deaths per year. Most malaria transmission occurs in developing countries, especially in rural areas of South America and South Asia. Young children and pregnant women are among the most vulnerable groups with little or no immunity against the disease [2]. There has been significant effort to control the spread of the disease by the vector mosquitoes. The most commonly used and effective methods to prevent mosquito bites is sleeping under insecticide-treated mosquito nets (ITNs) and practicing indoor residual spraying (IRS) of walls. The combined use of ITNs and IRS has helped reduce the global malaria burden since 2000 [2]. Aside from vector control, drug therapies are still heavily relied upon for treatment and prevention as there is currently no

FDA-approved vaccine.

Although several effective antimalarial treatments exist today, the threat and emergence of resistance to antimalarial drugs is a continuing public health concern [3–6]. Artemisinin-based combination therapy (ACT) remains the best option as the first- and second-line treatment [7–11]. However, several ACTs are beginning to fail in Southeast Asia due to the presence of parasites with reduced susceptibility to the artemisinins and/or the partner drugs [12–15]. Hence there is an urgent need to identify new drug targets or better understand the parasite mechanisms behind drug failure.

1.2 The life cycle of *Plasmodium falciparum*

Vaccine and drug discovery are challenging due to *P. falciparum*'s genetic plasticity and multi-stage development in humans and mosquitoes as shown in Figure 1.1. Within the mosquito or human, each stage of the parasite life cycle has a unique morphology and protein complements. To evade immune clearance, parasite surface proteins and metabolic pathways evolve quickly hence creating more complexity for drug and vaccine development.

Transmission begins when an infected mosquito simultaneously takes a blood meal and injects sporozoites into a human's skin. Sporozoites then migrate through the tissue and invade a blood vessel which will transport them to the liver and infect hepatocytes. During liver stage development, parasites undergo massive mitotic replication and form tens of thousands of merozoites. Eventually, liver cells rupture and liver-stage merozoites are released into the bloodstream where they invade red blood cells (RBCs).

In the intraerythrocytic cycle, parasites undergo further mitotic replication where merozoites progress through the developmental stages of rings, trophozoites and schizonts. The mature schizonts eventually burst out from the RBCs releasing merozoites which are then ready to infect new RBCs and continue the cycle. During schizont maturation, some merozoites will be predetermined to develop into the sexual stage gametocytes. When a

mosquito takes a blood meal from an infected person, male and female gametocytes will be ingested. Within the gut of the mosquito the gametocytes mate and undergo meiosis. The gametes then migrate through the midgut wall forming oocysts and eventually mature into sporozoites that will migrate to the salivary gland of the mosquito [16]. The majority of the life cycle of *Plasmodium* is spent in the haploid state (having only one set of chromosomes). *Plasmodium* only exists in the diploid state (having two copies of each chromosomes) after the fusion of gametes which lasts just long enough to invade a mosquito's gut and produce a new generation of haploid cells.

Research in the malaria field is heavily focused on understanding blood stage parasites as it is this stage of the life cycle that causes symptoms of the disease. Unlike other stages, blood stage parasites are easier to manipulate and culture in the *in vitro* system. The Rathod lab has established a systematic approach which allows us to perform drug resistance and genomics studies on the blood stage parasites [17–19]. Additionally, functional tools to study essential genes of blood-stage parasites may promote novel drug design which is badly needed in malaria chemotherapy.

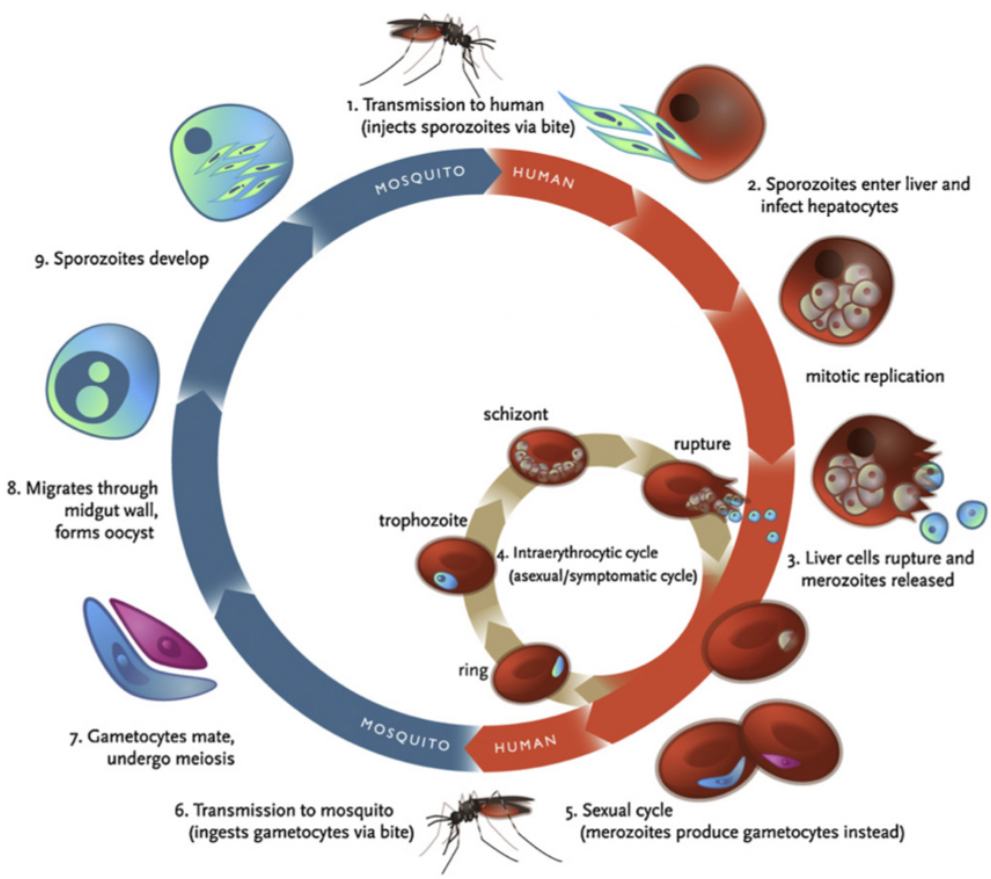

Figure 1.1: ***The life cycle of malaria parasites.*** *Parasites go through multiple stages of development both in a human and mosquito host. In the human host, parasites first infect the hepatocytes and subsequently red bloods cells and thereby entering the intraerythrocytic cycle. Gametocytes developed during the intraerythrocytic cycle can be ingested by the mosquito which will eventually become sporozoites during the mosquito stages. Figures adapted from Klein E.Y, 2013 [20]*

1.3 The role of the apicoplast organelle

The eukaryotic phylum Apicomplexa comprises more than 5000 species of parasitic protozoa, including the *Plasmodium* parasites [21]. Apicomplexan parasites possess a unique form of a plastid organelle called an apicoplast, and an apical complex structure. Phylogenetic studies show that apicomplexan parasites and the dinoflagellate algae arose from a common photosynthetic ancestor. However, whole genome sequencing of *P. falciparum* reveals that the apicoplast lacks any genes involved in photosynthesis [22]. Also, unlike the plant plastid, which is derived directly from a photosynthetic bacterium, the apicoplast is a secondary plastid derived from a photosynthetic eukaryote [23]. An apicomplexan ancestor engulfed a red algae and over time, incorporated the plastid and components necessary for its function while discarding the rest of the algal cell [24]. The most obvious remnants of this process are the third (algal outer membrane) and fourth (host cell endosome) membranes that surround the apicoplast and the transfer of genes to the nuclear genome [25, 26]. Hence the discovery of the apicoplast in *P. falciparum*, which is of prokaryotic origin and has no counterpart in the human host, presented new antimalarial targets.

The *P. falciparum* apicoplast consists of about 500 nuclear-encoded and apicoplast-targeted proteins as well as 35 proteins encoded within the apicoplast own circular genome [27–29]. The apicoplast carries out four identifiable metabolic pathways: isoprenoid precursor biosynthesis, fatty acid synthesis, heme synthesis and iron-sulfur cluster biogenesis [28, 30–33]. The apicoplast provides products that have housekeeping functions for genome transcription, replication, translation, and post-translational modification.

The apicoplast is clearly an essential organelle in blood stage parasites since perturbation of its housekeeping activities kill the parasites [34–37]. However, gene knockout studies have shown that fatty acid synthesis and heme synthesis are dispensable in blood stage parasites, while the role of iron-sulfur cluster biogenesis has been widely thought to be one of self-maintenance to generate reducing equivalents [28, 30, 38, 39]. This leaves isoprenoid precursor biosynthesis as the indispensable role of the apicoplast. It had been well-established that

inhibition of the apicoplast protein expression with antibiotics, such as doxycycline lead to parasite death due to lack of apicoplast formation in the daughter cells [34]. Remarkably, these apicoplast-minus parasites survive and continue to replicate when isopentenyl pyrophosphate (IPP), the product of isoprenoid precursor biosynthesis, is added to the growth media [40]. Chemical rescue demonstrated that the only essential function of the apicoplast in blood stage *P. falciparum* is the biosynthesis of the isoprenoid precursor. The singular role of the apicoplast is simple but essential to parasite survival and therefore has tremendous potential for drug discovery. Further studies of the essentiality of different apicoplast-targeted proteins that plays an important role in the apicoplast housekeeping functions as discussed in Chapter 2 might offer insight into potential drug targets.

1.4 Genetic Manipulation of *Plasmodium falciparum*

Despite the revelation of the completely sequenced genome of malaria parasites in 2002 [22], there are still over half the genes that have no known functions. In order to elucidate essential genes or pathways that could inform new drug design strategies and further understand the mechanism of drug resistance, molecular tools capable of manipulating the parasite during the blood stage development are needed.

1.4.1 Transfection of *Plasmodium falciparum*

Parasites transfection is generally accomplished by one of two methods. The first method utilizes the direct electroporation of ring stage parasites [41]. In this case, the plasmid DNA has to pass through four different membranes (RBC membrane, parasitophorous membrane, parasite membrane, and nuclear envelope) in order to enter the parasite's nucleus. The second method, termed "spontaneous uptake" involves the electroporation of uninfected RBCs to preload them with the plasmid DNA. The preloaded RBCs are then exposed to schizont stage parasites, so that when schizonts mature and rupture, merozoites will be released to infect the preloaded RBCs and uptake the plasmid DNA [42]. In both cases, however, the underlying mechanism of how the plasmid DNA enters the nucleus remains unclear and the low efficiency of plasmid-based transfections is problematic for *Plasmodium* genetics research. Moreover, the relative efficiency of these transfection approaches varies among different laboratories. Hence optimization of the transfection protocol is critical to adapt the method that works best in our laboratory system.

Transformed parasites are usually selected with different compounds based on the selectable marker in the plasmid DNA. Commonly used positive selectable markers include human dihydrofolate reductase (hDHFR) which conveys resistance to the antifolate compound WR99210, Blasticidin-S-deaminase (BSD) which conveys resistance to blasticidin, Neomycin phosphotransferase II (nptII) which conveys resistance to neomycin analogs such

as G418, and yeast dihydroorotate dehydrogenase (yDHODH) which conveys resistance to a triazolpyrimidine compound, DSM1 as shown in Table 1.1. In addition, negative selectable markers such as thymidine kinase (TK), cytosine deaminase (CD) and yeast cytosine deaminase combined with uridyl phosphoribosyl transferase (yFCU) are used to select for double-crossover recombination events and the loss of episomal plasmid DNA.

Selectable marker	**Selectable marker (Full name)**	**Selection agent**	**Selection target**	**Selection concentration**
hDHFR	Human dihydrofolate reductase	WR99210	*P. falciparum* hDHFR	2.5 nM
BSD	Blasticidin S-deaminase	Blasticidin	*P. falciparum* ribosome	2 μg/μl
NEO	Neomycin phosphotransferase II	G418	*P. falciparum ribosome*	500 μM
yDHODH	Yeast dihydroorotate dehydrogenase	DSM1	*P. falciparum* DHODH	1.5 μM
TK	HSV thymidine kinase	Ganciclovir	DNA synthesis	4 μM
CD	*E.coli* Cytosine deaminase	5-Flurocytosine	DNA synthesis	300 μM
yFCU	Yeast cytosine deaminase and uridyl phosphoribosyl transferase	5-Flurocytosine	DNA synthesis	300 μM

Table 1.1: *List of selectable markers [43–47].*

Optimizing transfection protocol

In order to ensure an optimal transfection protocol for downstream genome manipulation experiments, a transfection experiment was performed. Dr. Devaraja Mudeppa and Bennett Guo from the Rathod lab designed a small peptide that interferes with the folding of *Pf*Thymidylate synthase (*Pf*TS). This peptide prevented functional activity of the *Pf*TS enzyme both in the *in vitro* system as well as in *E. coli* cells. In order to test the effect of the peptide on the growth of parasite culture, a Dd2 clone was transfected with either control plasmid that carries sfGFP (super-fluorescent Green Fluorescent Protein) or plasmid that carries sfGFP-reverse peptide, as well as a test plasmid that carries sfGFP-peptide (Figure 1.2).

Transfections of each plasmid were done in triplicate using the direct electroporation method on sorbitol-synchronized ring-stage parasites as described previously with some modifications [41, 43]. Several transfection experiments were performed with various concentrations of starting parasites and plasmids concentrations. Below is the optimized protocol that result in consistent successful transfections. Dd2 clones of 3-5% parasitemia were first washed and pelleted with incomplete cytomix [1] at 3000rpm for 7 minutes with low deceleration. Supernatants were removed and RBC pellets were resuspended with 100 μl of the appropriate plasmid (either pUF1-sfGFP or pUF1-sfGFP-peptide or pUF1-sfGFP-reverse peptide) and 500 μl of the incomplete cytomix for a final volume of 800 μl. Half of the mixture was transferred to a 0.2-cm cuvette and electroporated at a setting of 0.31 kV and 960 μF using the BioRad Gene Pulser II electroporator. The time constant of the electroporation was about 7-11 ms. Electroporation was repeated with the remaining 400 μl and the sample was transferred back to the same flask. Selection pressure of 1.5 μM DSM1 was applied to each flask at 48 hours post-transfection. Media supplemented with selection pressure was renewed

[1] Preparation of 250 ml stock solution of incomplete cytomix: Mix 10 ml of 3 M KCl, 0.375 ml of 100 mM $CaCl_2$, 10 ml of 50 mM EGTA, 1.25 ml of 1 M $MgCl_2$, 6.25 ml of 1 M HEPES, pH 7.6, 0.217 g of K_2HPO_4, 0.170 g of KH_2PO_4, and 221.1 ml of sterilized deionized water. The pH of the final solution was adjusted to 7.6 by adding appropriate amount of KOH. The solution was then filtered sterilize and stored at 4°C.

every day for the first 6 days. Parasite proliferation was then monitored by Giemsa stained thin smeared blood samples taken at each media change, three times a week.

As expected, all 3 flasks of parasites transfected with pUF1-sfGFP plasmid were positive by microscopy at around week 3 post-transfection while all 3 flasks of parasites transfected with pUF1-sfGFP-peptide remained negative for parasites throughout the 60-day experiment. Interestingly, 2 out of 3 flasks transfected with pUF1-sfGFP-reverse peptide were positive by microscopy at around week 4-5 post-transfection with slower growth (Figure 1.3). This might be due to some low level growth inhibition due to the presence of the foreign peptide.

Positive transfected clones were then assayed by flow cytometry to confirm that the GFP is indeed being expressed in parasites cultures. Resuspended positive cultures (10 μl) were transferred to a 96-well plate and the volume is brought to 200 μl with 1X PBS. Flow cytometry recorded fluorescent signals from approximately 200,000 cells per well. Results were plotted in terms of GFP intensity as shown in Figure 1.4. Dd2 clone that was not transfected with any plasmid did not show any GFP signal while all other Dd2 clones that had been transfected with either pUF1-sfGFP or pUF1-sfGFP-reverse peptide showed positive GFP signals [*Manuscript in Preparation*].

Overall, with some optimization of the transfection protocol, this experiment has shown successful transfection of *P. falciparum* in nine independent flasks using direct electroporation method. Among the positive clones, parasites retained the plasmid and expressed the GFP as seen in the flow cytometry assay. The initial success in transfection has increased our confidence in performing gene manipulation with more complex experimental setups as discussed in the next few chapters.

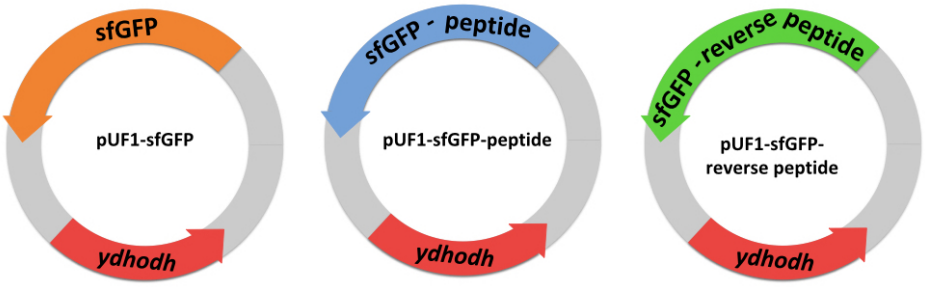

Figure 1.2: ***Plasmids used in transfection optimization.*** *sfGFP plasmid was used as a control to confirm plasmid is retained in parasites and the GFP is expressed. sfGFP-peptide was used to test the peptide inhibition of PfDHFR-TS function in parasite culture. sfGFP-reverse peptide was used as a control to ensure the inhibition by the peptide is sequence specific and that the reverse peptide does not affect parasites growth.*

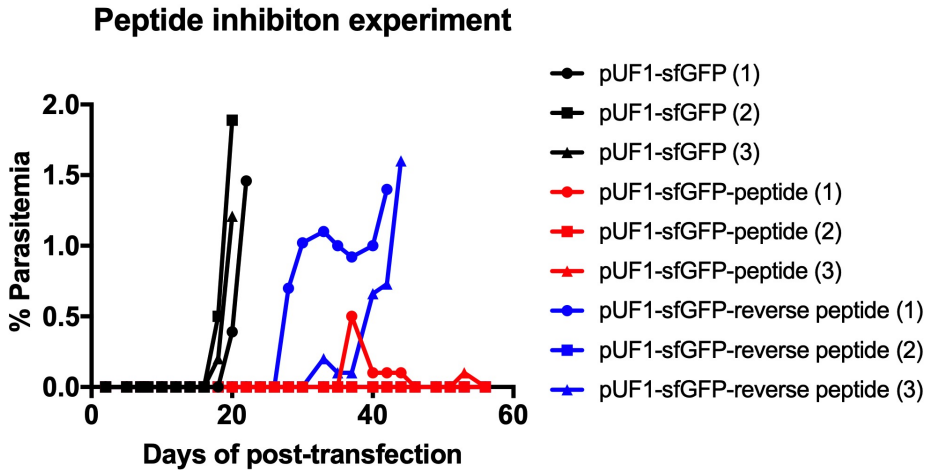

Figure 1.3: ***Result of peptide inhibition experiment.*** *All three flasks transfected with pUF1-sfGFP were positive by microscopy at week 3 post-transfection while all three flasks transfected with pUF1-sfGFP-peptide remained negative for parasites throughout the 60-day experiment. Two out of three flasks transfected with pUF1-sfGFP-reverse peptide were positive by microscopy at around week 4-5 post-transfection.*

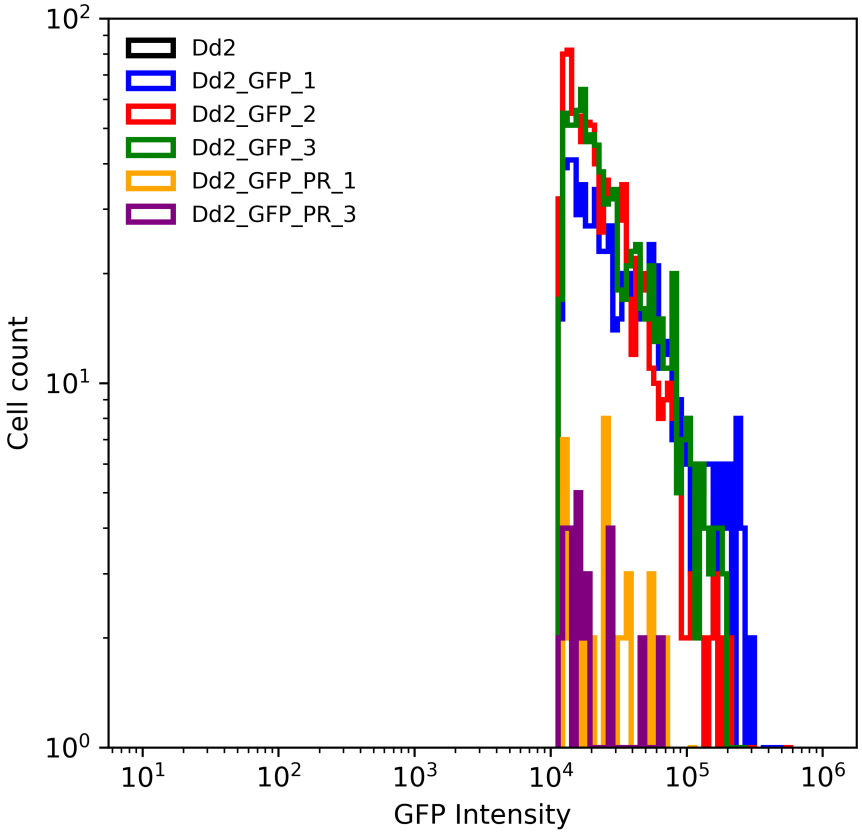

Figure 1.4: ***GFP intensity in positive transfected clones.*** *Dd2 parental clone does not exhibit any GFP signal while all the other positive transfected clones showed positive GFP signals. Dd2 clones transfected with pUF1-sfGFP plasmid were shown here as Dd2_GFP_1, Dd2_GFP_2, and Dd2_GFP_3 while Dd2 clones transfected with pUF1-sfGFP-reverse peptide plasmid were shown here as Dd2_GFP_PR_1 and Dd2_GFP_PR_3.*

1.4.2 Gene-editing tools

With advancements in transfection of *Plasmodium falciparum* and the availability of different selectable markers, genome manipulation techniques have vastly improved over the past few decades [48]. Targeted gene disruption via homologous recombination is a powerful method capable of providing information regarding gene function [49]. This includes the use of different plasmids that promote either single-crossover integration or double-crossover recombination (Figure 1.5). In the case of double-crossover recombination, a plasmid carrying the homologous regions of the gene of interest (GOI) flanking a selectable marker is transfected into the parasites to disrupt the function of the GOI. However, the use of this method has been hampered by several factors, including the low efficiency of the engineered constructs being correctly inserted into the target site, and the need for time-consuming and labor-intensive screening of clones that have the construct potentially integrated into the genome via single-crossover recombination. Alternatively, negative selection can be used to select for clones that have double-crossover recombination events [47]. However, this approach is still limited by the time required to obtain a positive transfectant.

Random gene insertional mutagenesis in *Plasmodium* spp. genome using the *PiggyBac* transposon system was introduced in 2005. This system works by randomly inserting the *PiggyBac* element at a tetranucleotide target site (TTAA) in the parasite's genome (Figure 1.6). Insertions can occur in a random gene or can flank a protein-coding sequence. After a library of parasite clones has been obtained, the *PiggyBac* insertions and their flanking genes can be identified by polymerase chain reaction (PCR) [50]. Since *Plasmodium falciparum* genomes are rich in TTAA sites, this system allows a high coverage of random-screen libraries based on phenotype. In fact, this system has been used to uncover essential genes in *Plasmodium falciparum* as shown in a recent paper published in Science in 2018 [51]. However, this method does not allow recovery of gene knockout mutations in essential genes nor can it be used to modify a specific target gene.

In circumstances in which the same gene locus is to be edited on multiple occasions, the

Bxb1 integrase system offers a more rapid way to obtain the desired integrant [52]. The Bxb1 integrase catalyzes recombination between an *attB* site already present in the *Plasmodium falciparum* genome and an incoming *attP* in a plasmid containing the desired transgene (Figure 1.7). This method usually inserts the gene of interest as a single copy into the target site without drug selection. However, the drawback in using this method is that it is restricted to using strains modified to contain the *attB* site.

Zinc Finger Nucleases (ZFNs) induce DNA double-strand breaks and trigger homologous-directed repair pathway to restore the integrity of the genome (Figure 1.8). Rapid modification of the target gene was achieved within two weeks. This insertion was possible with or without drug selection because homologous-directed repair is the only repair mechanism that occurs in *Plasmodium* spp. [53–55]. The alternative repair mechanism which stiches broken ends of DNA together by non-homologous end joining (NHEJ) pathway is absent in *Plasmodium* spp. as several crucial components of the NHEJ pathway are missing. An alternative NHEJ pathway based on microhomology has been described, although it appears to be very inefficient [56, 57]. Although ZFNs can be customized by modification on the DNA-binding domain to recognize virtually any sequence, it has not been proven to be straightforward to assemble zinc finger domains to bind an extended stretch of nucleotides with high affinity [58]. The constructs are expensive to generate and require extensive verification before being used in the parasite.

Despite advancements in genome editing, each method has its own drawbacks which might limit the type of questions that can be addressed. The emergence of CRISPR/Cas9 gene editing tool *(discussed in the next section)* in *P. falciparum* in 2014 has shed light on the possibility of improving the efficiency of gene manipulation.

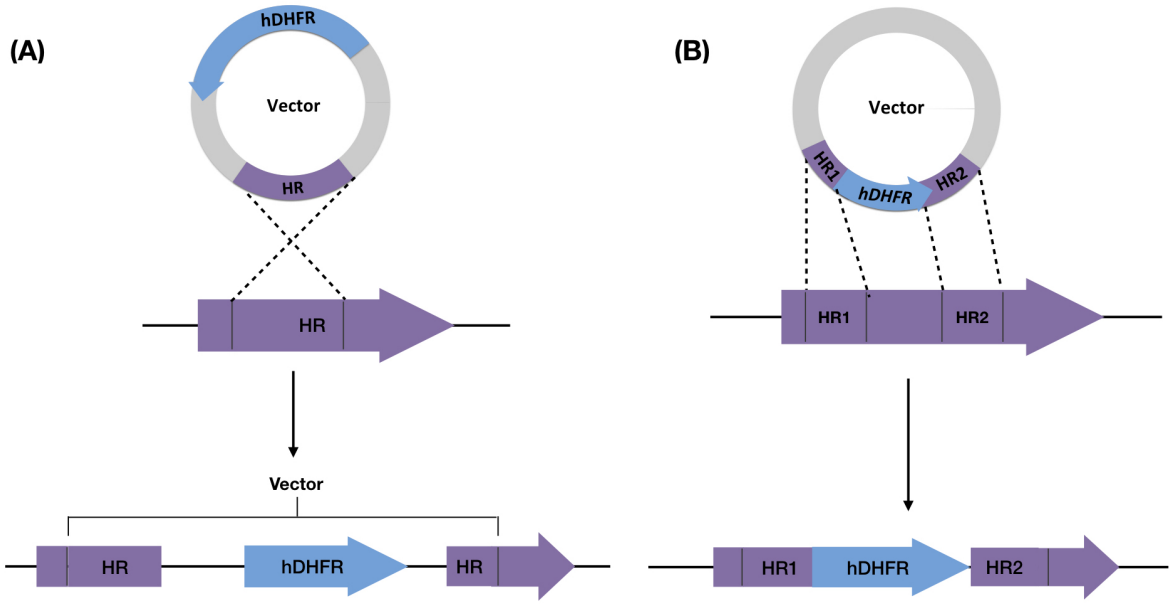

Figure 1.5: ***(A) Vector integration via single-crossover integration.*** *The targeted gene is represented by the purple arrow. In the single-crossover event, the plasmid carrying the homologous region (HR) as the target gene (shown by the purple block) will undergo recombination with the target gene. This event will lead to plasmid integration into the genome.* ***(B) Double-crossover recombination.*** *In this event, the plasmid carries the homologous regions of the targeted gene, flanking a selectable marker, in this case hdhfr. The successful recombination results in the insertion of the selectable marker into the targeted gene.*

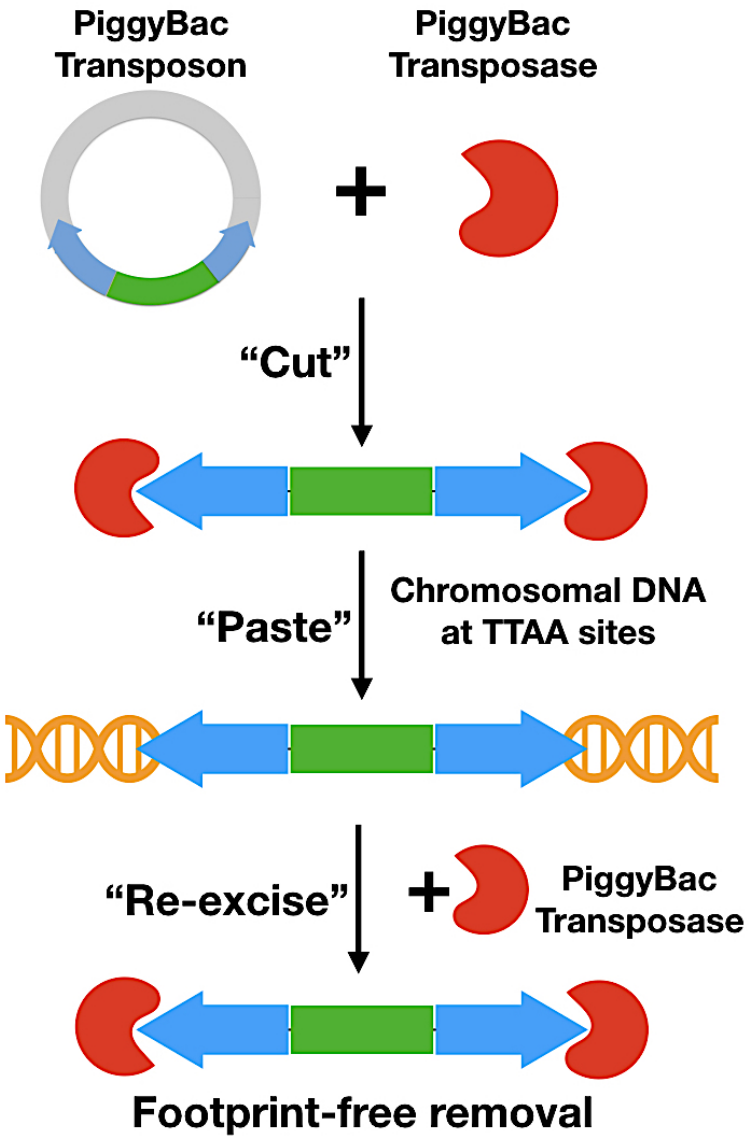

Figure 1.6: ***PiggyBac mutagenesis.*** *During transposition, the PiggyBac transposase recognizes the transposon-specific inverted repeat sequences (blue) located on both ends of the transposon vector and makes a "cut" in the sequence. The sequence is then moved from the original sites and efficiently integrates ("paste") into the TTAA chromosomal sites. The editing is reversible if the genome is treated with PiggyBac transposase to remove the inserted sequence.*

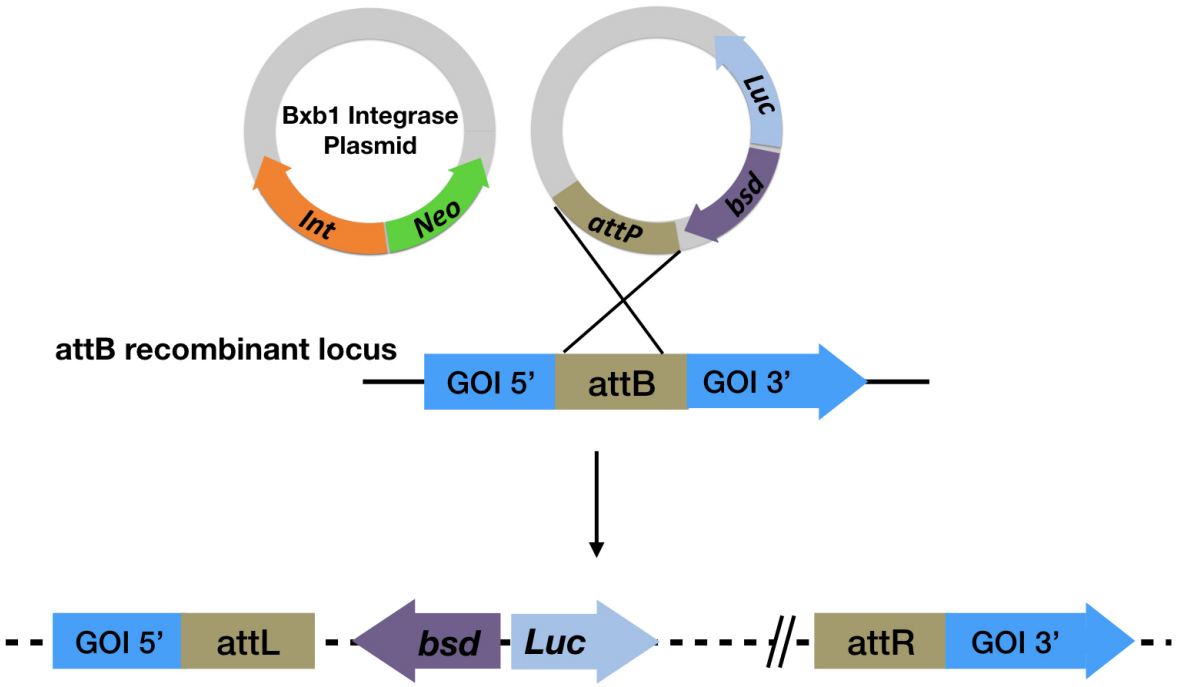

Figure 1.7: ***BxbI integrase system.*** *This system utilizes a two plasmid system as well as the genome with an integrated attB site. The Bxb1 Integrase (as shown by the orange arrow) mediates recombination of the attB site with the attP site on the second plasmid. This results in the disrupted gene, attL, which is the product of attB/attP recombination, followed by the blasticidin marker, the desired transgene (in this case, luciferase gene), the attR site flanked by the extraneous plasmid DNA, and the remaining gene of interest (GOI).*

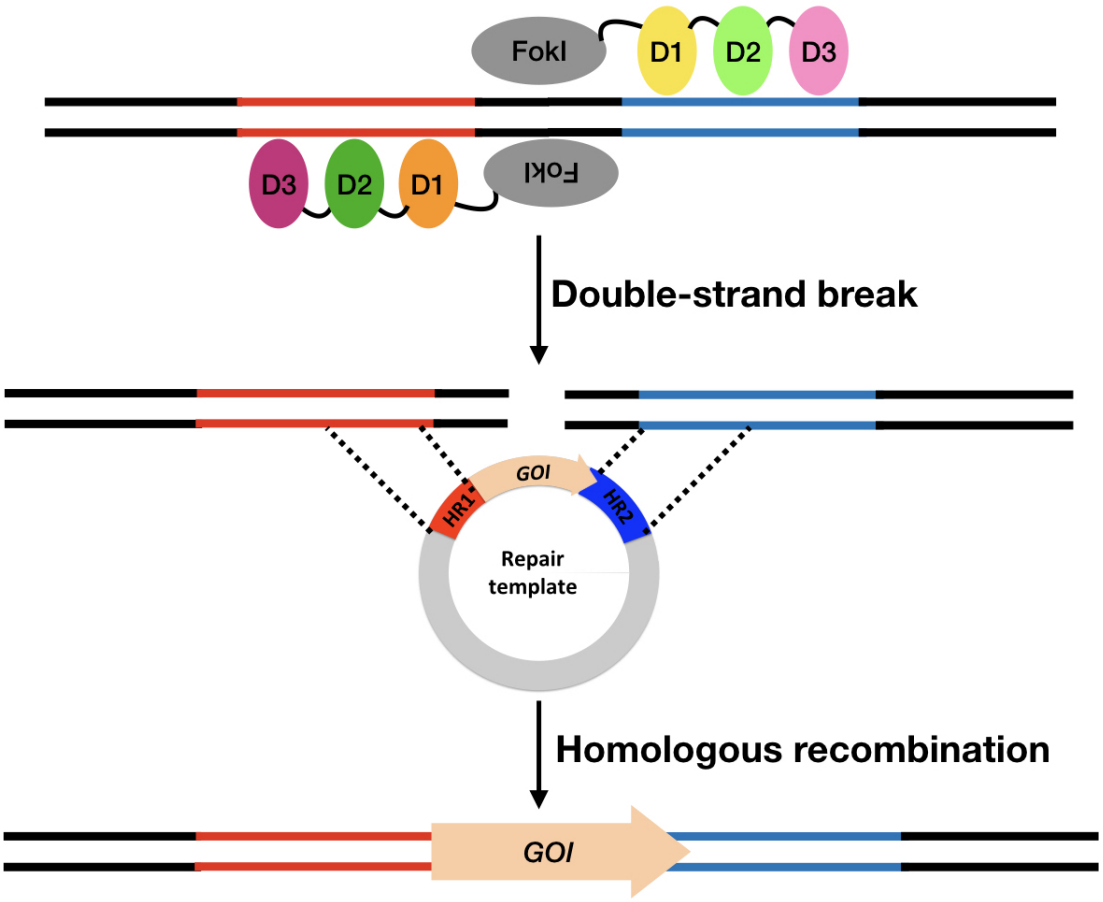

Figure 1.8: ***Editing with Zinc Finger Nucleases (ZFNs).*** *ZFN consists of two functional domains: (i) The DNA-binding domain comprised of a chain of two finger modules as shown in the figure as D1, D2, and D3, each recognizing a unique DNA sequence. These two finger modules form a Zinc Finger Protein that targets a specific sequence with high specificity; (ii) The DNA-cleaving domain comprised of the nuclease domain of FokI. When the DNA-binding and DNA-cleaving domains are fused together, it creates a highly-specific "gene-cutting" tool. The double-strand break is usually repaired through supplementation of the repair template in the form of plasmid. The repair template carries the homology regions of the target gene flanking the gene of interest (GOI) to be inserted.*

1.5 Genome editing with CRISPR technology

Genome editing by CRISPR (Clustered Regularly Interspaced Short Palindromic Repeats)/Cas9 (CRISPR-associated gene9) system has been transformative in biology. It has revolutionized the genetic manipulation of many organisms, ranging from yeast to mammalian cells as well as protist parasites [59–66].

CRISPR/Cas9 was developed from a microbial self-defense mechanism that records and targets foreign viral and plasmid DNA sequences [67]. The CRISPR/Cas-mediated prokaryotic immunity involves three stages as shown in Figure 1.9: (i) *Adaptation*, occurs when new spacers containing foreign DNA sequences are inserted into the CRISPR locus; (ii) *Expression*, occurs when *cas* genes are expressed and the CRISPR array is transcribed into a non-processed CRISPR RNA (crRNA) and further processed by Cas proteins into a mature crRNA; (iii) *Interference*, the last stage of bacterial defense, occurs when the DNA target is recognized and cleaved by ribonucleoprotein complex formed by crRNA and Cas proteins [68].

Type II CRISPR system relies primarily on a large, multifunctional protein known as Cas9, with additional modular RNAs to carry out the processes [69]. CRISPR/Cas9 is the most commonly used system for genome editing and has been adapted to many organisms [70–72]. Repurposed from the prokaryotic immune system to target and cleave foreign DNA, this system consists of an endonuclease(Cas9) and a RNA duplex (crRNA and trans-activating crRNA, tracrRNA) that targets DNA [73]. The RNA duplex has been engineered into an RNA chimera called single-guide RNA (sgRNA), for genome editing purposes. The sgRNA can be programmed to target a 20-bp sequence of interest (the protospacer). The only constraint of the molecular design used in the CRISPR system is that the protospacer has to be located immediately upstream of a protospacer adjacent motif (PAM) which is an NGG sequence (where N can be any nucleotide and G is the base Guanine) used for *S. pyogenes* Cas9 recognition (Figure 1.11) [74, 75].

Genome manipulation using CRISPR/Cas9 in *Plasmodium falciparum* was first illus-

trated by Ghorbal et al. and the utilization has since increased in the past few years [63, 76–81]. The manipulations were carried out using the two plasmids system as shown in Figure 1.10 where one plasmid carries the Cas9 endonuclease and the sgRNA, while the other plasmid carries the homologous regions of the target DNA to facilitate the homologous recombination after the introduction of the double-strand break. Since *Plasmodium falciparum* genome is highly AT-rich with overall (A + T) composition of more than 80%, the required NGG-recognition sequence will be a limitation to perform certain targeted gene manipulation. Another family of enzymes, CRISPR-Cas12a (Cpf1) recognizes a T nucleotide-rich PAM sequence [82]. Although this enzyme has not been optimized for use in the manipulation of *Plasmodium* genome, it will be useful in the future to investigate this posibility.

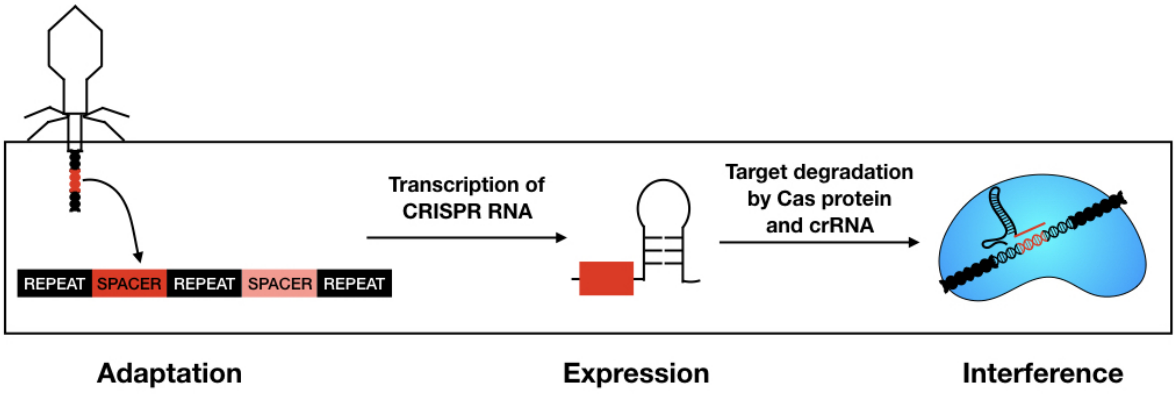

Figure 1.9: ***The key steps of CRISPR/Cas immunity.*** *(i) Adaptation: Insertion of spacers containing foreign DNA into the CRISPR locus; (ii) Expression: Expression of cas genes and transcription of CRISPR array into mature CRISPR RNA; (iii) Interference: Recognition and cleavage of DNA target by the ribonucleoprotein complex.*

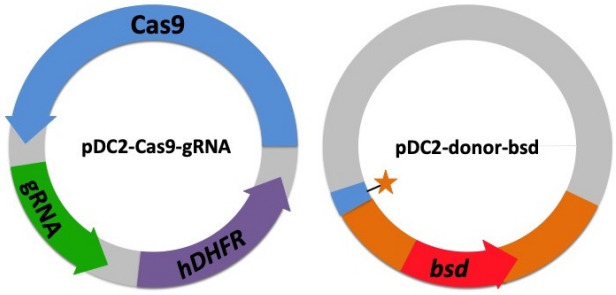

Figure 1.10: ***CRISPR/Cas9 two plasmids system.*** *pDC2-Cas9-gRNA plasmid consists of the Cas9 nuclease, a guide-RNA and a hDHFR selectable marker. pDC2-donor-bsd consists of the homology region of the target site (as shown by the orange boxes) flanking the bsd selectable marker.*

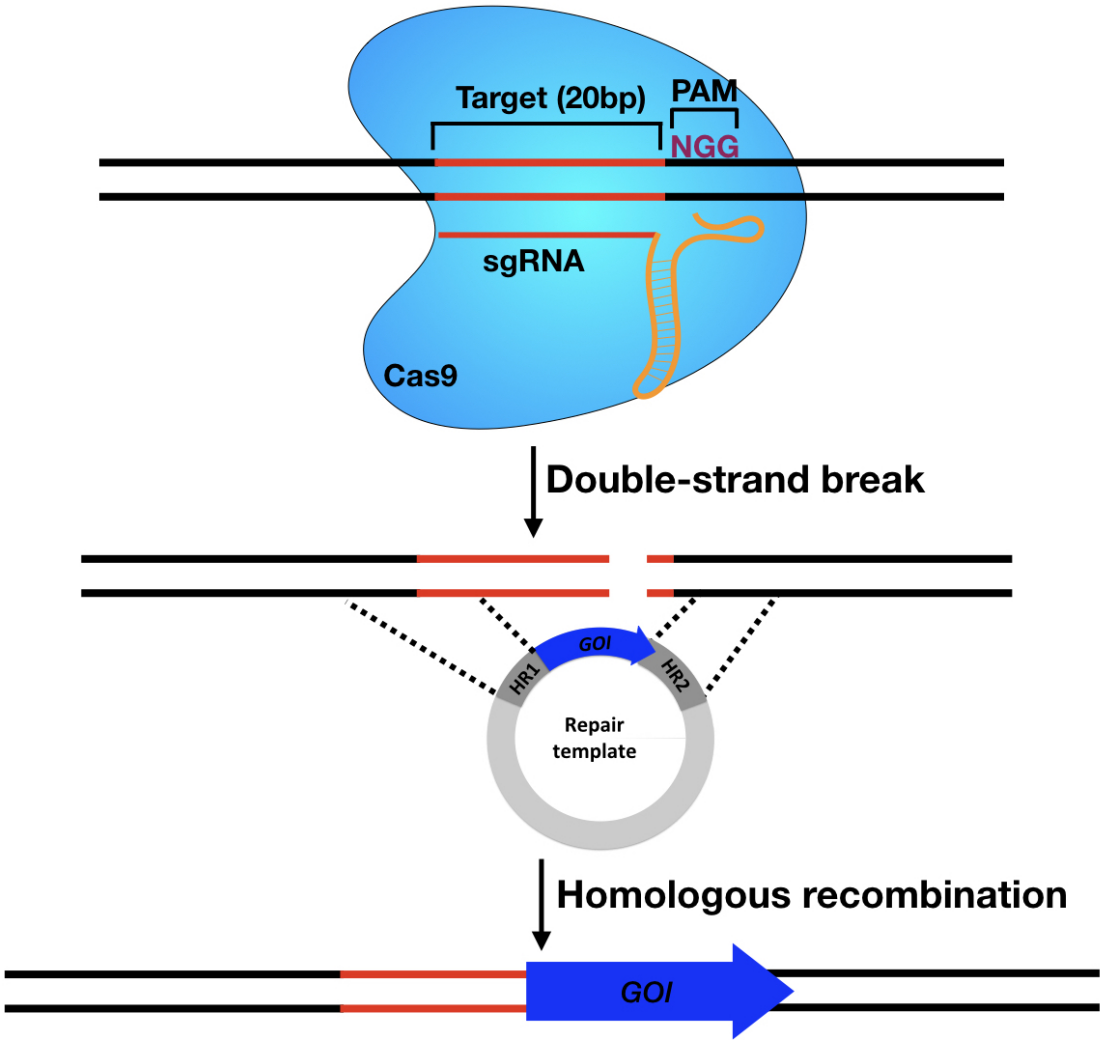

Figure 1.11: ***Editing with CRISPR/Cas9 system.*** *The sgRNA consists of a 20bp RNA complementary to the target sequence (red) that binds to the target sequence. This allows the Cas9 (blue) nuclease to be brought in close proximity to the target site through binding of the sgRNA-Cas9 binding region (yellow). The Cas9 nuclease can then mediate a double-strand break three base pairs upstream of the NGG-PAM sequence. Supplementation of the cell with the repair template allows the cell to undergo homologous recombination and hence insertion of the desired gene of interest into the target site.*

1.6 Summary

Eradication of malaria remains one of the most important global health priorities despite the emergence of resistance to our best antimalarial, artemisinin combinations therapy. Advancement in the transfection and genome manipulation techniques will likely accelerate the discovery of new drug targets, validation of mutations that lead to resistance phenotype, and the identification of essential genes that are important for the critical parasite transitions between the human and mosquito hosts.

In previous years, the Rathod lab established various tools in performing resistance studies. This includes the systematic selection of resistant parasites to antimalarial compounds and a workflow for analysis of whole genome sequences of resistant mutants. These systematic approaches have contributed to our understanding of the target of some compounds as well as the resistance mechanism.

In this thesis project, we hope to expand the toolbox to include the usage of genome manipulation to perform target identification/validation as well as understanding the detailed mechanism of mutagenesis in parasites. CRISPR/Cas9 system is a powerful alternative system for genome editing because it utilizes RNA-DNA base pairing to guide DNA cleavage and avoids inherent ZFN design problems. Taking advantage of this robust and inexpensive system, we investigated different hypotheses in malaria research. In the upcoming chapters, we are going to explore the usage of CRISPR/Cas9 tool to advance our understanding on the following topics:

- Chapter 2: Target validation of a difficult-to-purify malaria protein - *Plasmodium falciparum* DNA gyrase.
- Chapter 3: Validation of point mutations that lead to resistance to an antimalarial compound, BMS-388891.
- Chapter 4: Preliminary results on the use of genome manipulation techniques to understand the underlying mechanism of resistance acquisition.

Chapter 2

Knockout of *Plasmodium falciparum* DNA gyrase reveals its essentiality

2.1 Introduction

The complete genome sequence of *Plasmodium falciparum* published in 2002 is the first to reveal the sequences of three malaria parasite genomes: (1) a 23Mb, 14 chromosomes nuclear genome; (2) a 6kb mitochondria genome; and (3) a 35kb circular apicoplast genome [22]. During cell division DNA topoisomerases play a major role in DNA replication, DNA transcription and DNA repair in order to maintain the integrity of the whole genome throughout the life cycle of parasites [83–86]. This integrity is achieved through transesterification processes where DNA topoisomerases can (i) unlink two strands of DNA during replication or transcription, (ii) relax supercoiling tension in the DNA generated by translocating RNA polymerase or association of DNA with histones, and (iii) untangle completely replicated chromosomes [87–91]. In a strand-breakage reaction by DNA topoisomerase, a tyrosyl oxygen of the enzyme attacks a DNA phosphorus, forming a covalent phosphotyrosine link and breaking a DNA phosphodiester bond at the same time (Figure 2.1). Rejoining of the strand occurs by a second transesterification, which basically the reverse of the first reaction - the oxygen of the DNA hydroxyl group that is generated in the first reaction attacks the phosphorus of the phosphotyrosine link, breaking the covalent bond between the enzyme and DNA, and re-forming the DNA backbone bond. These reactions create transient enzyme-mediated gates

in the DNA for the passage of another DNA strand or double helix. There are two types of DNA topoisomerases (Type I and Type II) based on their ability to break single stranded or double stranded DNA [83]. Type I topoisomerases transiently break one DNA strand at a time; type II topoisomerases, in contrast, break a pair of DNA strands in a DNA double helix in concert by a dimeric enzyme molecule.

Malaria parasites have two type I (topoisomerase I and III) and three type II (topoisomerase II, VI and DNA gyrase) topoisomerases [22]. Biochemical functions for the majority of these topoisomerases remain uncertain due to the difficulty in expressing functional malaria enzymes. Previous work from the Rathod group showed successful expression of the full length topoisomerase II and the results point to a clear role for it in maintaining nuclear DNA [92]. Meanwhile Chalapareddy et al. work suggests topoisomerase VI might be important for the maintenance of the mitochondrial genome [93]. Based on the bioinformatics, DNA gyrase which consists of A and B subunits, is known to carry the apicoplast-targeting signal peptide and is believed to have a major role in retaining the apicoplast genome [25, 26, 94]. *Pf*DNA gyrase is the only apicoplast-specific type II topoisomerase and this opened possibilities for finding new targets in the development of antimalarials [25, 37, 95]. For decades, different groups have tried to understand the importance of this enzyme in malaria parasites. Functional complementation studies in *E.coli* have been performed to determine whether the *PfgyrA* and *PfgyrB* genes code for functional gyrase proteins. *PfgyrA* failed to complement *E. coli* temperature-sensitive cells at the restrictive temperature, where *PfgyrB* could do that nicely at the restrictive temperature. Also, *E. coli gyrA* and *gyrB* genes could rescue these temperature-sensitive phenomena at the restrictive temperature nicely. Although the expression of *Plasmodium falciparum* DNA gyrase A (*Pf*GyrA) was not successful, Dar et al. showed successful expression of *Pf*GyrB and its localization to the apicoplast. In that experiment, they have shown that *PfgyrB* is a true *gyrB* homologue while more optimization on the protocols have to be done to confirm the function of *Pf*GyrA enzyme [96]. Other independent studies have also been carried out to understand the function of the *Pf*GyrA

based on different versions of truncated *Pf*GyrA [97–100]. However, the essentiality and exact mode of action of *Pf*GyrA for blood stage malaria parasites have not been established.

In this chapter, we utilize CRISPR/Cas9-mediated gene editing to demonstrate that *Pf*GyrA is targeted to the apicoplast and that it is important for the function of the apicoplast. Previously, Yeh and Derisi showed that parasites lacking apicoplast functions can be chemically rescued with isopentenyl pyrophosphate (IPP) supplementation. In that study, they showed that the production of the IPP might be the sole function of the apicoplast in blood stage parasites [40]. Hence, if *Pf*GyrA enzyme is localized in the apicoplast and that it is essential in blood stage parasites, we hypothesized that *Pf*ΔGyrA parasites may survive with the addition of IPP (Figure 2.2). If successful, this would allow us to understand the importance of *Pf*GyrA in malaria parasites and drugs that target the apicoplast *Pf*GyrA.

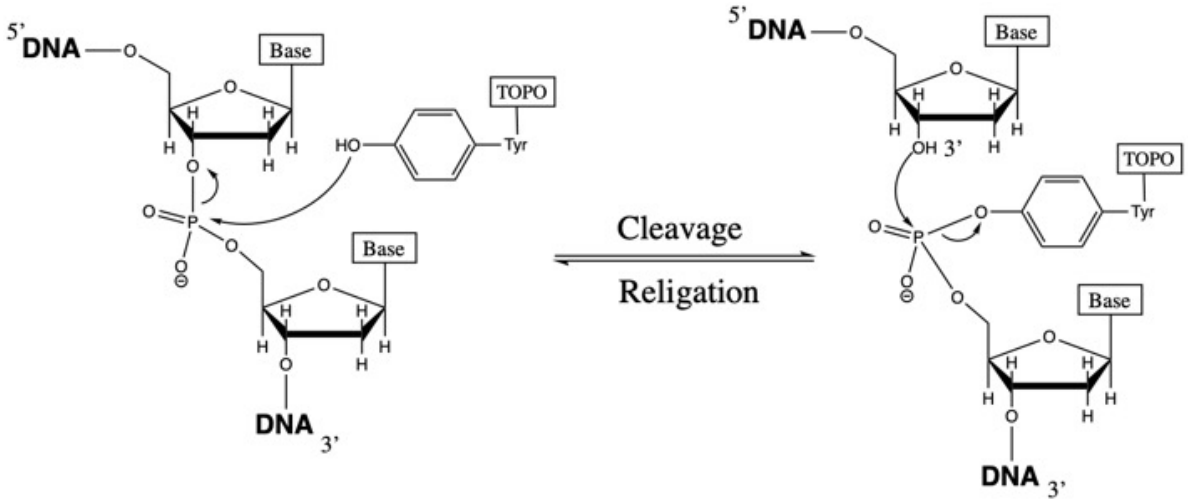

Figure 2.1: ***Catalysis of transient breakage of DNA by DNA topoisomerases.*** *Transesterification between an enzyme tyrosyl and a DNA phosphate group leads to the cleavage of a DNA backbone bond and the formation of a covalent enzyme-DNA intermediate. Religation of the DNA backbone bond occurs by the reversal of the reaction.*

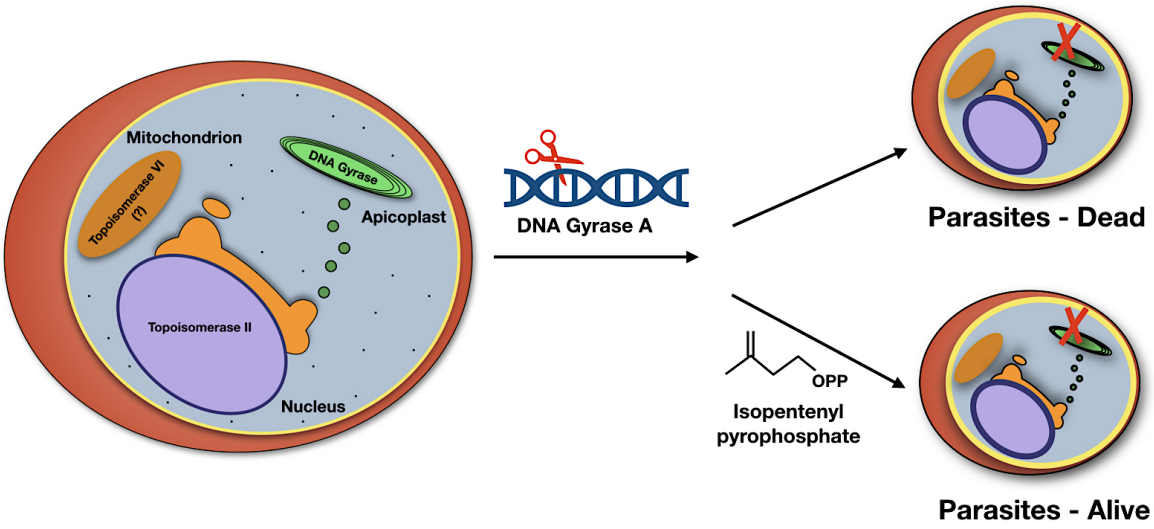

Figure 2.2: ***Experimental Model.*** *PfGyrA is a type II topoisomerase predicted to localized in the parasite apicoplast. Disruption of PfGyrA will lead to parasite death if its function is important to the maintenance of the apicoplast. However, we hypothesized that the genetically modified parasite that has lost its apicoplast can be chemically rescued with the supplementation of isopentenyl pyrophosphate (IPP).*

2.2 Results

2.2.1 Gene knockout of *Pf*GyrA

This experiment utilized the CRISPR/Cas9 method that has been adapted recently for genome editing in *Plasmodium falciparum* [63, 76, 77, 101]. The plasmid labeled as pDC2-gRNA-Cas9 expressed the Cas9 nuclease that introduces the double-strand break, the sgRNA that carries the 20-bp nucleotides complementary to the target site and the human dihydrofolate reductase (*hdhfr*) that is selectable with the antifolate WR99210. The donor plasmid labeled as pDC2-donor-bsd was designed to act as a repair template to leverage the homologous directed repair pathway. It carries the homology regions from the targeted gene sequence flanking the blasticidin-S-deaminase (BSD) selectable marker (Figure 2.3). A point mutation to insert a stop codon on the 3' end of the apicoplast-signal peptide was included in the homology region on the donor plasmid. The stop codon aims to further disrupt the production of the full-length *Pf*GyrA enzyme and its potential localization to the apicoplast.

The prepared gRNA-Cas9 and donor plasmids were electroporated into a parental Dd2 laboratory clone. At 48 hours post-transfection, parasites were supplemented with IPP and maintained with WR99210 and Blasticidin for six days, followed by culturing in the IPP-supplemented media. Modified parasites were observed microscopically at day 21-24 post-transfection in most flasks when IPP was supplemented in each culture. Genomic DNA was extracted from each positive transfected clone for downstream confirmation assays. PCR target gene amplification was done for each transfected clone using different primer sets to confirm the disruption of the *PfgyrA* gene (Figure 2.4). Amplification with primers P1/P2 yield a specific fragment length in the Dd2 clone while amplification using the same primer set yield a larger PCR fragment in the modified clones (Dd2ΔGyrA). Since Dd2 clone did not include the *bsd* gene, no fragment was observed when amplified with P1/P3 or P4/P2 primer sets. On the other hand, amplification with P1/P3 or P4/P2 primer sets yield a specific fragment length in the modified clones and hence confirmed the insertion of

the selectable marker. Among 5 out of 13 independent populations that were positive by microscopy, only two transfected clones carried the desired modification based on the PCR confirmation. Sequencing of the amplified PCR products further confirmed the disruption of the gene. Although the other three positive clones showed disruption of the *PfgyrA* gene, sequencing of those PCR products indicated that the point mutation inserted at the 3' end of the apicoplast-targeting signal was absent.

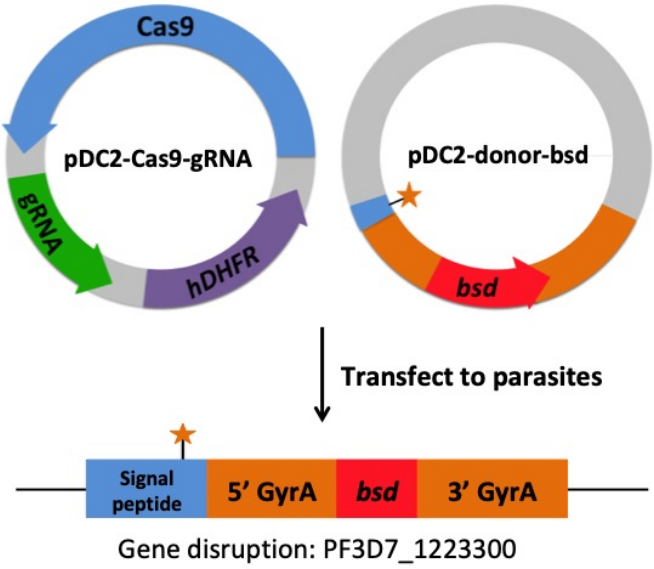

Figure 2.3: ***Experimental Design.*** *Gene manipulation was done via CRISPR/Cas9 method. The Cas9 enzyme is encoded on a plasmid that also expresses gRNA and a hdhfr selectable marker. The donor plasmid carries the homology arms of the PfgyrA gene with a point mutation inserted on the 3' end of the apicoplast-signal peptide. Transfected parasites would have the PfgyrA gene disrupted with the insertion of bsd.*

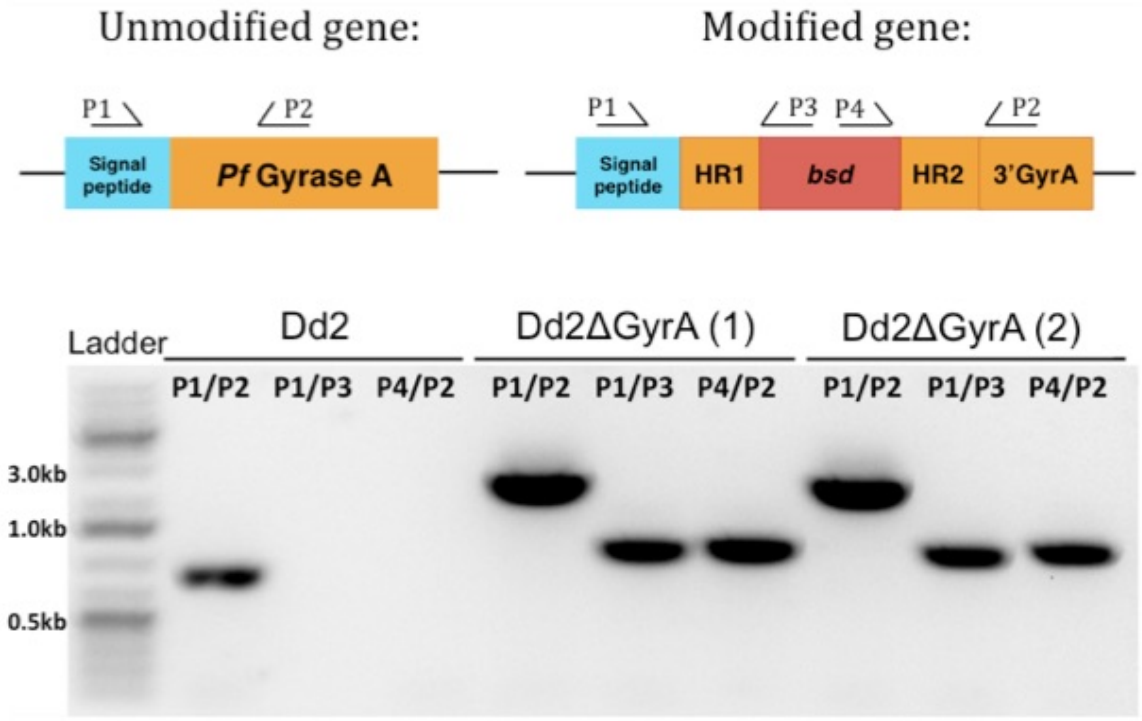

Figure 2.4: ***Confirmation of the disruption of the PfgyrA.*** *PCR with different primer sets was used to assess the disruption of the gene. Genetically modified parasites yield a larger PCR fragment when amplified with P1/P2 primers. Amplification with P1/P3 and P4/P2 primers furthers confirmed the insertion of the selectable marker in the modified parasites.*

2.2.2 Loss of apicoplast in Dd2ΔGyrA

In order to determine whether the apicoplast remained intact after the disruption of the *PfgyrA* gene, genetically pure populations of Dd2ΔGyrA generated through limiting dilution were isolated. Immunofluorescence assay was carried out to confirm the loss of the apicoplast. Apicoplast structure was visualized through staining of an apicoplast-targeted acyl-carrier protein (ACP) with the ACP-antibody. Anti-rabbit secondary antibody conjugated with the Alexa-Fluor 488 (green fluorescence) was used to confirm the apicoplast staining through microscopy. As expected, the ACP localized to a discrete structure (the apicoplast) in the Dd2 clone while ACP appeared to be diffused in the cytoplasm of the Dd2ΔGyrA clone where apicoplast was lost (Figure 2.5). As the control, the nucleus was stained with DAPI (blue fluorescence) and the mitochondria was stained with Mitotracker CMX-ROS (red fluorescence). In both conditions, there were no difference in the staining pattern between Dd2 and Dd2ΔGyrA clones, suggesting that the nuclear and mitochondria remained intact in both clones.

The loss of the apicoplast in the Dd2ΔGyrA clone was further confirmed through whole genome sequencing. The coverage of the whole genome sequences in a Dd2ΔGyrA was compared to that of a Dd2 clone. The coverage plot as shown in Figure 2.6 indicated that Dd2ΔGyrA has lost its apicoplast genome (with no coverage) while Dd2 clone displayed a good coverage for its apicoplast genome. The coverage of both mitochondrial and nuclear genomes (represented by Chromosome 1) shown by both Dd2 and Dd2ΔGyrA clones were very similar, indicating that both genomes remained intact in both clones. Coverage of chromosomes 2 - 14 of both clones were also plotted and shown to display similar trend as chromosome 1 (plots not included here).

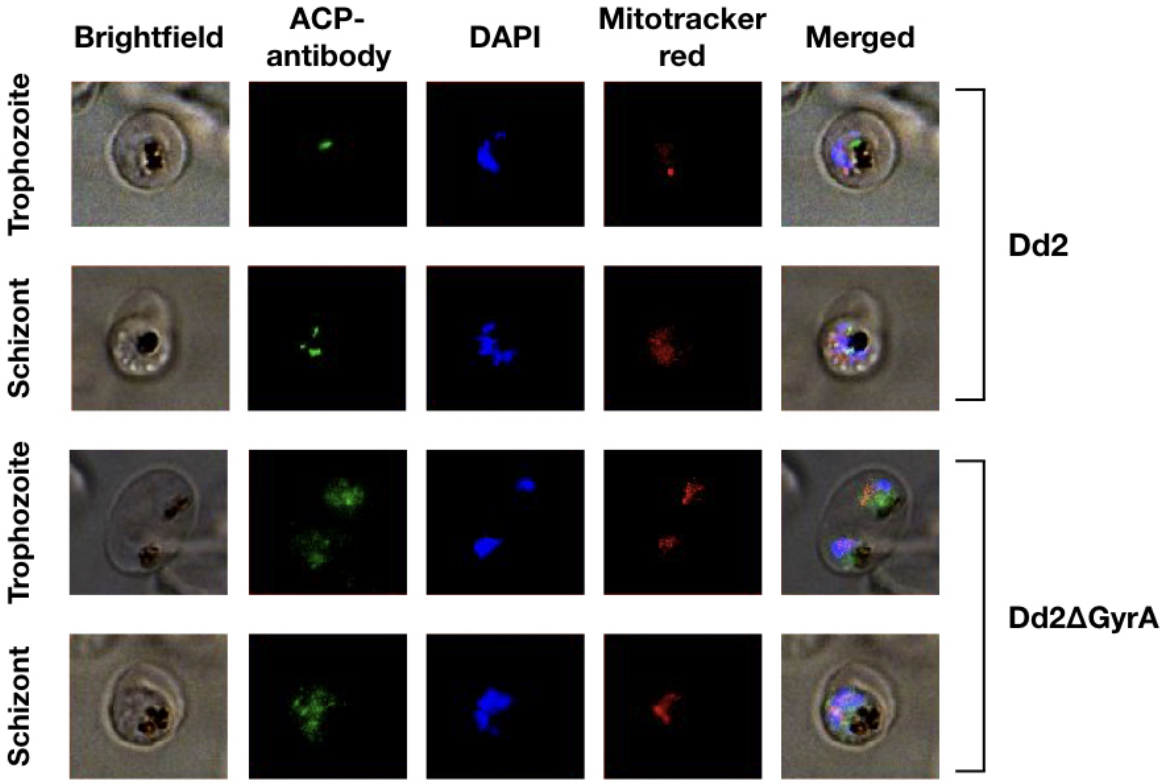

Figure 2.5: ***Loss of apicoplast confirmed through Immunofluorescence assay.*** *The apicoplast was stained with the ACP-antibody, which was then visualized with the anti-rabbit secondary antibody conjugated to Alexa Fluor 488. Nucleus was stained with DAPI while Mitochondria was stained with the Mitotracker CMX-ROS. The apicoplast remained intact in the Dd2 clone where ACPs were localized to a specific location. However, in the Dd2ΔGyrA clone, ACPs were dispersed throughout the cytoplasm of parasites, indicating loss of the apicoplast structure. Nuclear and mitochondrial genomes remained intact in both Dd2 and Dd2ΔGyrA clones.*

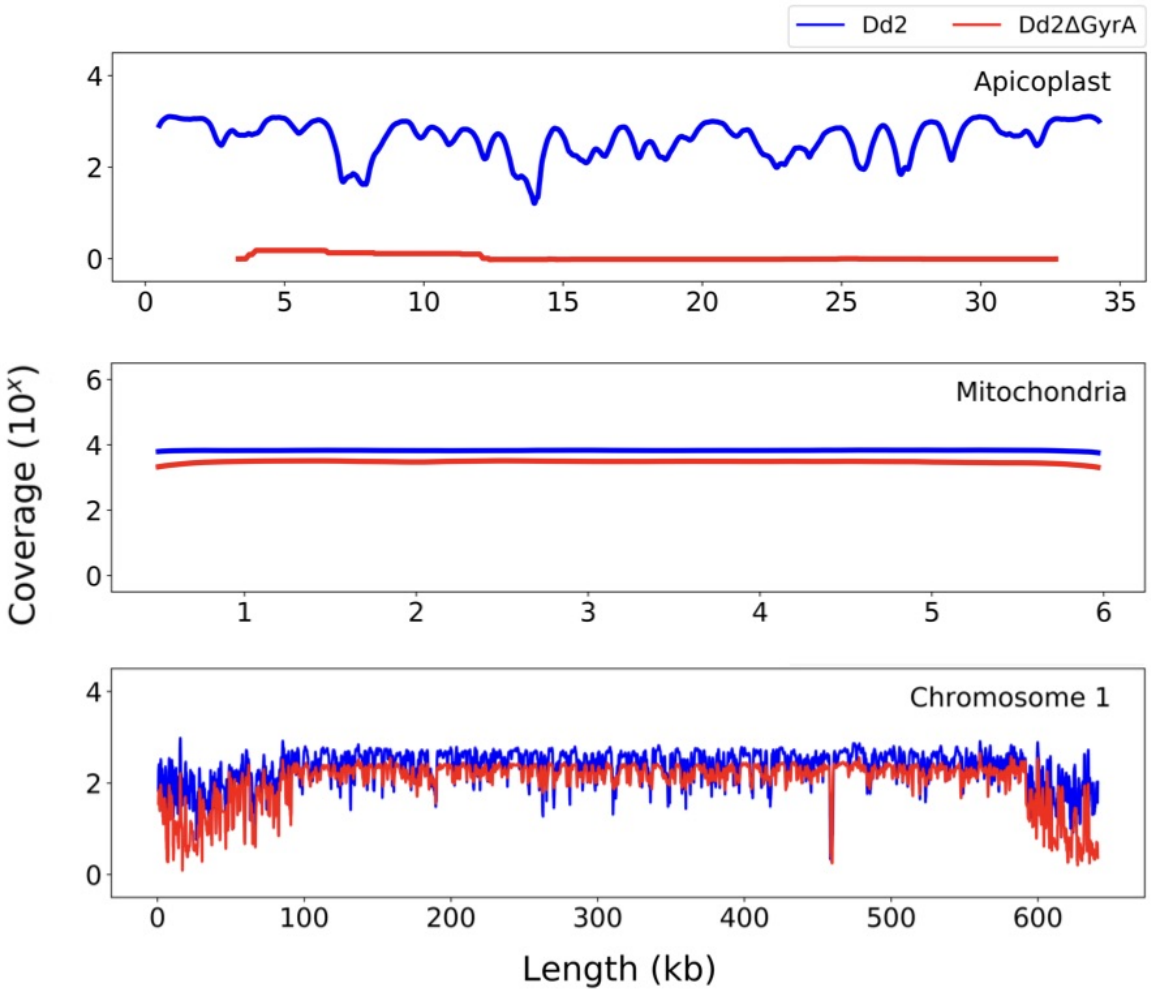

Figure 2.6: ***Loss of apicoplast genome confirmed through WGS data.*** *The depth of sequenced reads indicated that Dd2ΔGyrA has lost its apicoplast genome while still retaining the mitochondria and nuclear genomes. The unmodified Dd2 clone has all its apicoplast, mitochondrial and nuclear genomes remained intact.*

2.2.3 Dependence of Dd2ΔGyrA on IPP for growth

In order to test whether Dd2ΔGyrA clone was dependent on IPP for growth; each flask was split into two. One flask was maintained in the presence of IPP while the other flask has IPP removed from the culture and parasites were observed microscopically 48 hours later (Figure 2.7 A). Based on the microscopic images at 48 hours post-IPP removal, cytoplasm in each parasite appeared to be less condensed and the morphology of parasites was distorted compared to parasites cultured in IPP-supplemented media (Figure 2.7 B). Parasites were able to proliferate normally in cultures supplemented with IPP. However, reduced parasites growth was observed in cultures at 48 hours post-IPP removal. Most parasites were considered unhealthy or non-viable at 72 hours post-IPP removal (Figure 2.7 C).

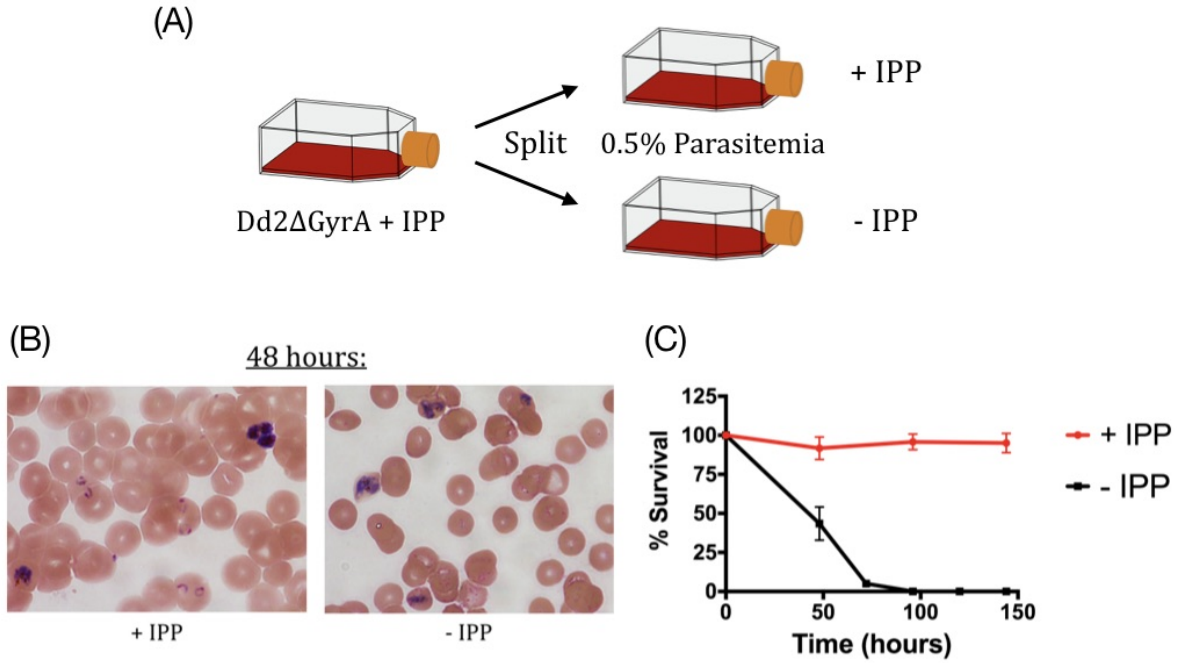

Figure 2.7: ***Dependence of Dd2ΔGyrA on IPP for growth.*** *(A) Dd2ΔGyrA clone was split into two independent flasks, one with continuous supplementation of IPP while the other flask has IPP removed. (B, C) Parasites with continuous IPP supplementation were able to proliferate healthily. Parasites in flask where IPP has been removed were unhealthy and were not viable after 48 hours.*

2.2.4 IPP rescues parasites from delayed-death phenotype

Previous studies have shown that parasites display a delayed-death phenotype when treated with antibacterial targeting apicoplast housekeeping processes [36, 102, 103]. In those cases, parasites can proliferate normally for one cycle but the daughter cells would have lost their apicoplasts and could not complete another cycle. In order to determine the properties of Dd2ΔGyrA clone, we tested the clone using doxycycline, ciprofloxacin and etoposide in 48 hours, 72 hours, 96 hours or 120 hours drug-sensitivity assays. Doxycycline is an antibacterial known to inhibit bacterial protein synthesis by binding to the 30S ribosomal subunit; Ciprofloxacin is an antibacterial known to inhibit bacterial DNA gyrase; Etoposide on the other hand, is known to inhibit nuclear topoisomerase II. Similar to what have been shown in previous publication, Dd2 exhibited a delayed-death phenotype when treated with doxycycline or ciprofloxacin, demonstrating that they are indeed targeting the apicoplast proteins. When IPP was supplemented in the assay (Dd2+IPP), chemical rescue of apicoplast-specific inhibition was observed, consistent with previous findings [40, 104, 105]. Dd2ΔGyrA displayed a similar inhibitor-response profile as Dd2 clone when IPP was supplemented (Figure 2.8). This suggests that our CRISPR-generated Dd2ΔGyrA parasite line displays similar characteristics as the apicoplast-minus parasites generated through inhibition by small molecules. Inhibition by the control compound, etoposide, did not result in delayed-death and chemical rescue was not observed. This indicated that our parasite line was not perturbed in regards to normal topoisomerase activity.

Next we also tested various commercially available fluoroquinolone compounds (ciprofloxacin derivatives) as shown in Figure 2.9 to determine their effect on the Dd2ΔGyrA clone. Majority of the fluoroquinolone compounds displayed similar inhibition and IPP-rescue profiles as ciprofloxacin. Surprisingly, moxifloxacin and nadifloxacin did not show delayed-death or IPP-rescue effect when being tested on the Dd2ΔGyrA clone (Figure 2.10). Other compounds such as flumequine, cinoxacin and nalidixic acid displayed EC_{50} values of >125 μM and their inhibition profiles were not determined (results not shown here).

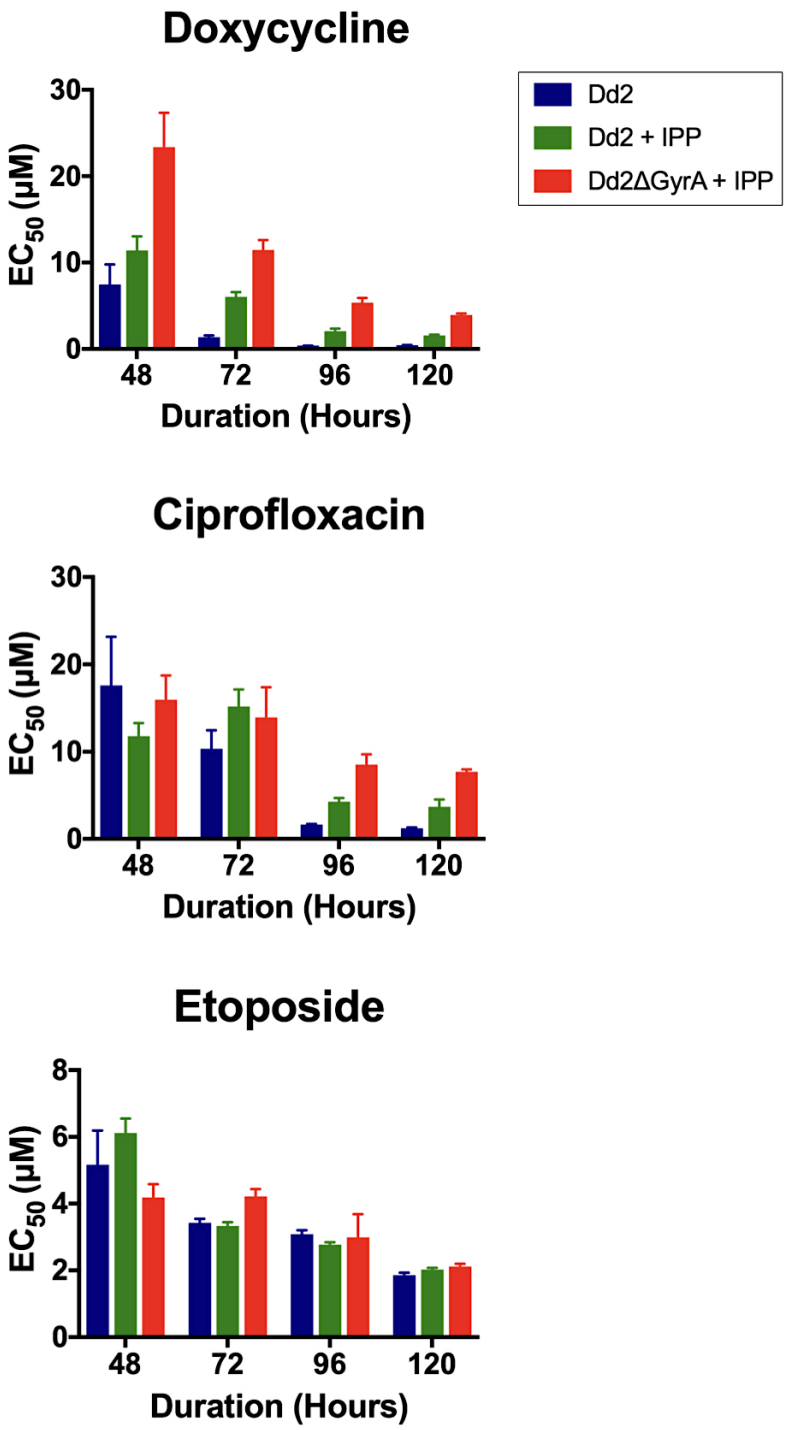

Figure 2.8: ***Drug sensitivity assays with different antibacterial compounds.*** *Delayed-death phenotype was observed when Dd2 clone was treated with doxycycline or ciprofloxacin. The parasite inhibition at 96 hours or 120 hours can be partially rescued with IPP in both Dd2 and Dd2ΔGyrA clones. Inhibition by etoposide was shown here as controls where no delayed-death or chemical rescue properties were observed.*

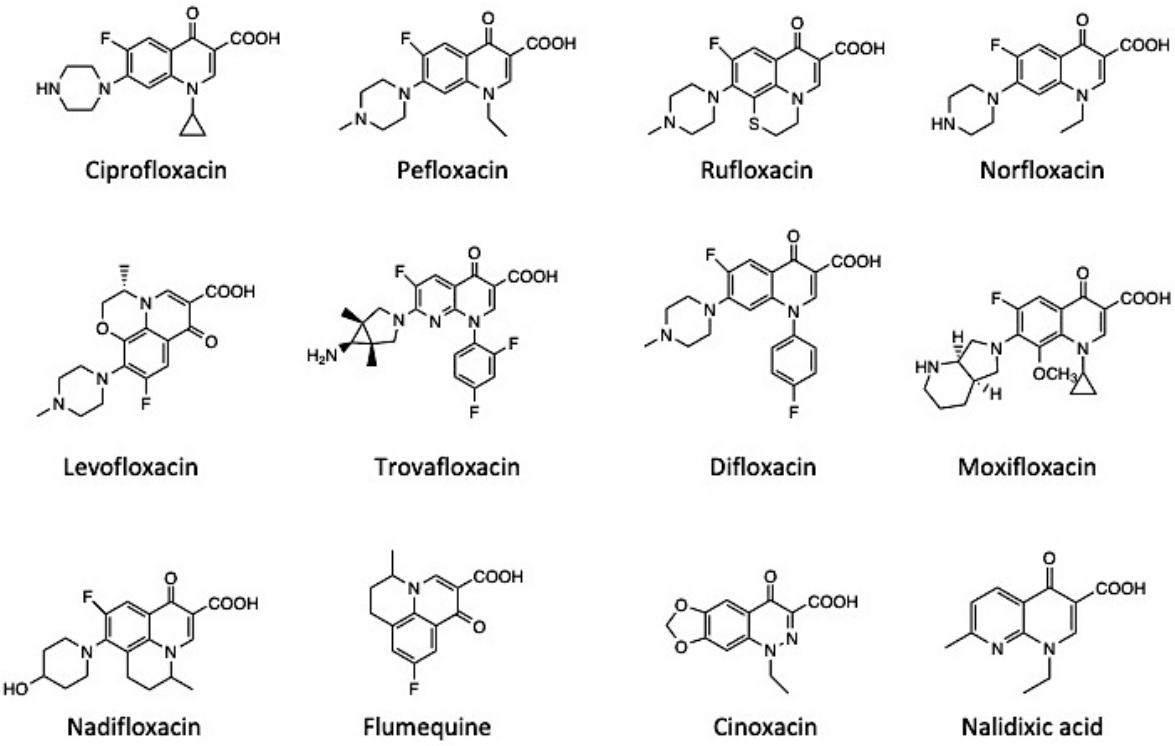

Figure 2.9: ***Structures of fluoroquinolone derivatives.*** *List of some commercially available fluoroquinolones derivatives. ciprofloxacin, pefloxacin, norfloxacin, levofloxacin, trovafloxacin, difloxacin, nadifloxacin, flumequine, cinoxacin, and nalidic acid were purchased from SigmaAldrich. Rufloxacin was purchased from MedChem Express while moxifloxacin was purchased from Cayman Chemicals.*

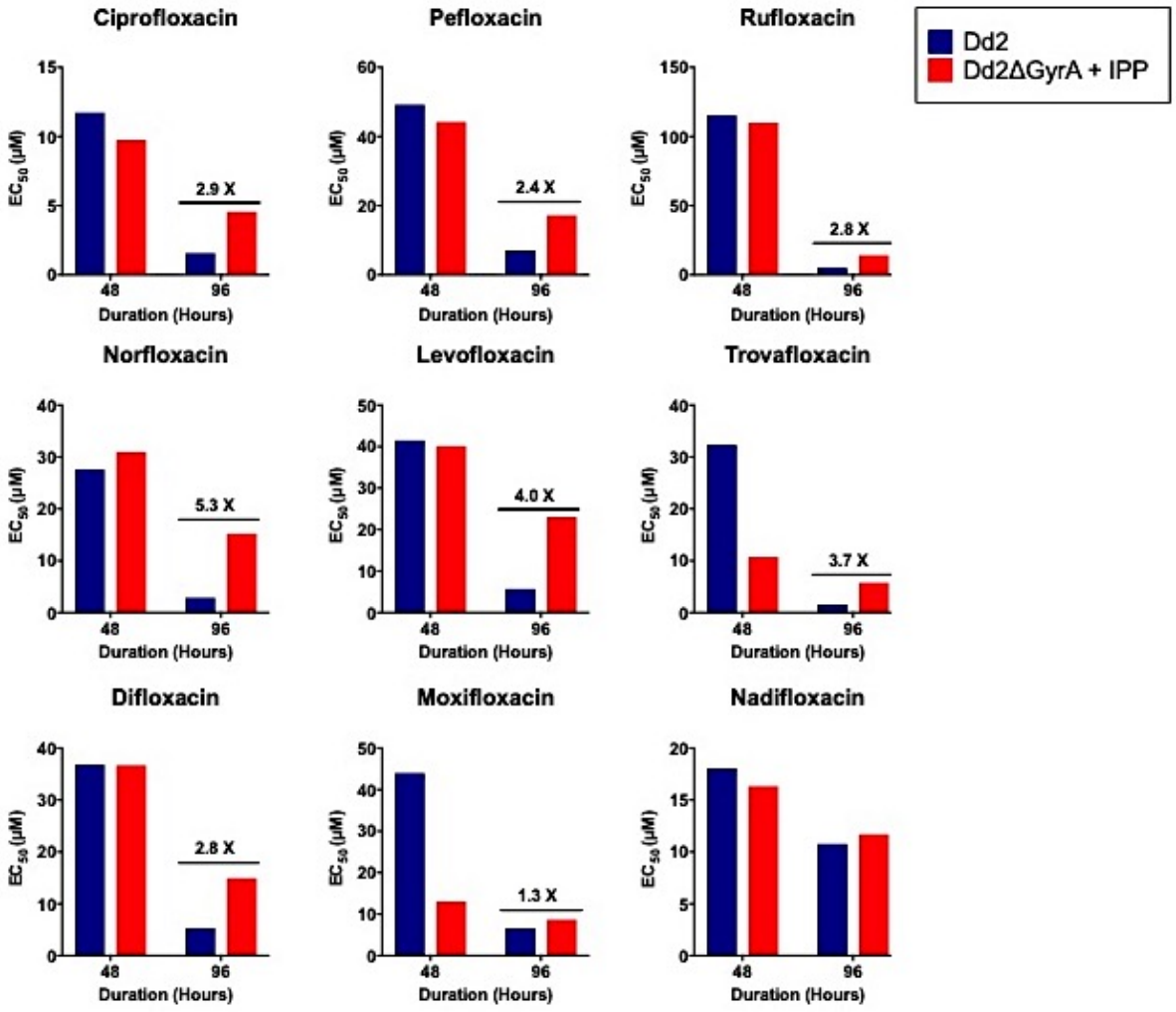

Figure 2.10: ***Drug-senstivity of fluoroquinolone derivatives.*** *Dd2ΔGyrA clone exhibit similar inhibition and IPP-rescue profiles when tested with ciprofloxacin, pefloxacin, rufloxacin, norfloxacin, levofloxacin, trovafloxacin, and difloxacin. No significant delayed-death or IPP-rescue effects were seen in the Dd2ΔGyrA when tested with moxifloxacin or nadifloxacin.*

2.3 Discussion

CRISPR/Cas9-mediated gene knockout of *Pf*GyrA clearly confirms its importance to the function of the apicoplast in blood-stage parasites. Here we showed through immunofluorescence and whole genome sequencing that the disruption of the *PfgyrA* gene led to the loss of the apicoplast. This further supports previous findings that *Pf*GyrA is localized to the apicoplast and that it has a major role in the maintenance of the integrity of the apicoplast [25]. Previous report by Yeh and Derisi showed that IPP can be used to chemically rescue parasites that have been treated with apicoplast-targeting compounds [40]. In this study, we have shown that we could use a similar chemical rescue strategy to understand the importance of the apicoplast-targeted enzyme. The gene knockout and chemical rescue approach could be a useful tool in screening for essential apicoplast-targeted enzyme.

Although apicoplast can be lost through chemical inhibition by small molecules, there are several advantages of generating apicoplast-minus parasites using a genomic approach. Uddin et al. demonstrated that apicoplast-targeting drugs can be validated with the chemical rescue method. For instance, parasites exhibit delayed-death phenotype when treated with doxycycline or ciprofloxacin and that the inhibition can be chemically rescued with the supplementation of IPP. [105]. We showed that similar work can be done using the Dd2ΔGyrA clone generated in this study. In fact, the IPP-rescue effect is more prominent when tested with Dd2ΔGyrA as compared to the Dd2 clone (Figure 2.11). This is a major advantage because the use of Dd2ΔGyrA clone for inhibitor screening would result in a more accurate inhibition-rescue profile.

Given the difficulties in performing biochemical assays to characterize inhibitors of *Pf*GyrA in malaria parasites, CRISPR/Cas9-mediated gene knockout of the enzyme has proved to be useful to characterize inhibitors that target the apicoplast in blood-stage parasites. Drug sensitivity assays of various fluoroquinolones compounds revealed that there are more than one mode-of-action of this class of compounds on malaria parasites; one with an apicoplast target while the other with a non-apicoplast target. This phenomenon was

also observed at high concentrations where ciprofloxacin continued to inhibit IPP-rescued Dd2ΔGyrA suggesting that this compound has an additional target in *P. falciparum*. Previous biochemical experiments conducted in our lab indicate that ciprofloxacin can inhibit nuclear topoisomerase II and the crystal structure showed binding of ciprofloxacin in the topoisomerase II catalytic pocket (*Manuscript in Preparation*) [92]. Among 12 fluoroquinolone compounds tested in this study, ciprofloxacin exhibit lowest EC_{50} values (i.e. the most potent compound). In the future, a resistant selection experiment with ciprofloxacin on the Dd2ΔGyrA clone would enable us to potentially dissect the secondary mode of action of this class of compounds.

Overall, gene-editing of *Pf*GyrA allows for formal dissection of antimalarial activity directed at this high value target. In the future as we reach forward and design novel potent inhibitors that specifically target *Pf*GyrA from malaria parasites, the present validation model would allow us to stay on track. Furthermore, by untangling the two inhibitory functions of ciprofloxacin, we hope to help identify the additional target and a potential new mode of action of ciprofloxacin in malaria parasites.

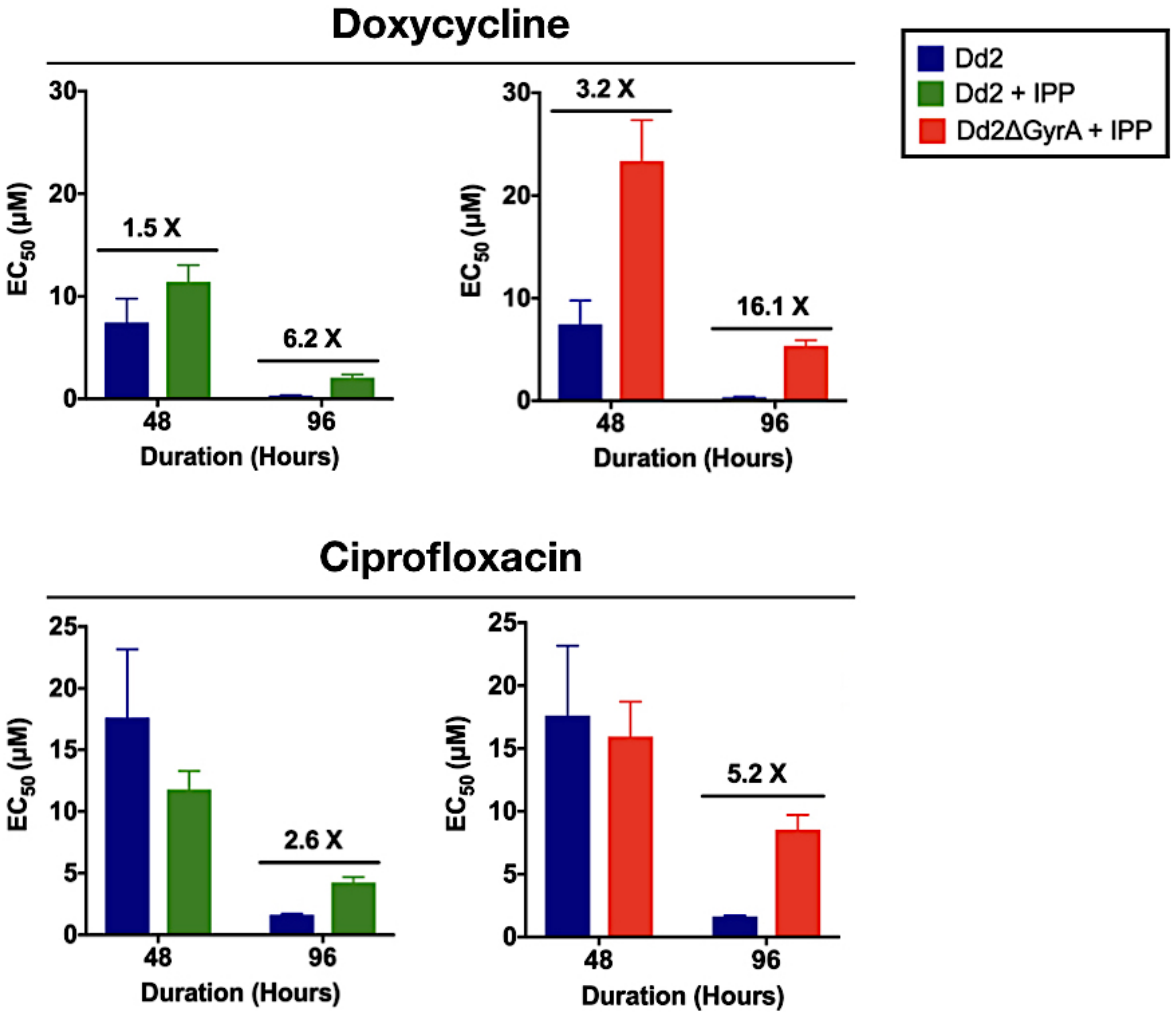

Figure 2.11: ***Fold of IPP-rescue in Dd2 and Dd2ΔGyrA clones.*** *Clones treated with doxycycline exhibit a low-level IPP-rescue at 48 hours (1-3 fold) while establishing a higher-level of IPP-rescue at 96 hours (6-16 fold) when the delayed-death effect is prominent. Clones treated with ciprofloxacin do not exhibit any IPP-rescue at 48 hours while establishing some low-level IPP-rescue at 96 hours (3-5 fold).*

2.4 Methods

2.4.1 Plasmids construction

Plasmids pDC2-gRNA-Cas9 and pDC2-donor-bsd as shown in Section 2.5.1 were provided by Marcus Lee (Wellcome Sanger Institute, UK). The plasmid pDC2-gRNA-Cas9 was modified to include 20 nucleotides gRNA sequence (ATAGGTAAATATCATCCACA) targeting *PfgyrA*. gRNA construct was designed using the CRISPR tool on the Geneious software. The gRNA selected has an on-target score of 0.709 (higher score denoting higher activity) based on method proposed by Doench et al. [106] and an off-target score of 100% (higher score denoting less off-target activity) based on method proposed by Zhang et al. [107]. 100 μM of each gRNA-Oligo 1 and gRNA-Oligo 2 (ordered from Eurofins Genomics) were phosphorylated and annealed using T4 polynucleotide kinase and T4 ligation buffer in a thermocycler by incubating at 37^{o}C for 30 minutes, increase the heat to 94^{o}C for 5 minutes then ramp down to 25^{o}C at 5^{o}C/min. Annealed gRNA-oligos (1:200 dilution) were then ligated with 50 ng of BbsI-digested plasmid. Ligated product was transformed into DH5α competent cells (Invitrogen). The sequencing primer (gRNA primer) was used for sequencing to confirm insertion of gRNA into the plasmid. The plasmid pDC2-donor-bsd was modified to carry homology arms of *PfgyrA* (PlasmoDB ID: PF3D7_1223300) flanking the selectable marker Blasticidin S-deaminase (BSD) to facilitate homology recombination. 5' homology arm of 307bp starts from nucleotide +415 of the GyrA coding sequence while 3' homology arm of 306bp starts from nucleotide +740. Nonsense mutations at nucleotide 437-438 (CT $\rightarrow$ GA) were inserted to introduce a stop codon at the beginning of the gene to stop further translation of the protein. 5'GyrA-F and 5'GyrA-R primers were used to amplify the 5'homology arm from the Dd2 clone; GyrA-BSD-F and GyrA-BSD-R primers were used to amplify BSD selectable marker from the pDC2-donor-bsd plasmid; 3'GyrA-F and 3'GyrA-R primers were used to amplify the 3'homology arm from the Dd2 clone. These three PCR fragments were then assembled into a single piece that carries BamHI restriction site on the 5' end and SacI

restriction site on the 3' end. The final assembled PCR construct was then digested with BamHI and SacI restriction enzymes and ligated into the double-digested pDC2-donor-bsd plasmid. Ligated plasmid was transformed into DH5α competent cells.

Primers	**Sequence**
gRNA-Oligo 1	ATTGATAGGTAAATATCATCCACA
gRNA-Oligo 2	AAACTGTGGATGATATTTACCTAT
gRNA-primer	GTTGTGTGGAATTGTGAGCGG
5'GyrA-F	TTACTCGGATCCAAAGATGATATAGTTAATGCATCTAATGATATAACAAATGA
5'GyrA-R	AAGCGAATTAGCTAAGCATGCTACCTATAACTTCACCAACTAT
GyrA-BSD-F	ATAGTTGGTGAAGTTATAGGTAGCATGCTTAGCTAATTCGCTT
GyrA-BSD-R	CTAAAGCATCATATACACTCTTATTTTCTCTGCGGTTTAATAAATATG
3'GyrA-F	CATATTTATTAAACCGCAGAGAAAATAAGAGTGTATATGATGCTTTAG
3'GyrA-R	TGATAAGAGCTCAAGGTATACTGCTTAATATACTTAC

Table 2.1: *List of primers for plasmids construction used in PfGyrA knockout experiment.*

2.4.2 Parasite cultures and transfection

Parasites were cultivated using established methods with some changes [108, 109]. Cultures of the *Plasmodium falciparum* clone Dd2 were grown *in vitro* at 37°C in solutions of 2% hematocrit (serotype A positive human erythrocyte) in RPMI-1640 medium (Invitrogen) containing L-Glutamine and 25mM HEPES, and supplemented with 0.5% Albumax I and 0.1 g/L Hypoxanthine (ThermoFisher). Cultures were maintained in sterile, sealed flasks, flushed with blood gas mixture (5% CO_2, 5% O_2 and 90% N_2). Transfections were done with the direct electroporation method on sorbitol-synchronized ring-stage parasites as

described previously [41, 43, 110]. Dd2 clones of 3-5% parasitemia were pelleted at 3000 rpm for 7 minutes with low deceleration. Supernatants were removed and RBCs pellets were resuspended with 100 μl of each 1 μg/μl plasmid (pDC2-Cas9-gRNA and pDC2-donor-bsd) and 400 μl of the incomplete cytomix to bring the final mixture to 800 μl. 400 μl of the mixture was transferred to a 0.2-cm cuvette and electroporated at a setting of 0.31 kV and 960 μF using the BioRad Gene Pulser II electroporator. The time constant of the electroporation was about 7-11 ms. Electroporation was repeated with the remaining 400 μl and the sample was transferred back to the same flask. Selection pressure (2.5 nM WR99210 and 2 μg/μl Blasticidin) and 200 μM IPP (Isoprenoids, LC and in-house synthesis) were applied to each flask at 48 hours post-transfection. Media supplemented with IPP and selection pressure were renewed every day for 6 days. On day-8 post-transfection, selection pressure was removed and media supplemented with IPP was changed every other day. Parasites proliferation was monitored by Giemsa-stained thin smeared blood samples taken at each media change, three times a week.

2.4.3 Analysis of Dd2ΔGyrA clone

Parasite pellets from Dd2ΔGyrA clone ($\sim$ 2-3% parasitemia) was lysed using 0.15% saponin solution [111]. Genomic DNA was then extracted using Qiagen DNA Mini Kit according to the manufacturer's instructions. 50 ng of genomic DNA was used in the PCR reaction for targeted gene disruption and BSD-cassette integration verification. Different primers sets as discussed in the result section were used. After verification of the product size by gel electrophoresis, 10 μl of the PCR products were then mix with 5 μl of EXO-SAP-IT PCR cleanup reagent (ThermoFisher) at 37^{o}C for 15 minutes to degrade remaining primers and nucleotides. The mixture was then heat inactivated at 80^{o}C for 15 minutes. The cleaned-up PCR product was then sent to Eurofins Genomics for sequencing using the same primers.

Primers	Sequence
P1	GAGTAATCGTTCAACATATACAG
P2	ACCAGTTGAAAAATCAGGTCC
P3	GTGGATTCTTCTTGAGACAAAG
P4	TCAAAGCCATAGTGAAGGAC

Table 2.2: *List of primers for analysis of Dd2ΔGyrA clone.*

2.4.4 Parasite sub-cloning

To isolate pure populations of Dd2ΔGyrA parasites for further analysis, aliquots of 10 or 20 parasitized red blood cells (pRBCs) were plated across an entire 96-well plate according to an established method [112]. These plates were maintained in the presence of IPP. As soon as parasites were observed proliferating, the well contents were extracted from the plate and transferred to a new 10 ml culture flask for further expansion, sample storage and analysis.

2.4.5 Drug sensitivity assay

Drug sensitivity assays were performed in 96-well plates containing serial dilution of compounds in triplicate. Concentration range used for each compound is shown in Table 2.3. Media was supplemented with IPP as indicated. To determine the EC_{50} of different compounds, plates of 0.5% parasitemia were incubated for 48 hours or 72 hours. To determine if parasites clones show delayed-death phenotype, cultures were initiated at 0.2% parasitemia and incubated for 96 hours or 120 hours, 75% of the media was exchanged every 48 hours. For all assays, parasitized cells were stained using SYBR Green I (Invitrogen) at the end of the assay and counted by flow cytometry (BD Accuri C6). Parasite proliferation in each well was expressed as a percentage of the solvent control. EC_{50} were determined using GraphPad PRISM software.

Compounds	Concentration range	Fold-dilution
Doxycycline	120 mM - 7.32 nM	4-fold
Ciprofloxacin	250 mM - 15.26 nM	4-fold
Etoposide	250 mM - 15.26 nM	4-fold
Pefloxacin	250 mM - 15.26 nM	4-fold
Rufloxacin	200 mM - 12.20 nM	4-fold
Norfloxacin	125 mM - 57.16 nM	3-fold
Levofloxacin	125 mM - 57.16 nM	3-fold
Trovafloxacin	125 mM - 57.16 nM	3-fold
Difloxacin	125 mM - 57.16 nM	3-fold
Moxifloxacin	125 mM - 57.16 nM	3-fold
Nadifloxacin	125 mM - 57.16 nM	3-fold
Flumequine	125 mM - 57.16 nM	3-fold
Cinoxacin	125 mM - 57.16 nM	3-fold
Nalidixic acid	125 mM - 57.16 nM	3-fold

Table 2.3: *Concentration range used for each compound in drug sensitivity assay*

2.4.6 Immunofluorescence Microscopy

5 ml cultures of Dd2 and Dd2ΔGyrA clones with parasitemia of ∼3%, respectively, were incubated in 100 nM MitoTracker Red CMXRos (Invitrogen) stain for 30 minutes at 37^{o}C. The dye will diffuse passively across the membranes and accumulate in active mitochondria. Cells were then prepared for microscopy as illustrated previously [113]. In a microcentrifuge tube, 1 ml of Mitrotracker-stained cells were washed and fixed in 4% paraformaldehyde (Electron Microscopy Sciences) with 0.0075% glutaraldehyde (Electron Microscopy Sciences) for 30 minutes at room temperature. Cells were then permeabilized with 0.1x Triton-X-100 in PBS for 10 minutes and blocked with 3% BSA/PBS for 2 hours with end-over-end rotation. Cells were then incubated with 1:500 diluted ACP-antibody for 1 hour and then incubated with 1:500 diluted anti-rabbit secondary antibody conjugated with Alexa Fluor 488 for 30 minutes. Nuclear DNAs were stained with 1 μg/ml DAPI for 10 minutes at room temperature. Cells were washed twice with PBS in between each step to remove excess chemicals or stains. The pellet was then resuspended in 40 μl of PBS. 10 μl of the resuspendend cells were mounted onto the slides with 5 μl of Hard Mount VectaShield (Vector Laboratories). The edges of the slides were sealed with nail polish. Slides were left at room temperature for at least 15 minutes to allow immobilization of cells to the surface of the slide. Fluorescence images were obtained on a Nikon Eclipse Ti-E equipped with a camera using a 100x / 1.4 oil immersion objective. Images were analyzed using Nikon NIS-Elements software.

2.4.7 Whole genome sequences analysis

400 ng of genomic DNA extracted from sorbitol-synchronized ring-stage Dd2 and Dd2ΔGyrA clones were sent to MedGenome, California for genomic libraries preparation and whole genome sequencing. The resulting FASTQ files with paired-end reads were trimmed from bases with a quality score below 28 (Phred) using TrimGalore, and then mapped to the 3D7 reference genome (Pf3D7v9) using BWA. Downstream processes were done following Genome Analysis Toolkit (GATK) best practices pipeline where reads are sorted and duplicated reads

were marked using Picard tools [114, 115]. After Indel realignment and base recalibration steps using GATK software, final reads were piled using SAMtools to generate Variant Calling Files. Coverage of each chromosome including mitochondria and apicoplast were generated using SAMtools from the final pileup file, from which read depth at each nucleotide position was recorded. Results were generated into coverage plots using Matplotlib. Detailed workflow of the genome analysis was discussed in Section 2.5.2.

2.4.8 Synthesis of Isopentenyl pyrophosphate, IPP

Note: Synthesis was done by Dr. Sreekanth Kokkonda from the Rathod lab.

Isopentenyl pyrophosphate was synthesized from the corresponding alcohol (1) according to the procedure as depicted in Scheme 2.1 [116]. 3-methyl-3-butene-1-ol was converted to 3-methylbut-3-en-1-yl 4-methylbenzenesulfonate using para toluenesulfonyl chloride in dichloromethane. The tosyl intermediate (2) was treated with tris(tetra-n-butylammonium) hydrogen pyrophosphate to obtain isopentenyl pyrophosphate. The final product was first passed through cation exchange resin (ammonium form) for complete ion-exchange. Subsequent purification on cellulose flash column chromatography resulted in the final product.

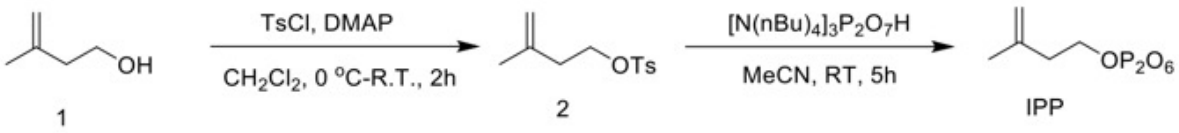

Scheme 2.1: *Synthesis scheme of IPP.*

Synthesis of 3-methylbut-3-en-1-yl 4-methylbenzenesulfonate (2):

P-toluenesulfonyl chloride (2.2 g, 11.6 mmmol) and 4-(N,N-dimethylamino) pyridine (1.5 g, 12.76 mmol) were mixed with 50 mL of anhydrous dichloromethane in a 100 mL round bottom flask at 0°C under argon. A solution of 3-methyl-3-butene-1-ol (1) (1 g, 11.6 mmol) in anhydrous dichloromethane (5 mL) was then slowly introduced with a syringe through a septum in the flask, and the ice bath was then removed. The reaction was stirred for 1-2

hours until silica-gel TLC (Hexane/Ethylacetate, 85:15 (v/v)) indicated that the reaction has completed. The reaction mixture was quenched with water (10 mL) at 0^{o}C and poured in to 1 M HCl. The layers were separated and the organic extract was washed with water (20 mL), dried and concentrated in vacuo and purified by flask column chromatography, using Hexane/Ehtylacetate (5:1) as the eluent, to give the title compound 3-methylbut-3-en-1-yl 4-methylbenzenesulfonate (2) as a colorless oil (2.31g, 80% yield). ^{1}H-NMR ($CDCl_3$): δ 1.67 (s, 3H), 2.36 (t, J = 6.8 Hz, 2H), 2.48 (s, 3H), 4.15 (t, J = 6.8 Hz, 2H), 4.69 (brs, 1H), 4.80 (brs, 1H), 7.36 (d, J = 8.0 Hz, 2H), 7.80 (d, J = 8.0 Hz, 2H). ESI-MS m/z: 258$[M+NH_4]^+$.

Synthesis of 3-Methyl-3-butenyl diphosphate (Isopentenyl pyrophosphate) (3): Tris(tetra-n-butylammonium) hydrogen pyrophosphate (3.25 g, 3.6 mmol) in 3.5 mL of acetonitrile was added to 3-methyl-3-buten-1-yl tosylate (2) (288 mg, 1.20 mmol), and the resulting solution was allowed to stir for 2 hours. The resulting material was converted to the ammonium form with 30 equivalents of DOWEX AG 50W-X8 cation exchange resin (100-200 mesh). After lyophilization the resulting powder was dissolved in 3 mL of 0.1 M ammonium bicarbonate extracted twice with 7 mL of 1:1 (v/v) acetonitrile/isopropyl alcohol. Flash chromatography on a 3.5 cm X 15 cm cellulose column (4.5:2.5:3 (v/v/v) isopropyl alcohol/acetonitrile/0.1 M ammonium bicarbonate) yielded 59 mg (20% yield) of a white solid. ^{1}H-NMR (300 MHz, D_2O): δ 1.67 (s, 3H), 2.29 (t, 2H, J = 6.3 Hz), 3.96 (qd, J = 6.6, 2.3 Hz, 2H), 4.70-4.85 (m, 2H); ^{31}P-NMR (32 MHz, D_2O): δ -10.41 (d, J = 20.1 Hz, 1P), -7.54 (d, J = 20.1 Hz, 1P). ESI-MS m/z: 247.4 $[M+H]^+$.

2.5 Supplemental Information

2.5.1 Plasmids maps provided by Dr. Marcus Lee

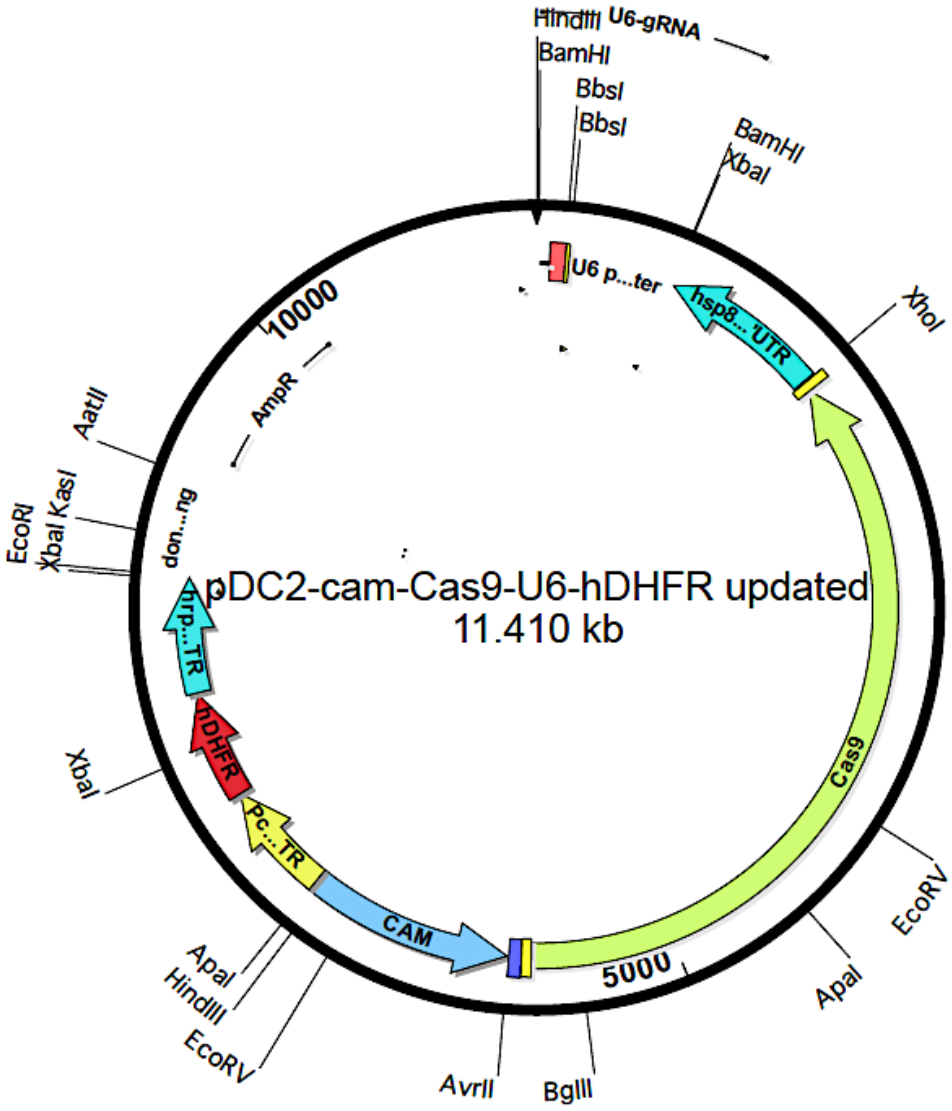

Figure 2.12: ***Plasmid map of pDC2-gRNA-Cas9.*** *This plasmid carries the Cas9 endonuclease, U6-gRNA and a hDHFR selectable marker. The U6-gRNA cassette can be modified to include a 20-nucleotide gRNA sequence that targets gene of interest.*

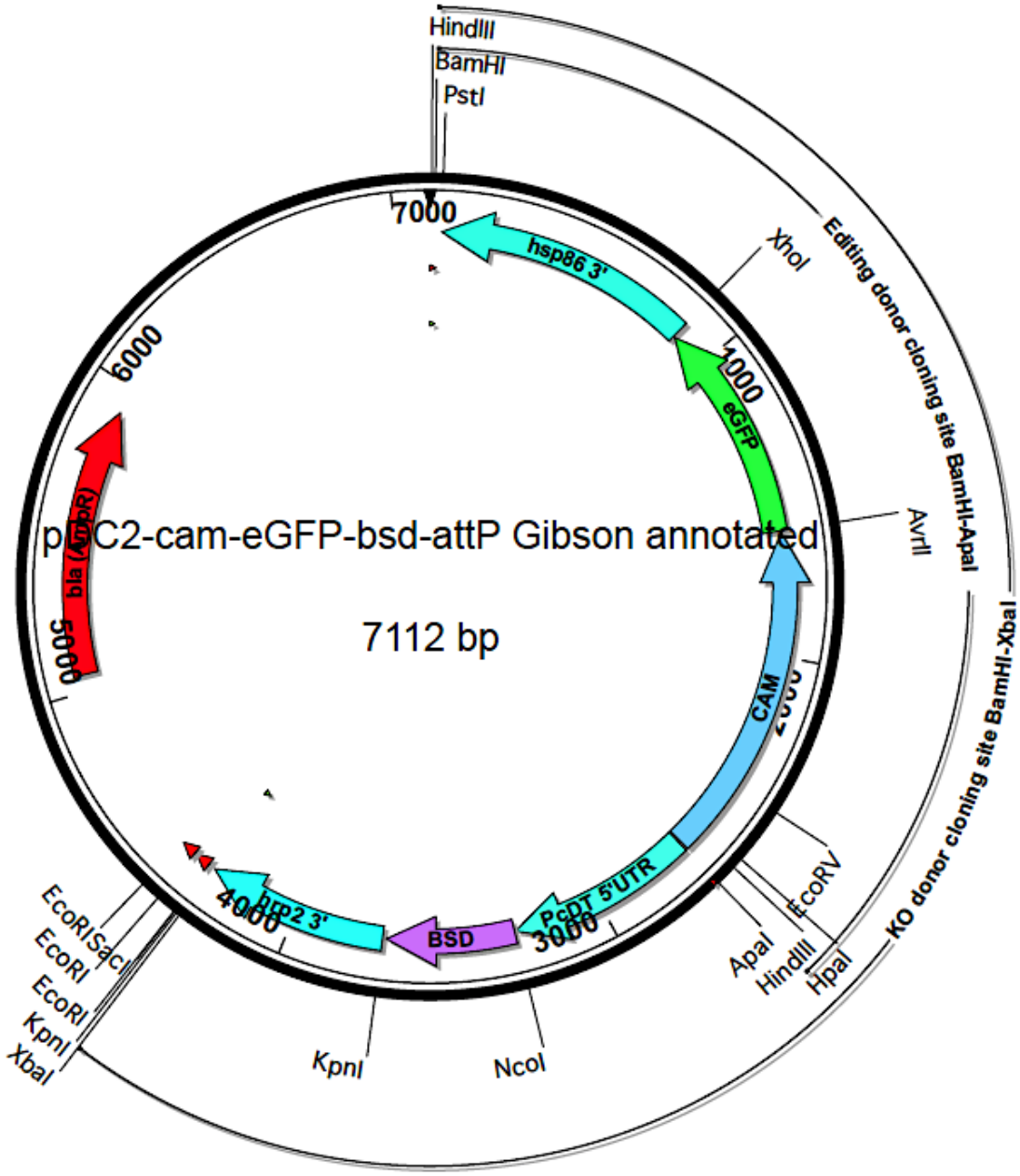

Figure 2.13: ***Plasmid map of pDC2-donor-bsd.*** *This plasmid carries the BSD selectable marker. The donor template shown here as eGFP can be easily modified to include other templates of interest.*

2.5.2 Whole genome sequences analysis workflow

GATK Best Practices workflow was designed to perform variant discovery analysis in high-throughput sequencing data [114, 115]. The workflow was modified here for the study of *Plasmodium falciparum* genome. The reference genome used in this workflow was *Pf*3D7v9 (https://plasmodb.org/common/downloads/release-9.0/Pfalciparum3D7/).

Below are the scripts used in the analysis of Dd2 and Dd2ΔGyrA clones in this study:

Trim Sequences (Tool: TrimGalore)

```
</path/to/TRIMGALORE> --quality 28 --fastqc --gzip --length 70 --paired --
   path_to_cutadapt </path/to/cutadapt> FileToWorkOn[1] FilesToWorkOn[2] --
   output_dir </path/to/output/directory>
```

Map to Reference (Tool: BWA-MEM)

```
</path/to/BWA> mem -t 1 -M -k 20 -w 105 -d 105 -r 1.4 -c 12000 -A 1 -B 4 -O
   6 -E 1 -L 5 -U 9 -R '@RG\\tID:<barcode>\\tCN:UW\\tDT:<Current date>\\tLB
   :<SampleName>\\tPL:ILLUMINA\\tPU:<barcode>\\tSM:<SampleName>\\tDS:<
   FilesToWorkOn[1]> and <FilesToWorkOn[2]>' </path/to/ReferenceGenome> <
   FilesToWorkOn[1]> <FilesToWorkOn[2]> | </path/to/PICARD
   SamFormatConverter COMPRESSION_LEVEL=5 I=/dev/stdin O= <OutPutFileName>
```

Sort Reads (Tool: SortSam)

```
</path/to/PICARD> SortSam I= <FilesToWorkOn> OUTPUT= <OutPutFile> SORT_ORDER
   =coordinate CREATE_MD5_FILE=false CREATE_INDEX=false MAX_RECORDS_IN_RAM
   =500000 QUIET=false COMPRESSION_LEVEL=5 TMP_DIR= </path/to/temp/
   directory>
```

Mark Duplicates (Tool: MarkDuplicates)

```
</path/to/PICARD> MarkDuplicates I= <FilesToWorkOn> OUTPUT= <OutPutFile>
   METRICS_FILE= <path/to/Metrics/output/file.duplicate_metrics.txt> AS=
   true CREATE_MD5_FILE=false CREATE_INDEX=true
   OPTICAL_DUPLICATE_PIXEL_DISTANCE=100 QUIET=false PROGRAM_RECORD_ID=null
   TMP_DIR= </path/to/temp/directory> REMOVE_DUPLICATES=false
   COMPRESSION_LEVEL=5
```

Estimate Indel Sites (Tool: RealignerTargetCreator)

```
java -d64 -Xmx3G -jar </path/to/GATK> -T RealignerTargetCreator -nt 1 -I <
   FilesToWorkOn> --maxIntervalSize 500 --minReadsAtLocus 4 --
   mismatchFraction 0.0 --windowSize 10 -R <path/to/ReferenceGenome> -o <
   OutPutFile>
```

Realign around Indel Sites (Tool: IndelRealigner)

```
java -d64 -Xmx3G -jar </path/to/GATK> -T IndelRealigner --knownAlleles </
   path/to/DBSNP> --entropyThreshold 0.10 --maxConsensuses 30 --
   maxIsizeForMovement 2000 --maxPositionalMoveAllowed 175 --
   maxReadsForConsensuses 120 --maxReadsForRealignment 25000 --
   maxReadsInMemory 150000 -I <FilesToWorkOn> -R /path/to/ReferenceGenome> -
   targetIntervals </path/to/ouputfile/from/last/command> -o <OutPutFile>
```

Base (Quality Score) Recalibration (Tool: BaseRecalibrator)

```
java -d64 -Xmx3G -jar </path/to/GATK> -T BaseRecalibrator -nct 1 -R <path/to
   /ReferenceGenome> -knownSites </path/to/DBSNP> -rf BadCigar -cov
   CycleCovariate -cov ContextCovariate --deletions_default_quality 45 --
   indels_context_size 3 --insertions_default_quality 45 --low_quality_tail
    3 --maximum_cycle_value 500 --mismatches_context_size 2 --
```

```
   mismatches_default_quality -1 -I <FilesToWorkOn> --quantizing_levels 16
   --out <OutPutFile>
```

Print Recalibrated Scores (Tool: PrintReads)

```
java -d64 -Xmx3G -jar </path/to/GATK> -T PrintReads -R <path/to/
   ReferenceGenome> -I <FilesToWorkOn> -o <OutPutFile> -BQSR </path/to/
   outputfile/from/previous/command>
```

Extract Coverage Information (Tool: SamTools)

```
</path/to/SamTools/samtools-1.2/samtools> mpileup -r <LocationOfInterest> <
   FilesToWorkOn> -o <Output.csv>
```

2.5.3 Plotting Coverage Data with Python Libraries

Pandas is an easy-to-use data structures and data analysis tools for the Python programming language [117]. Coverage data for Dd2 and Dd2ΔGyrA clones were analyzed with *Pandas* and plotted with *Matplotlib* [118]. Codes were implemented at an interactive computing platform, The Jupyter Notebook. Each genome (apicoplast, mitochondrial and nuclear) was plotted as independent plot.

Import Python Libraries and Coverage Files

```
import matplotlib
import matplotlib.pyplot as plt
import pandas as pd
import math
df1 = pd.read.csv('</path/to/Dd2_coverage/file.csv>', names = ['Chr','
   Position','a','Coverage','b','c'], delimeter='\t')
df2 = df1 = pd.read.csv('</path/to/Dd2_GyrAKO_coverage/file.csv>', names =
   ['Chr','Position','a','Coverage','b','c'], delimeter='\t')
```

Define Window Size and Scale

```
df1['Coverage_MA'] = df1['Coverage'].rolling(window=500).mean()
df2['Coverage_MA'] = df2['Coverage'].rolling(window=500).mean()
df1['Coverage_new'] = df1['Coverage_MA'].apply(math.log10)
df2['Coverage_new'] = df2['Coverage_MA'].apply(math.log10)
df1['Position_new'] = df1['Position']/1000
df2['Position_new'] = df2['Position']/1000
```

Create the Plot

```
fig1 = plt.figure(figsize=(14, 7), dpi=500)
ax1 = fig1.add_subplot(2,1,1)
plt.plot(df1['Position_new'],df1['Coverage_new'],'b', df2['Position_new'],
   df2['Coverage_new'], 'r', linewidth=2)
ax1.set_yscale("linear", nonposy='clip')
ax1.set_xlabel('Length (kb)',size=20)
ax1.set_ylabel('Coverage ($10^x$)',size=20)
ax1.set_ylim(-0.5, 4.5)
ax1.legend(['Dd2', 'Dd2$\Delta$GyrA'],bbox_to_anchor=(0.1, 0.4, 0.9, 0.8),
   fontsize = 'xx-large',loc=1, ncol=2, borderaxespad=0.)
ax1.yaxis.set_minor_locator(plt.NullLocator())
ax1.tick_params(axis = 'both', which = 'major', labelsize = 20)
ax1.set_title('<title_of_the_graph>', position=(0.87, 0.8), size = 20)
plt.savefig('<name_of_the_plot.png>')
```

Chapter 3

Validation of point mutations that lead to BMS-388891 resistance in malaria parasites

3.1 Introduction

Recent improvements in sequencing and gene-editing technology have advanced our understanding of mutations that confer resistance to different antimalarials. In this chapter, we will explore the resistance mechanism of protein farnesyltransferase (PFT) inhibitors, BMS-388891 compound.

Isoprene is a five-carbon unit that constitutes the basic building block of isoprenoids. Prenyl groups are a subset of isoprenoids and are found on a variety of biological structures, including proteins. Prenylated proteins or peptides arise from the post-translational attachment of a 15-carbon farnesyl or a 20-carbon geranyl group to the C-termini of a specific set of proteins. PFT catalyzes the transfer of the 15-carbon farnesyl group while protein geranylgeranyltransferase-I (PGGT-I) catalyzes the transfer of the 20-carbon geranyl group. Previous reports have shown that blood-stage *Plasmodium falciparum* contains PFT activity and the complete genome sequences of parasites reveal the absence of PGGT-I activity [119, 120]. The lack of PGGT-I enzyme in *P. falciparum* suggests that inhibition by the PFT inhibitors will be highly toxic to parasites since vital proteins that are normally geranylgeranylated by PGGT-I and farnesylated by PFT in mammalian cells are likely to be

farnesylated by *Pf*PFT in *P. falciparum*.

PFT inhibitors (PFTIs) have been developed by the pharmaceutical industry because of their anti-cancer properties [121–123]. Ras proteins play a pivotal role in the transduction of cell-growth-stimulating signals, and mutation of the *ras* gene leads to constant activation of the protein, ultimately resulting in uncontrolled cell proliferation [124]. The high prevalence of mutated *ras* genes, found in 30% of all human cancers, makes this pathway an attractive target for anticancer drug development [125]. To become functionally active, the Ras protein has to undergo several post-translational modifications. The first step in this process is the farnesylation of the C-terminal cysteine by PFT in order to activate the Ras protein. By inhibition of Ras farnesyltransferase, a blockade of the signal transduction pathway is accomplished with cessation of cell growth [126–128]. Thus it was predicted and proven that PFTIs would be effective therapeutic agents in the treatment of cancer.

Several inhibitors of the PFT enzyme were developed following rational design strategies, as well as on screening of combinatorial libraries [129, 130]. Four companies (Janssen/Johnson & Johnson, Schering-Plough, Merck, and Bristol-Myers Squibb) have entered clinical trials for the development of PFTIs as a cancer chemotherapuetic agent [131–136]. Because of strong interest in the development of PFTIs for the treatment of cancer, there is a wealth of pharmocologic information about PFTIs. This pharmacologic information, the lack of toxicity and a rich source of small molecule PFTI libraries provide an excellent opportunity for the "piggy-back" investigation of PFTIs for the treatment of malaria. Previous work has demonstrated the development of low nanomolar concentrations of tetrahydroquinolones (THQ)-based PFTIs based on these available resources. These inhibitors are cytotoxic to parasites both *in vitro* and *in vivo* [137]. Among those, BMS-388891 compound (Figure 3.1) showed promising efficacy with IC_{50} (dose that inhibits 50% of *Pf*PFT enzyme activity) of 0.6 nM and ED_{50} (dose that inhibits 50% of *P. falciparum* growth) of 7 nM. The *P. falciparum* resistance to BMS-388891 compound was investigated and results have shown that resistant parasites carried a single point mutation on either subunits of *Pf*PFT enzymes [17, 138].

Biochemical assays of the purified *Pf*PFT enzyme indicated that point mutations affect both the enzyme affinity for the peptide substrate and the inhibitor, which likely contribute to the drug-resistance phenotype. Altogether, these results support that *Pf*PFT is the target of the tetrahydroquinolone compounds.

Although results look promising that a single point mutation on the *Pf*PFT enzyme (either on the PFT-α-subunit or PFT-β-subunit) led to BMS-388891 resistant parasites as shown in Table 3.1, whole genome sequencing on those mutants are yet to be done. Identification of point mutation was done through targeted sequencing of both *Pfpft-α-subunit* and *Pfpft-β-subunit* of those resistant mutants. Hence, we could not draw a conclusion and eliminate the possibility that other mutations might have occurred elsewhere in the genome and contributed to the resistance phenotype. Considering advancements in whole genome sequencing this past decade, we hope to revisit this experiment and utilize both whole genome sequencing and CRISPR/Cas9 gene-editing tool to prove that a single point mutation on the *Pf*PFT enzyme is sufficient for parasites to confer resistance to BMS-388891 compound.

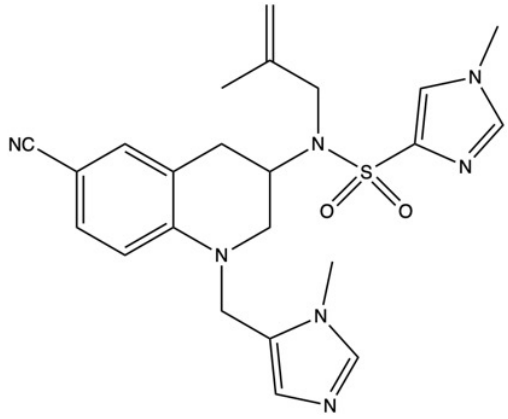

Figure 3.1: ***BMS-388891 compound***

Variant	Mutation	Sequenced "Clones"	Fold resistant
1	α D308Y	10	10
2	none	9	0.5-20
3	β Y837C*,**	3	5-10
4	α N315Y*,**	2	10
5	β Y837S	1	10
6	β G612A**	1	>10
7	β Q774R + Q902H**	1	>10
8	β Q774R + Y837S	1	unknown
9	Pft beta amplification ***	1+	10

* Observed in multiple experiments
** Identified by Richard Eastman
*** Nimblegen and spot array (Rapatbhorn Patraputrich)

Table 3.1: *BMS-388891 mutants selected by John White and Richard Eastman*

3.2 Results

3.2.1 Resistance selection studies of BMS-388891

(*Experiments in this section were conducted by Dr. John White and Jordan Rixon*)

Previous studies have shown that *P. falciparum* clone Dd2 was sensitive to growth inhibition by BMS-388891 with an EC_{50} of 10 nM [17, 138]. To replicate the experiment, a new set of selection experiments as shown in Figure 3.2 were carried out. Freshly thawed Dd2 clone was first diluted to 10 parasitized red blood cells (pRBCs), with a total of 10 independent flasks. This step was done to ensure that the experiment started with parasites from similar genetic background. Parasites were then monitored from day 10-14. When there were $>10^7$ pRBCs/flask, each flask were split into two; one flask was then challenged with 100 nM BMS-388891 while the other flask was treated with DMSO. These DMSO treated flasks act as control to make sure parasites are able to grow well and also as a parental reference when analyzing its corresponding mutant in the downstream assay. In cultures treated with 100 nM BMS-388891, 2 out of 10 flasks were positive for parasites at day 21. After at least 30 days of continuous culturing, remaining flasks challenged with 100 nM BMS-388891 remained negative for parasites. Clonal parasites were derived from each of the two 100 nM BMS-388891 treated flasks where outgrowth occurred. Three clones were isolated from each independent resistant mutant and further characterized by drug-sensitivity assays and whole genome sequencing.

Resistant clones obtained from two independent BMS selection experiments showed an increase in EC_{50} values when compared to the parental Dd2 clone, which has an EC_{50} of 6 nM (consistent with previously reported values). Clonal resistant mutants isolated from mutant 1 (1B11, 1F02 and 1E04) have EC_{50} values at around 220-250 nM, a 40-fold increase in resistance; while clonal resistant mutants isolated from mutant 2 (2D11, 2E05 and 2G06) have EC_{50} values at around 250-300 nM, a 40- to 50-fold increase in resistance to the BMS-388891 compound (Figure 3.3).

In previous publications, the basis of resistance was identified through sequencing of both the *Pfpft-α-subunit* and *Pfpft-β-subunit* of the resistant mutants. This method had successfully determined different point mutations on either *Pf*PFT genes that confer resistance to BMS-388891 compound. However, this method does not allow us to further understand the possibility of other mutations at other parts of the genome that might have contributed to the resistance mechanism. Hence whole genome sequencing was carried out on the resistant clones isolated from this experiment. Through whole genome sequencing, clones 1B11, 1F02 and 1E04 were found to carry a missense mutation (Ser603Arg) on *Pfpft-β-subunit* and 5 other mutations in repeats intergenic region. On the other hand, clones 2D11, 2E05 and 2G06) were found to carry a missense mutation (Tyr837Asn) on *Pfpft-β-subunit* and either six (3971-3976bp) or three (3974-3976bp) nucleotides in-frame deletion on a Ubiqutin-like protein (PF3D7_0922100). Although the result observed was consistent with previous publications where resistant mutants established a point mutation on either *Pf*PFT genes, other mutations on other parts of the genome were present as well. This result opens up debate on whether the point mutation on the *Pf*PFT genes is the sole contributor of the BMS-388891 resistance mechanism.

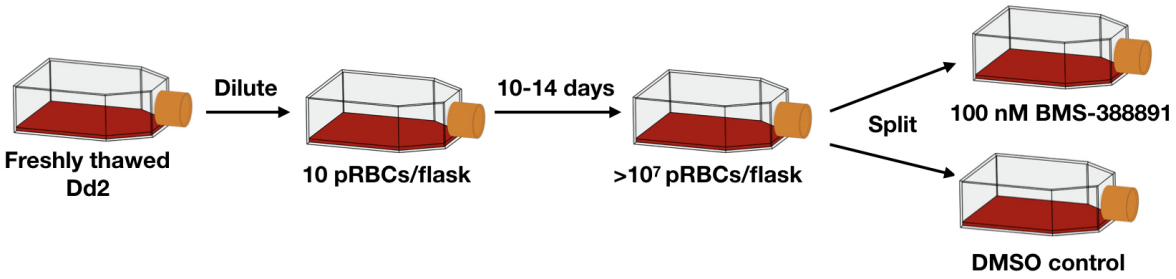

Figure 3.2: ***Selection scheme of BMS-388891 compound.*** *Freshly thawed Dd2 clones were diluted to 10 pRBCs/flask and allowed to proliferate for 10-14 days. When parasite density in each flask was greater than 10^7, each flask was split into two. One set of flasks were challenged with 100 nM BMS-388891 while the corresponding set of flasks were treated with DMSO and act as the control.*

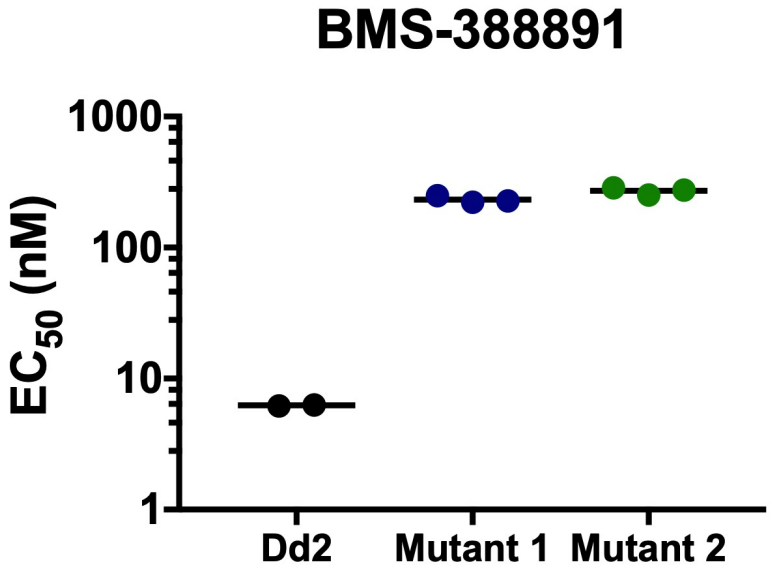

Figure 3.3: ***EC_{50} of BMS-388891 mutants.*** *Parental Dd2 clones showed higher sensitivity with EC_{50} values of approximately 10 nM. BMS-388891 resistant mutants showed a lower sensitivity to the compound with EC_{50} values at around 220-300 nM.*

3.2.2 Gene alteration of *Pfpft-β*-subunit

Since whole genome sequencing results identified other mutations present in the background of the clonal BMS-388891 mutants, a single-base gene alteration experiment was performed to prove that a particular single point mutation on either *Pf*PFT genes is sufficient for parasites to confer resistance to BMS-388891 compound. The missense mutation on amino acid 837 of *Pfpft-β-subunit* appeared multiple times in previous experiment (Table 3.1) as well as the current experiment (Y837N). Hence, gene alteration of amino acid 837 on *Pf*PFT-β-subunit was done using the CRISPR/Cas9 tool utilizing the two plasmid system; a Cas9-gRNA plasmid and a donor plasmid. The homology region on the donor plasmid consists of a desired point mutation of either BMS-388891 mutant (Y837N/Y837S/Y837C) or the silent mutation that acts as a control (Y837*). Some silent mutations on the gRNA binding regions and the PAM sequence (Figure 3.4) were also included to prevent binding of the Cas9 nuclease to the homology region on the donor plasmid or the modified gene in parasites.

Four different pDC2-donor-bsd plasmids (pDC2-Y837*-control, pDC2-Y837N-mutant, pDC2-Y837S-mutant, and pDC2-Y837C-mutant) that carry different desired point mutations were constructed. Each set of gRNA-Cas9 and the donor plasmid were electroporated into parental Dd2 laboratory clone, respectively. At 48 hours post-transfection, parasites were maintained with WR99210 and Blasticidin for six days, followed by culturing in the drug-free media. Parasites were observed microscopically between 21-24 days post-transfection in most of the flasks. Genomic DNA was extracted from each positive clone for downstream confirmation assays. Full-length *Pf*PFT-β-subunit was amplified from each clone and sent for sequencing to confirm the insertion of point mutations. As shown in Figure 3.5, the sequence of the non-transfected Dd2 clone was identical to the reference sequence provided. For the modified clones, the sequences surrounding the cut site were identical to the template provided in the donor plasmids, with the desired mutation (either control or mutants) and all the adjacent silent mutations.

To confirm that these CRISPR-induced mutations on *Pf*PFT-β-subunit confer resistance

to BMS-388891 compound, 72-hours drug sensitivity assays were performed. The EC_{50} of BMS-388891 compound on the non-modified (Dd2) and modified-control (Dd2-Y837*) clones were around 10-18 nM; whereas the modified-mutants (Dd2-Y837N, Dd2-Y837S, Dd2-Y837C) clones showed 10-20 fold increase in resistance (Figure 3.6). Since there was no change in sensitivity to BMS-388891 compound between Dd2 and Dd2-Y837*, the modification made on the *Pfpft-β-subunit* region was not harmful to parasites. The increase in resistance of Dd2-Y837N, Dd2-Y837S and Dd2-Y837C to BMS-388891 compound was consistent with the previously acquired data on parasites that spontaneously adopted these mutations while under drug selection pressure in culture. Hence this result confirms that a single point mutation on the *Pf*PFT gene is sufficient for parasites to confer resistance to BMS-388891 compound.

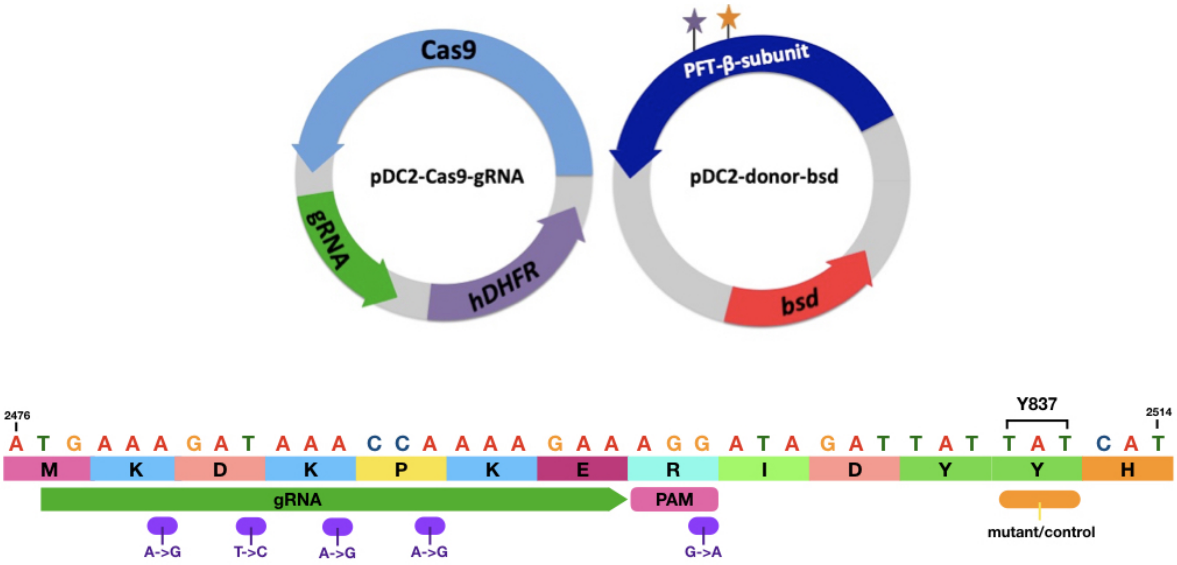

Figure 3.4: ***Experimental Design.*** *pDC2-Cas9-gRNA plasmid carries the gRNA sequence targeting the Pfpft-β-subunit. pDC2-donor-bsd plasmid carries the homology region of the Pfpft-β-subunit along with some silent mutations and the desired point mutation. The snippet of the sequence shown is part of the Pfpft-β-subunit gene from the donor plasmid. The purple annotations are silent mutations on the gRNA binding region and the PAM sequence while the orange annotation is the desired point mutation.*

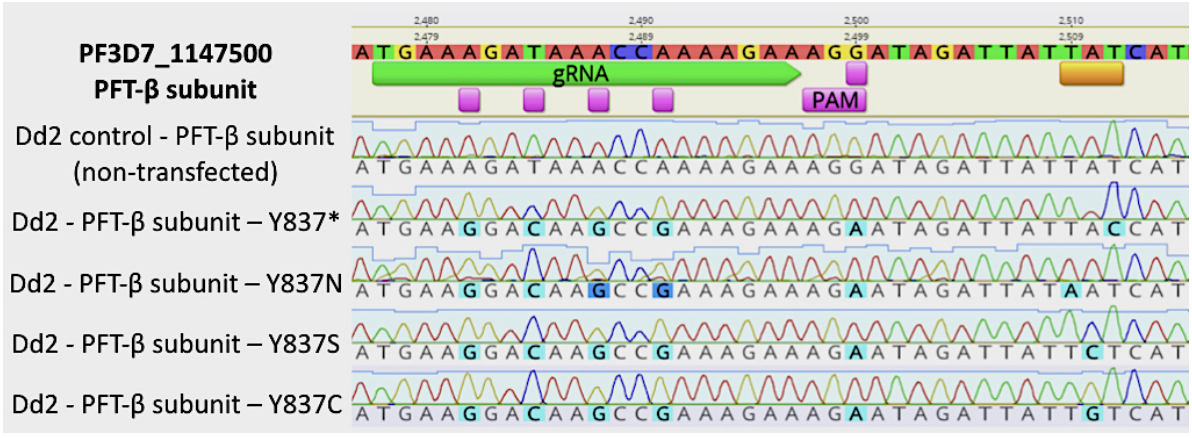

Figure 3.5: ***Gene alteration confirmation.*** *The sequence of the non-transfected Dd2 clone was identical to the reference sequence; the sequences of modified clones include the desired mutation (control or mutants) as well as all the adjacent silent mutations.*

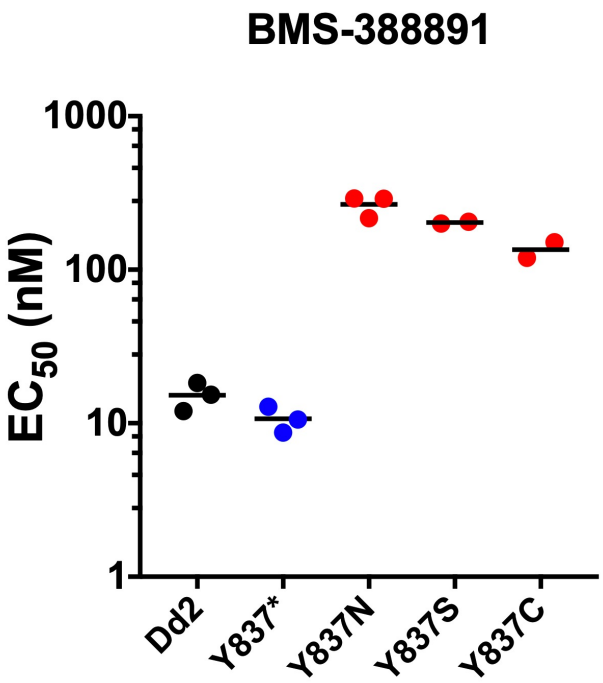

Figure 3.6: ***BMS-388891 sensitivity assays.*** *Non-modified (Dd2) and modified-control (Dd2-Y837*) clones showed similar sensitivity to BMS-388891 compound. All modified-mutants (Dd2-Y837N, Dd2-Y837S, and Dd2-Y837C) clones showed 10-20 fold increase in resistance.*

3.3 Discussion

Protein farnesyltransferase is known to be an essential enzyme in malaria parasites. Previous studies have illustrated that this enzyme is the target of the tetrahydroquinolone compounds and that selection studies have led to the findings of point mutations on either *Pf*PFT subunits [17, 138]. Although it is known through enzymatic assays that the BMS-388891 compound inhibits growth of parasites through binding of the compound on the enzymatic pocket of *Pf*PFT, it does not exclude the possibility that additional genes do not play a role in modulating the level of resistance [138, 139].

Selection assays in the Rathod lab have been optimized since the earlier selections done on the BMS-388891 compound. Studies on the frequencies of resistance to BMS-388891 indicated that 10^7 initial pRBCs resulted in a reproducible, low number of genetic mutation events per population. Similar to previous findings, resistance was associated with single point mutations in the target enzyme, protein farnesyltransferase. However, whole genome sequencing of the mutants revealed that other mutations were present in other parts of their genomes. The discovery of other mutations suggested that those might have also contributed to the increase resistance observed in the drug-sensitivity assay.

Gene alteration experiment using CRISPR/Cas9 tool has successfully confirmed for the first time that a single point mutation on the *Pfpft-β-subunit* is sufficient for parasites to confer resistance to BMS-388891 compound. The CRISPR-modified mutant parasites showed a 10-20 fold increase in resistance to BMS-388891. The increase in resistance of the modified parasites (10-20 fold) is lower than the drug-selected mutants (40-50 fold). This might suggest that although the point mutation itself is sufficient for parasites to confer resistance, other mutations contribute to higher level resistance to BMS-388891 compound. This can be determined through further modification of the CRISPR-mutants to carry additional mutation(s) identified from whole genome sequencing.

In conclusion, the emergence of resistance to various antimalarial compounds continues to be a significant challenge in finding efficient antimalarial drugs. The use of CRISPR/Cas9

gene alteration technique enables us to confirm the association of a point mutation to resistance. We conclude that a single point mutation on the *Pfpft* gene is sufficient for parasites to confer resistance to BMS-388891 compound. The combination of our systematic research techniques (drug selection, genome sequencing and gene-editing) will enable us to identify targets of inhibitors and/or non-target based resistance mechanisms. Better understanding of the target-inhibitor relationship may enable us to rationally design small molecules with improved drug-like properties and additional interactions that should reduce the propensity for resistance while maintaining selectivity.

3.4 Methods

3.4.1 Parasite cultures and selection experiment

Parasites were cultivated using established methods with some changes [108, 109]. Cultures of *Plasmodium falciparum* clone Dd2 were grown *in vitro* at 37°C in solutions of 2% hematocrit (serotype A positive human erythrocyte) in RPMI-1640 medium (Invitrogen) containing L-Glutamine and 25mM HEPES, and supplemented with 0.5% Albumax I and 0.1 g/L Hypoxanthine (ThermoFisher). Cultures were maintained in sterile, sealed flasks, flushed with blood gas mixture (5% CO_2, 5% O_2 and 90% N_2). Dd2 clone was diluted to 10 parasites in 7 independent flasks. Parasites were allowed to proliferate for about 10-14 days until each flask has parasite density of about 10^7. Each flask was then split into two, with one set of flasks challenged with 100 nM BMS-388891; while the other set of flasks were diluted to 10 parasites per flask and treated with DMSO. The 10 parasites, DMSO treated flasks act as positive controls to determine growth rates and evaluate the quality of blood products used in culture. The media was changed every other day while maintaining the initial drug concentration. Cultures were split 1:2 every two weeks and replenished with fresh RBCs. Parasites proliferation was monitored by Giemsa-stained thin blood smear. Clonal isolates of BMS-388891 resistant mutants were generated by limiting dilutions on a 96-well plate [112].

3.4.2 Whole genome sequencing

Clonal parasites were synchronized with 5% sorbitol for at least two continuous cycles [110]. RBCs containing highly synchronized parasites ($>$ 90% rings, 3% parasitemia) were lysed using saponin. DNA was then extracted from each clone using Qiagen DNA Mini Kit according to the manufacturer's instructions. Illumina compatible libraries were generated from 50 ng genomic DNA using Nextera DNA Sample Prep Kit (Epicenter Technologies) according to the manufacturer's instructions with two exceptions as described previously [19]. The bridge PCR step was limited to 5 cycles and the extension step was done at 65°C. Samples

were dual indexed and library fragments of 360 to 540 bp were isolated using a 5XT DNA 750 LabChip XT system (Caliper Life Sciences). Sequence ready fragments were enriched by limited cycle PCR using other sequencing adapters (6 cycles of 95^{o}C for 10 sec, 58^{o}C for 30 sec, 60^{o}C for 6 minutes). Prepared DNA libraries samples were sent for paired-end sequencing at the Northwest Genomics Center. The resulting FASTQ files with paired-end reads were processed to generate Variant Calling File (VCF) with steps as described in Section 2.4.5. SNPs were detected from the VCF by comparing the mutant clones to the parental clone.

3.4.3 Plasmids construction

The plasmid pDC2-gRNA-Cas9 was modified to include a 20 nucleotides gRNA sequence (TGAAAGATAAACCAAAAGAA) targeting *Pfpft-β-subunit*. The gRNA construct was designed using the CRISPR tool on the Geneious software. The gRNA selected has an on-target score of 0.30 and an off-target score of 100%. gRNA-Oligo 1 and gRNA-Oligo 2 were annealed and cloned into the the BbsI-digested pDC2-gRNA-Cas9 plasmid as discussed in section 2.4.1. The plasmid pDC2-donor-bsd was modified to carry a homologous region of *Pfpft-β-subunit* (PlasmoDB ID: PF3D7_1147500) with the desired point mutation that confer resistance and some silent mutations on the gRNA binding region. The homologous region of length 649bp starts from nucleotide +2124 of the PFT-β-subunit. Primers Y837N-F-1/Y837N-R-1 were used to amplify the half of the homologous region while primers Y837N-F-2/Y837N-R-2 were used to amplify the other half. The amplified fragments were then assembled into a single piece that carries HindIII restriction sites on both the 5' and 3' ends. The final assembled PCR construct was then digested with HindIII restriction enzymes and ligated into the HindIII-digested pDC2-donor-bsd plasmid to give the pDC2-Y837N-mutant plasmid. The pDC2-Y837*-control plasmid was constructed using the same process as discussed with the exception of using Y837N-R-1(C) and Y837N-F-2(C) primers during the fragment amplification step. Four silent mutations on the gRNA binding regions were introduced one at a time to both pDC2-Y837N-mutant and pDC2-Y837-control plasmids

using QuikChangeII Site-Directed Mutagenesis Kit (Agilent Technologies) with the primers Y837-Mut1-F/Y837-Mut1-R, Y837-Mut2-F/Y837-Mut2-R, Y837-Mut3-F/Y837-Mut3-R, and Y837-Mut4-F/Y837-Mut4-R primers as shown in Table 3.2. pDC2-Y837S-mutant plasmid was constructed by introducing point mutations on the PFT-β-subunit homology region on the pDC2-Y837N-mutant plasmid using the primer set Y837S-F/Y837S-R with the site-directed mutagenesis kit. pDC2-Y837C-mutant plasmid was constructed using the same method as the construction of pDC2-Y837S-mutant plasmid with the exception of using Y837C-F/Y837C-R primer set.

3.4.4 Transfection

Transfections of pDC2-gRNA-Cas9 and pDC2-mutant or control plasmids into Dd2 clones were carried out as discussed in section 2.4.2. Selection pressure (2.5 nM WR99210 and 2 μg/μl Blasticidin) was applied to each flask at 48 hours post-transfection. Media supplemented with selection pressure was renewed every day for 6 days. Selection pressure was removed on day-8 post-transfection and parasites proliferation was monitored by Giemsa-stained thin smeared blood samples taken at each media change, three times a week.

3.4.5 Confirmation of point mutation insertions

Parasite pellets from the modified parasites ($\sim$ 2-3% parasitemia) were lysed using 0.15% saponin solution. Genomic DNA was then extracted using Qiagen DNA Mini Kit according to the manufacturer's instructions. 50 ng of genomic DNA was used in the PCR reaction to amplify the full length *Pfpft-β-subunit* using primer set P5/P6. 10 μl of the PCR products were then mixed with 5 μl of EXO-SAP-IT PCR cleanup reagent and incubated at 37^{o}C for 15 minutes. The mixture was then heat inactivated at 80^{o}C for 15 minutes. The cleanup-up PCR product was then sent to Eurofins Genomics for sequencing using primer P6. The sequences received from Eurofins Genomics were mapped to the *Pf*PFT-β-subunit reference sequence using the "Assemble" tool on Geneious.

Primers	**Sequence**
gRNA-Oligo 1	ATTGTGAAAGATAAACCAAAAGAA
gRNA-Oligo 2	AAACTTCTTTTGGTTTATCTTTCA
Y837N-F-1	TAGAATACTCAAGCTGGATTATTCAAAATCACATGAAT
Y837N-R-1	CGTATGATTATAATCTATTCTTTCTT
Y837N-F-2	AAGAAAGAATAGATTATAATCATACG
Y837N-R-2	TAATAATTATAAGCTTCATTCTTGTAGTAACCTTTTTA
Y837N-R-1 (C)	CGTATGGTAATAATCTATTCTTTCTT
Y837N-F-2 (C)	AAGAAAGAATAGATTATTACCATACG
Y837-Mut1-F	GGAATGAAAGATAAGCCAAAAGAAAGAAT
Y837-Mut1-R	ATTCTTTCTTTTGGCTTATCTTTCATTCC
Y837-Mut2-F	AAGGAGGAATGAAGGATAAGCCAAAAG
Y837-Mut2-R	CTTTTGGCTTATCCTTCATTCCTCCTT
Y837-Mut3-F	GAGGAATGAAGGACAAGCCAAAAGAAA
Y837-Mut3-R	TTTCTTTTGGCTTGTCCTTCATTCCTC
Y837-Mut4-F	TGAAGGACAAGCCGAAAGAAAGAATAG
Y837N-Mut4-R	CTATTCTTTCTTTCGGCTTGTCCTTCA
Y837C-F	AGAATAGATTATTGTCATACGTGTTATGC
Y837C-R	GCATAACACGTATGACAATAATCTATTCT
Y837S-F	AGAATAGATTATTCTCATACGTGTTATGC
Y837S-R	GCATAACACGTATGAGAATAATCTATTCT

Table 3.2: *List of primers for plasmids construction used in PfPFT-β-subunit mutations validation experiment.*

Primers	**Sequence**
P5	ATGGAAAAAAATGATTCGTATTTATT
P6	TCATTCTTGTAGTAACCTTTTTAAAT

Table 3.3: *List of primers for point mutations confirmation*

3.4.6 BMS-388891 sensitivity assay

Drug sensitivity assays were performed in 96-well plates containing parasite solution of either the parental clone, BMS-388891 resistant clones, or modified parasites at 0.5% parasitemia and 0.5% hematocrit. A range of concentrations of BMS-388891 (from 2000 - 0.122 nM) were added to the parasites. In order to minimize DMSO concentrations in parasite cultures, 200x BMS-388891 concentrations (in 100% DMSO) were first diluted 1:20 into RPMI (final 5% DMSO) before being diluted further into the parasite-containing wells (final 0.5% DMSO). Each concentration was tested in triplicate and compared to solvent-only controls. After incubating for $\sim$ 72 hours, parasitized red blood cells were stained using SYBR Green I for 20 minutes and counted by flow cytometry (BD Accuri C6). Parasite proliferation in each well was expressed as a percentage of the solvent control. EC_{50} was determined using GraphPad PRISM software.

Chapter 4

Understanding mechanisms of mutagenesis

4.1 Introduction to mutagenesis

As discussed in Chapter 1.1, the emergence of drug resistance to various antimalarial drugs is a continuing public health concern. Drug resistance can occur through many types of phenomena; however the most common mechanisms involve gene amplifications or point mutations [4, 18, 19, 140, 141]. The Rathod lab has developed a systematic approach to characterize mechanisms that drive genetic change when the parasite is exposed to metabolic stress [142]. For example, *Rathod et. al.* demonstrated through *in vitro* selection that parasites acquire resistance to tetrahydroquinoline compounds through point mutations rather than larger genomic rearrangments [17, 138]. In other inhibitor selection outcomes, parasites acquired resistance through target gene amplification with no other nucleotide sequence changes in the locus. Amplification-based resistance was observed in parasites selected with compounds DSM1 or 1843U89, which target dihydroorotate dehydrogenase (DHODH) and thymidylate synthase (TS), respectively [19].

While it is known that amplification and point mutation are the possible outcomes of a selection for resistance, the order of the processes are less understood. Under lethal drug pressure, transcriptional and translational responses are not significantly up- or down-regulated in *P. falciparum*. Therefore, we propose parasites resort to rapid changes in the

genomic DNA in order to survive under metabolic stress [143]. In a model proposed by *Guler et. al.* as shown in Figure 4.1, a two-step process is utilized by *P. falciparum* to acquire resistance when challenged with DSM1 compound. Random mutations might be happening pre- or post-stress environment in the parasites and some might go through duplication in localized part of the genome as the first step to acquire resistance. The successful resistance event involves amplification at a resistance-conferring locus. It is accompanied by millions of parasites that do not amplify a useful portion of the genome and will die. After gaining an advantage through amplification of the target gene *Pfdhodh*, the second step occurs when the drug pressure is increased and parasites further increase copy numbers of their preexisting duplicated genome segment. Since malaria parasites are haploid organisms that carry only one copy of their genomes, we believe that pseudo-ploidy genes can eventually lead to other beneficial changes that confer resistance, such as acquisition of point mutations. After gaining point mutations, eventually, this would result in partial or even complete resolution of the amplified resistance locus. Through detailed whole genome sequencing studies of successful resistance events, mutations were found to occur at only one location in the genome. We believe that parasites employ this two-step strategy to acquire drug resistance without having extensive damage in other parts of the genome [19]. Overall, genome amplification is favored over the acquisition of point mutations as continual drug pressure demands an immediate solution from the parasite population with little tolerance for wrong guesses. The ease with which one can find the correct locus that confers drug resistance and the lack of severe penalties for expanding copy numbers in the neighborhood of the target gene made amplification event more favorable.

As discussed in Chapter 3, *P. falciparum* protein farnesyltransferase (*Pf*PFT) is the drug target of the tetrahydroquinoline class of compounds [18]. *Pf*PFT consists of alpha and beta subunits, which are encoded separately on different chromosomes. Both subunits must assemble to make a functionally active protein. Previous studies in the Rathod lab have shown that resistance to a *Pf*PFT inhibitor, BMS-388891, is associated with a single point

mutation on either the alpha or beta subunit of *Pf*PFT, but never on both subunits [17, 138]. In one mutant, a point mutation in the alpha subunit and an amplification of the beta subunit were observed (unpublished data). Amplification of both subunits resulting in resistance to BMS-388891 compound has not been observed because simultaneous amplification of both subunit loci is likely to be a rare event. The findings from studies on *Pf*PFT inhibitor resistance are consistent with what we observed in DSM1 resistant parasites where mutation is found to occur only at one location in the genome. The findings from DSM1 and BMS-388891 resistant parasites present an opportunity to test details of the model for acquisition of drug resistance in *P. falciparum* using the latest genetic manipulation tools, CRISPR/Cas9 system.

We hypothesize that genetically manipulation leading to pre-amplification of one of the *Pfpft* subunits (i.e. *Pfpft-α-subunit*), artificially, will not be sufficient for acquisition of resistance to BMS-388891. However, pre-amplification may lead to a more efficient acquisition of resistance through amplification of the other subunit, *Pfpft-β-subunit*, or through the generation of a point mutation in the alpha subunit. We postulate that point mutations will only happen on the pre-amplified subunit (*Pfpft-α-subunit*). In other words, once the initial amplification is established, acquisition of amplification or point mutations would occur more easily.

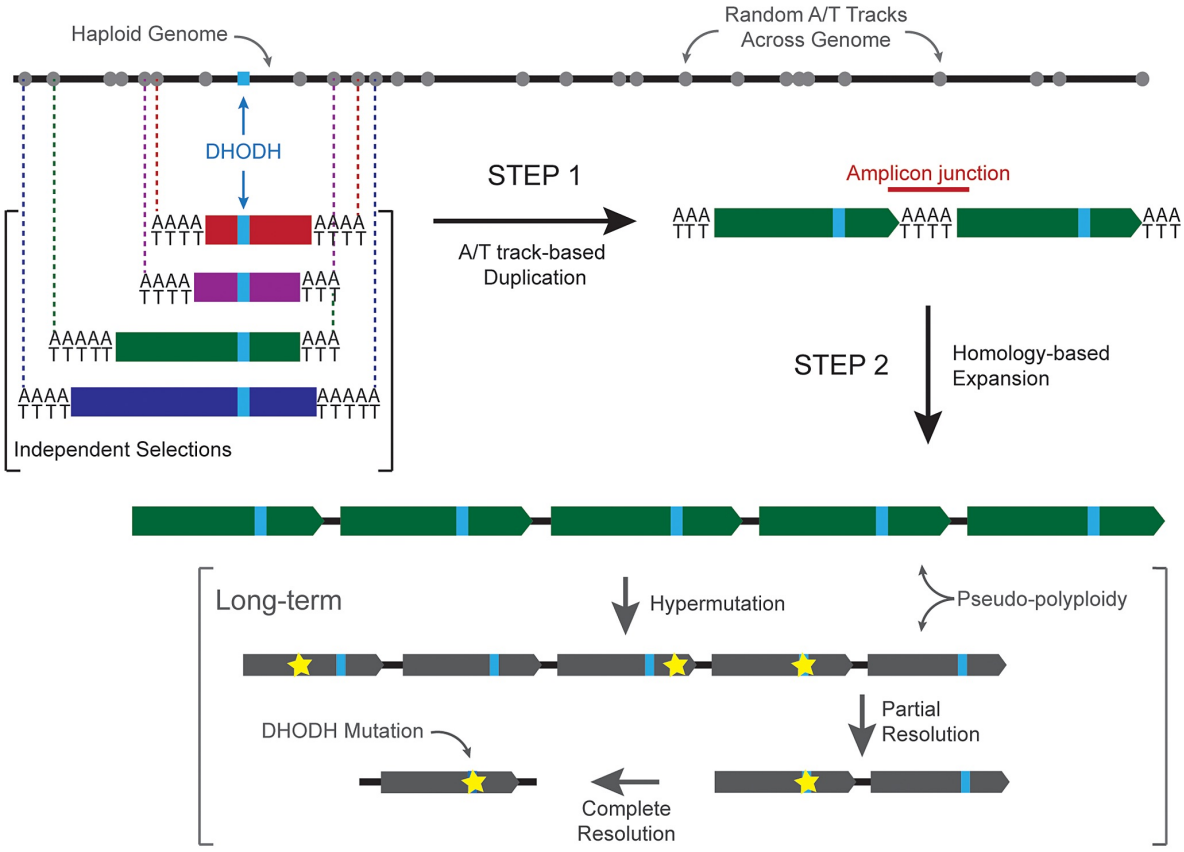

Figure 4.1: ***Model of acquisition of drug resistance in Plasmodium falciparum.*** *[19] Based on the model described by Guler et al., parasites undergo two-step process to acquire resistance. The first-step involves the duplication of the targeted gene with some nearby genes. After this initial duplication step, parasites can undergo homology-based expansion to increase the copy numbers of the duplicated region. These pseudo-polyploidy genes will aid in parasites acquiring a beneficial point mutation that confer resistance to the compound. Once the beneficial point mutation is introduced, complete resolution of the copy numbers of the amplified regions can be resolved.*

4.2 Experimental model

In order to test the hypothesis, one of the *Pf*PFT subunits (i.e. *Pfpft-α-subunit*) has to be pre-amplified. Previous studies have shown that when parasites are challenged with 333 nM of DSM1, amplification around the *Pfdhodh* gene on chromosome 6 is observed. A conserved region (gene #15-23) is always amplified from independent DSM1 resistant clones with gene 19 being the *Pfdhodh* gene. Insertion of the *Pfpft-α-subunit* into this conserved region would enable us to amplify the subunit along with the amplification of *Pfdhodh* when being selected with DSM1. After confirming the experimental pre-amplification of *Pfpft-α-subunit*, we can then test the hypothesis by doing a second selection experiment with *Pf*PFT inhibitor, BMS-388891 (Scheme 4.1). Successful selection of BMS-388891 resistant parasites can be achieved at higher frequency with lower starting parasite populations (i.e. 10^6 parasites).

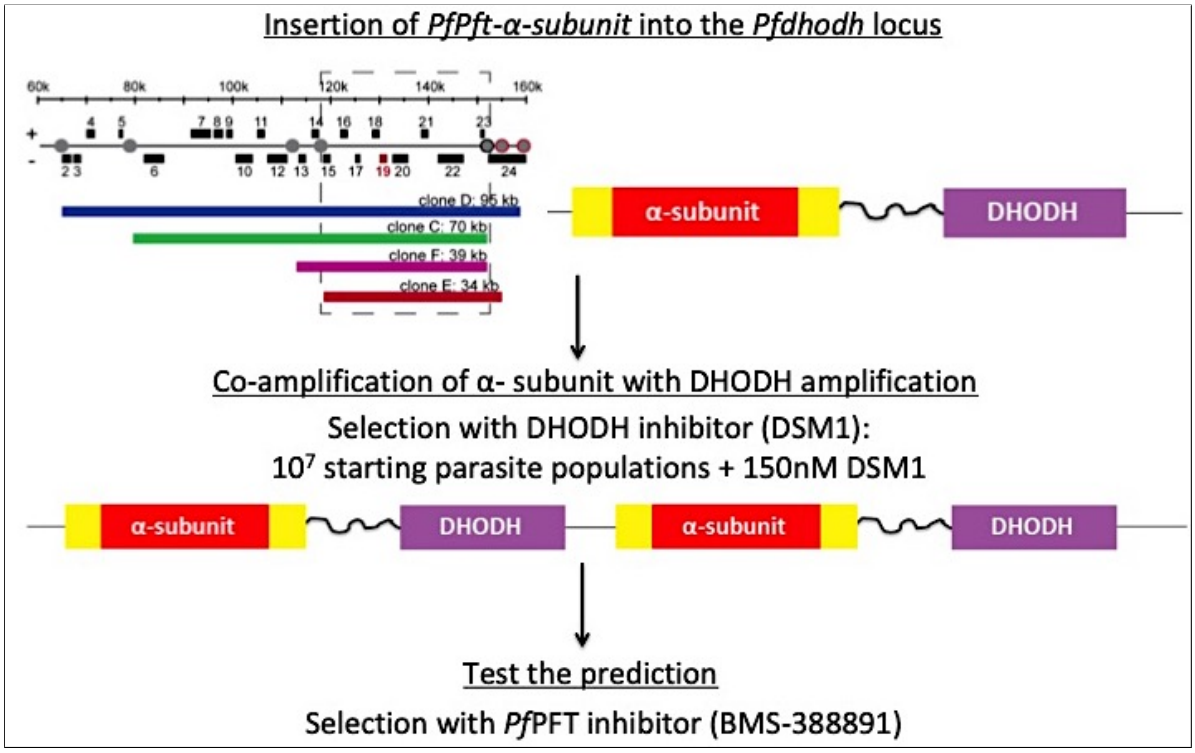

Scheme 4.1: ***Experimental scheme to test the model of mutagenesis.*** *Amplification of Pfpft-α-subunit could be achieved with the insertion of the gene at the Pfdhodh locus (gene # 15-23) followed by a resistant selection with DSM1. Parasites with pre-amplified Pfpft-α-subunit enable us to test the prediction through a resistant selection with BMS-388891 compound.*

4.3 Preliminary result and Discussion

4.3.1 Insertion of *Pfpft-α-subunit* into the *Pfdhodh* locus

Non-lethal (non-essential genes) locations on the conserved amplified regions near the *Pfdhodh* gene need to be determined for insertion of *Pfpft-α-subunit*. Based on the information from the database of Plasmodium Genomics Resource (PlasmoDB), genes 15, 16, 17 and 22 are annotated as conserved proteins, but of unknown functions (Figure 4.2). In order to determine whether those genes are essential for blood-stage parasites, knockouts for each gene were made utilizing the CRISPR/Cas9 method. As a positive control, we knocked out Exonuclease I (PF3D7_ 0725000), which is non-essential for blood-stage parasites [144]. As a negative control, we knocked out gene 23 (from the *Pfdhodh amplified region)*, which is known to be essential for blood-stage parasites (based on annotation on PlasmoDB).

As expected, parasites transfected with plasmid set to knockout Exonuclease I (positive control) were positive by microscopy at about week 3-4 post-transfection while parasites transfected with plasmid set to knockout gene 23 (negative control) remained negative for parasites throughout the experiment. Transfections with plasmid sets to knockout gene 15, 17 or 22 were positive for parasites by microscopy at about 3-4 weeks post-transfection. Transfections with the plasmid set to knockout gene 16 remained negative for parasites. Genomic DNA was extracted from each positive knockout parasites for downstream confirmation of gene disruption. PCR target gene amplification was done for each knockout clone using different primer sets to confirm the disruption of each gene, respectively (Figure 4.3). Sequencing of the amplified PCR products further confirmed the disruption of each gene in those independent clones. In this experiment, genes 15, 17 and 22 were proven to be non-essential for blood-stage parasites and hence insertion of *Pfpft-α-subunit* into one of these locations will not affect the viability of parasites.

Since gene 17 is located closest to the *Pfdhodh* gene on Chromosome 6, insertion of *Pfpft-α-subunit* was done at this location. The initial plan for insertion was to insert the

Pfpft-α-subunit gene with its own promoters. However, due to the AT-richness in the sequence of the promoters and the gene itself, we were not able to get the plasmid clone ready with the desired construct. Instead, modifications on the construct were made such that the *Pfpft-α-subunit* would be inserted directly downstream of the promoters of gene 17 in order to reduce the total AT-richness of the sequence in the plasmid. As the control, another plasmid construct was made with the insertion of Blasticidin S-deaminase (BSD) instead of *Pfpft-α-subunit*.

Parasites were then transfected with pDC2-Cas9-gRNA and pDC2-Gene17p-PFT or pDC2-Gene17p-BSD plasmids to insert either the *Pfpft-α-subunit* or BSD gene into the gene 17 locus. Some flasks were positive for parasites at around week 3-4 post-transfection. Genomic DNA was extracted from each modified parasite clone (Dd2-Gene17p-PFT-α-subunit or Dd2-Gene17p-BSD) for downstream confirmation of gene insertion. PCR target gene amplification and sequencing of the amplified PCR products confirmed the insertion of each gene in the independent clones. As shown in Figure 4.4, amplification with P1/P2 primers yield a smaller fragment in Dd2 parental clone compared to Dd2-Gene17p-BSD clone. Although the amplification fragment of P1/P2 primer set was not visible for the Dd2-Gene17p-PFT-α-subunit clone, the insertion was confirmed by the amplification fragment of P1/P3 and P4/P2 primer sets. Since the parental Dd2 clone did not carry the insertion of either gene, amplification with P1/P3 or P4/P2 primer sets did not yield any product as expected.

In addition, total RNA of modified parasites was isolated and reverse transcribed to complement DNA (cDNA) to confirm the expression of the inserted gene. Expression of the Heat Shock Protein 70 (HSP70) was used as the positive control of the assay. As shown in Figure 4.5, amplification of HSP70 from the cDNA product of Dd2, Dd2-Gene17p-PFT-α-subunit or Dd2-Gene17p-BSD yield a specific product. Amplification of HSP70 from the total RNA samples did not yield any product hence confirming that the total RNA samples did not contain any DNA contamination. Next, amplification with specific primer sets for either

Dd2-Gene17p-PFT-α-subunit and Dd2-Gene17p-BSD yield a specific product when amplified from the cDNA of both modified parasites but not in the parental Dd2 clone. Overall, this confirmed the expression of the inserted *Pfpft-α-subunit* or *bsd* gene driven by the Gene17 promoter.

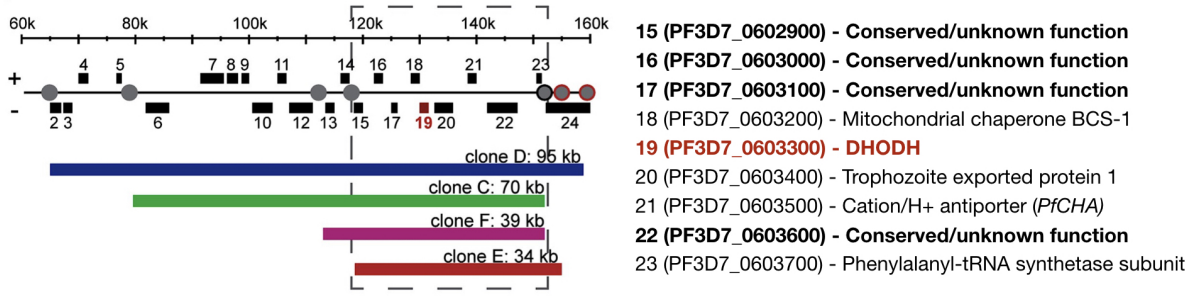

Figure 4.2: ***Summary of gene annotations of genes at the conserved amplified region of Pfdhodh.*** *Genes 15-23 located at the conserved amplified regions near the Pfdhodh gene. Among those, genes 15, 16, 17 and 22 are annotated as conserved proteins, but of unknown functions.*

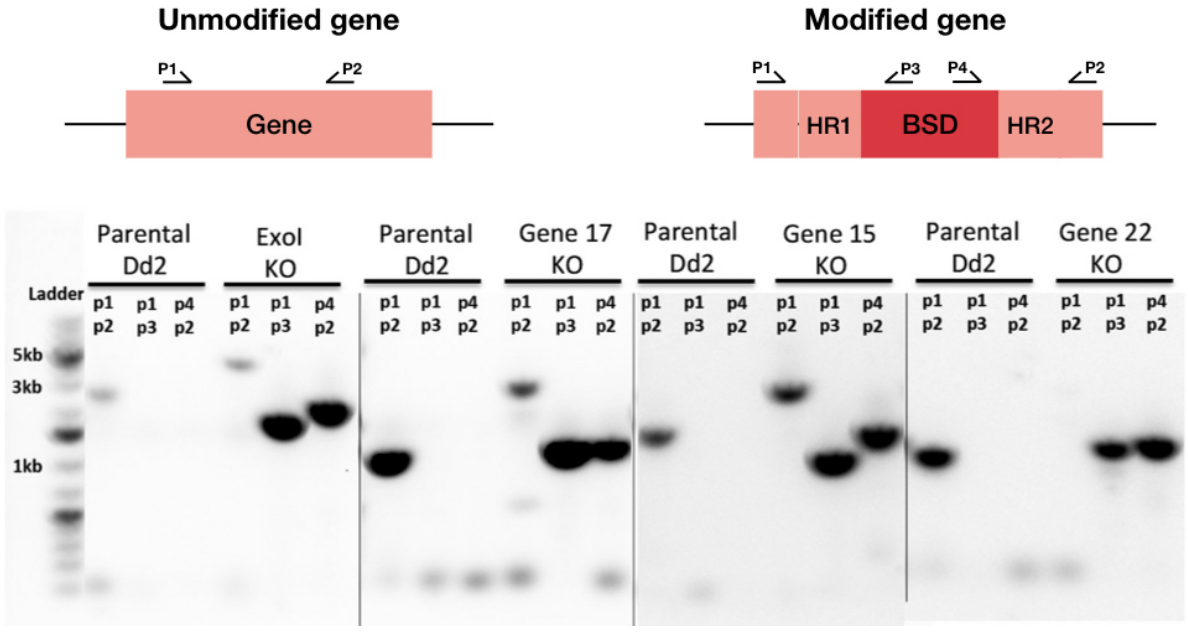

Figure 4.3: ***Gene disruption confirmation.*** *PCR with different primer sets were used to assess the disruption of each gene, respectively. Genetically modified parasites yielded a larger PCR fragment when amplified with P1/P2 primers. Amplification with P1/P3 and P4/P2 primers further confirmed the insertion of the selectable marker in the modified parasites.*

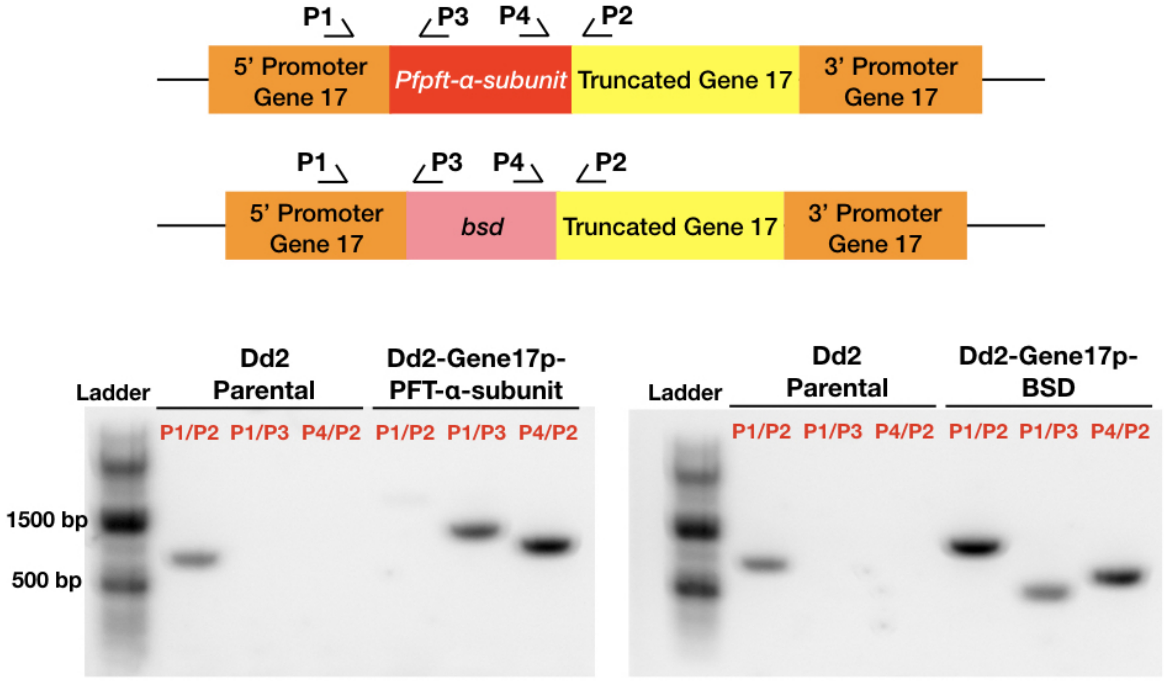

Figure 4.4: ***Gene insertion confirmation.*** *PCR with different primer sets were used to assess the insertion of each gene, respectively. Genetically modified parasites (Dd2-Gene17p-PFT-α-subunit or Dd2-Gene17p-BSD) yielded a larger PCR fragment when amplified with P1/P2 primers. Amplification with P1/P3 and P4/P2 primers further confirms the insertion of each independent gene in the modified parasites.*

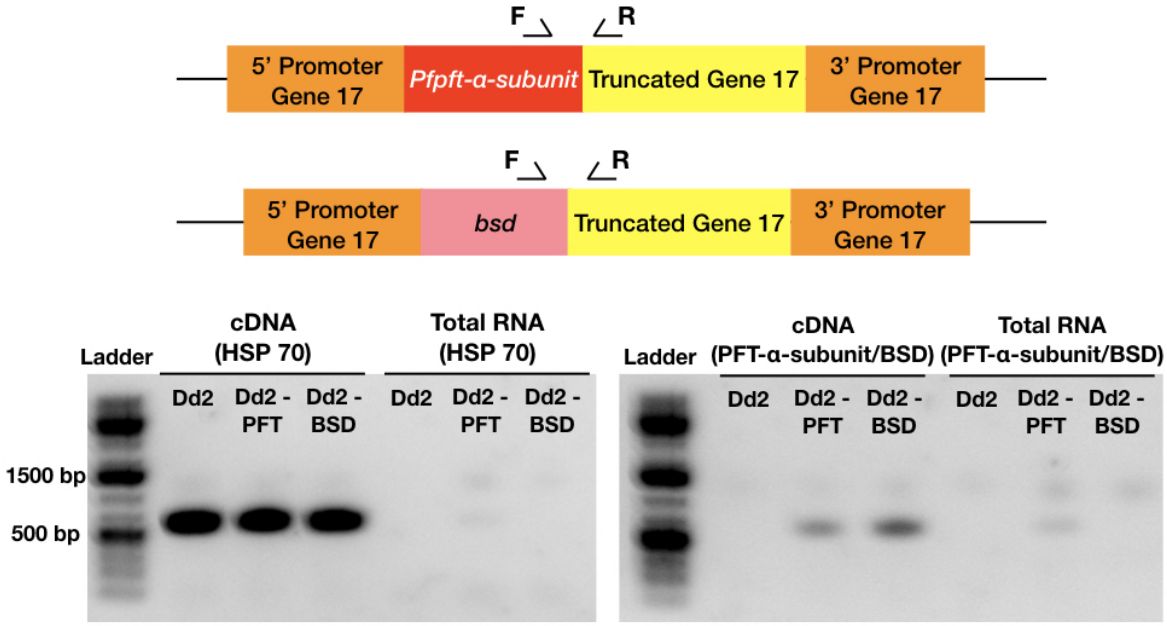

Figure 4.5: ***RNA expression confirmation.*** *PCR amplification with either HSP70 or PfPFT-α-subunit or BSD primers on cDNA products generated from Dd2, Dd2-Gene17p-PFT-α-subunit (shown here as Dd2-PFT), and Dd2-Gene17p-BSD (shown here as Dd2-BSD) indicated successful expression of the specific gene. Negative amplification as shown in the total RNA products indicate that no genomic DNA contamination was observed.*

4.3.2 DSM1 selection to amplify target locus

Based on Scheme 4.1, co-amplification of the inserted *Pfpft-α-subunit* with *Pfdhodh* can be achieved with DSM1 selection. A drug sensitivity assay was performed on the modified parasites to make sure that DSM1 sensitivity was not altered by the insertion experiment. As shown in Figure 4.6, the non-modified Dd2 clone showed an EC_{50} of 35.86 nM while the modified clones Dd2-Gene17p-PFTα-subunit and Dd2-Gene17p-BSD displayed EC_{50} values of 49.77 nM and 44.23 nM, respectively. This demonstrated that the initial transfection and modification made on parasites near the the *Pfdhodh* locus did not alter parasites' sensitivity towards DSM1 compound.

A DSM1 selection experiment was then carried out in triplicate with three independent cell lines (Dd2, Dd2-Gene17p-PFT-α-subunit and Dd2-Gene17p-BSD) each with 10^7 starting parasites (10^7pRBCs) and treated with 150 nM DSM1. As the positive control, 10 pRBCs were treated with DMSO. Similarly, 10 pRBCs were treated with 150 nM DSM1 in triplicate, as a negative control. Parasites were detected to be positive by microscopy at day 14-16 in all nine positive control flasks while the negative control flasks were absent of parasites throughout the length of the experiment (25 days). Parasite growth in cultures seeded with 10^7pRBCs (Dd2) and treated with 150 nM showed an initial drop in growth the first few days followed by the appearance of resistant parasites at around week 3 post-selection. However, this trend was not observed in most of the modified parasites lines. Continuous parasite growth was observed in 3 out of 3 flasks of Dd2-Gene17p-PFT-α-subunit clone and 2 out of 3 flasks of Dd2-Gene17p-BSD (Figure 4.7). Since modified parasites were shown to be sensitive to DSM1 compound prior to the selection experiment, the lack of initial inhibition of growth during selection pressure indicate that these parasites have an accelerated rate of resistance acquisition due to their altered genetic backgrounds. Drug sensitivity assays showed that these DSM1-mutants established higher resistance (higher EC_{50}) towards DSM1 compound as compared to each of their respective parental lines (Figure 4.8).

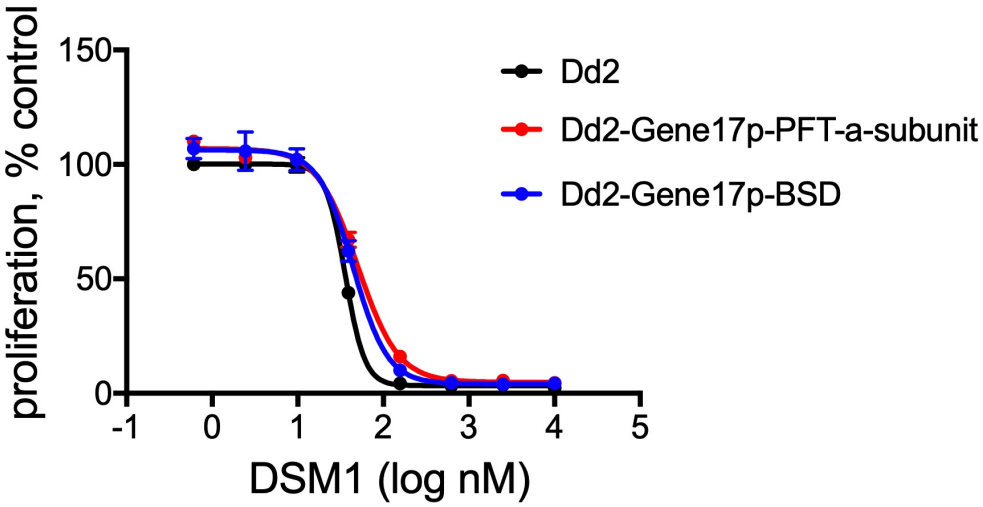

Figure 4.6: ***DSM1 sensitivity of modified clones.*** *The modified and non-modified parental Dd2 clones showed similar sensitivity towards DSM1 compound.*

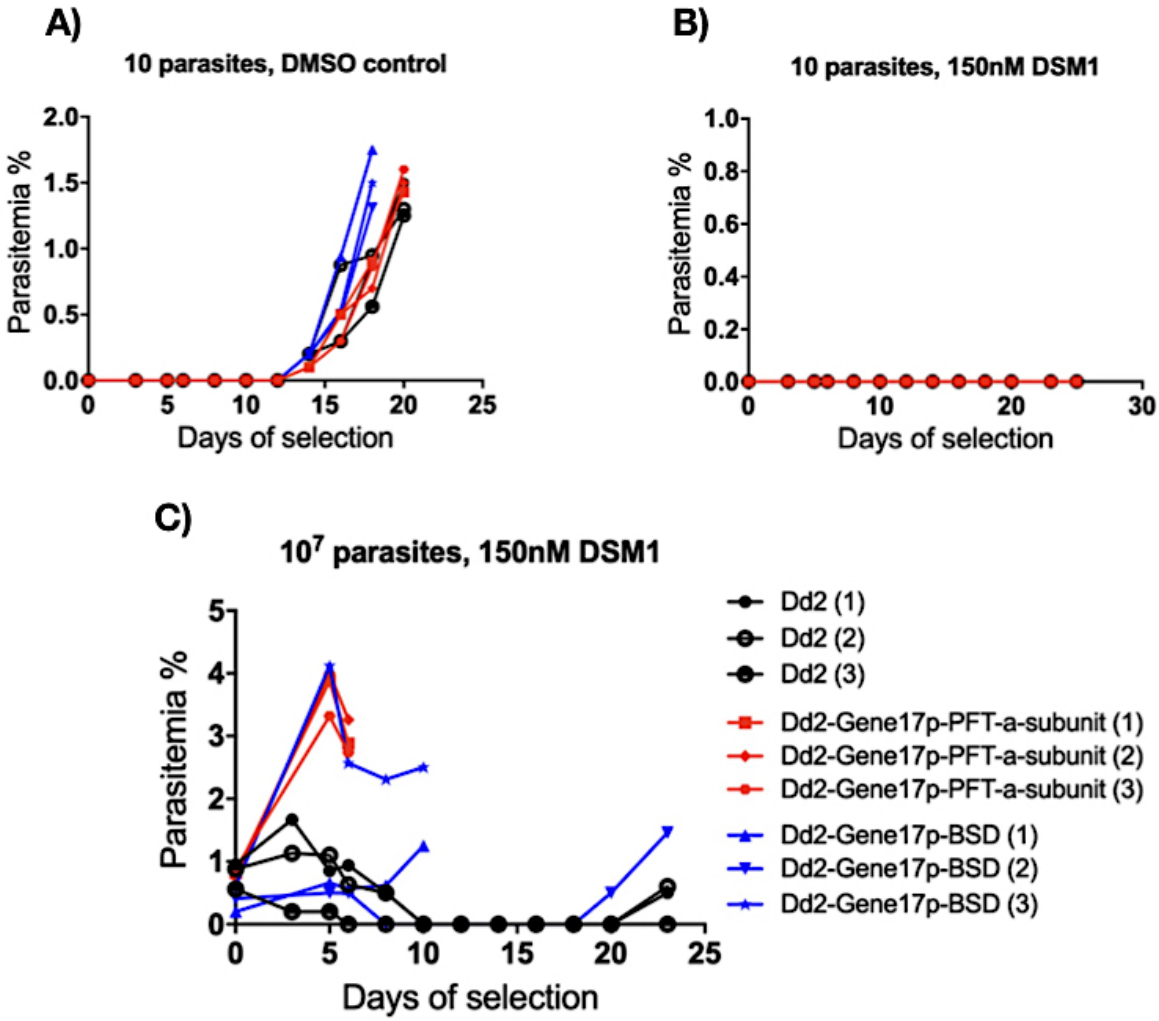

Figure 4.7: ***DSM1 selection result.*** *A) and B) Parasites growth in positive and negative control flasks behaved as expected as growth is observed around day 14-16 in positive control flasks while no parasites growth was observed up to day 25 in negative control flasks. C) Dd2 showed the typical selection trend where the growth of parasites plummeted in the first few days of selection and the reappearance of growth was observed around day 23. However, no initial death of parasites (Dd2-Gene17p-PFT-α-subunit and Dd2-Gene17p-BSD) was observed in most of the flasks where continuous parasites growth was observed at the beginning of the selection experiment.*

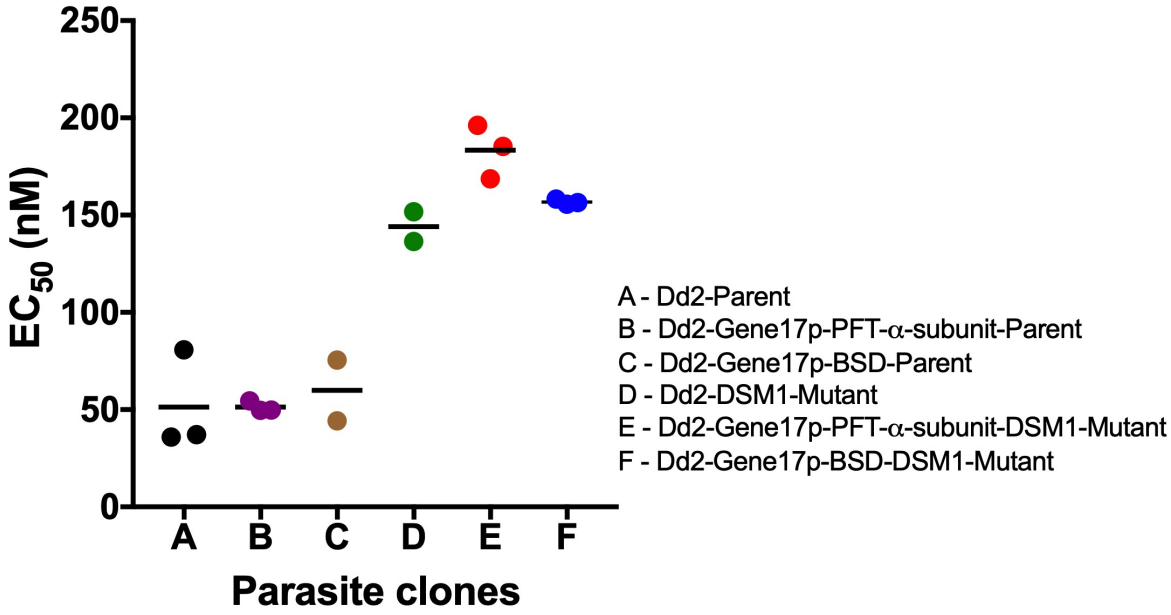

Figure 4.8: ***Sensitivity of resistant mutants to DSM1.*** *Dd2 and Dd2-modified parasites (either with Pft-α-subunit or bsd) displayed similar sensitivity to DSM1. Parasite clones that have been challenged with DSM1 (denoted here as DSM1-Mutant) showed resistance with higher EC_{50} values as compared to their respective parental lines.*

4.3.3 Characterization of modified parasite clones

We further investigated the genetics of the selected mutants harboring *Pfpft-α-subunit* at the *Pfdhodh* locus. Clonal parasites (Dd2-CloneD3-PFT, Dd2-CloneE7-PFT, Dd2-CloneB6-BSD and Dd2-CloneG1-BSD) were isolated from Dd2-Gene17p-PFT-α-subunit and Dd2-Gene17p-BSD. Quantitative PCR (qPCR) was performed on these clonal parasites in order to determine the copy number of the *Pfpft-α-subunit* gene in each modified clone. A standard genomic quantities curve was plotted using the parental Dd2 clone. Copy number determination of *Pfseryl-tRNA* gene was used as the control to make sure that the standard curve was accurate. Modified clonal parasites should only carry one copy of *Pfdhodh* and *Pfpft-β-subunit*. On the other hand, Dd2-CloneD3-PFT and Dd2-CloneE7-PFT are expected to carry two copies of *Pfpft-α-subunit* (one endogenous gene, and the other from the gene inserted at the Gene17 locus); while Dd2-CloneB6-BSD and Dd2-CloneG1-BSD are expected to have only one copy of *Pfpft-α-subunit* (endogenous gene only). However, as shown in Table 4.1, Dd2-CloneD3-PFT and Dd2-CloneE7-PFT showed elevated copies of *Pfpft-α-subunit*. Further analysis of the whole genome sequences of these modified clones reveal the presence of plasmid constructs (pDC2-gRNA-Cas9 and pDC2-donor plasmids used during transfection experiment) in the parasites genome. Consequently, the observed elevated copy numbers of *pfpft-α-subunit* in the qPCR experiment were contributed by the presence of the gene in the donor plasmid. Although this experiment confirms that modified clones carry only one copy of the *Pfdhodh* gene, copy numbers of *Pfpft-α-subunit* could not be determined due to plasmid retention in the genome samples.

Overall, successful insertion and expression of the inserted *Pfpft-α-subunit* were confirmed through different assays, however copy numbers of the inserted gene could not be confirmed due to plasmid retention in the experiment. This finding not only affects the ability to determine the copy numbers of the inserted gene in the pre-selected parasite lines, but proposed downstream selection experiments will also be impacted. For example, we would not be certain about the number of *Pfpft-α-subunit* amplifications in DSM1-selected mutants.

If *Pfpft-α-subunit* is inserted multiple times outside of the *Pfdhodh* locus, it would not be possible to resolve amplifications that evolved to point mutations. How the phenomena of rapid DSM1 resistance acquisition is mediated by additional copies of *Pfpft-α-subunit* is unknown and may warrant further exploration since DHODH-based inhibitors are in human clinical trials. This preliminary data is under review. The model and tools available remain a solid approach to understanding the initiation of mutagenesis in *Plasmodium falciparum*.

	CloneD3-PFT	**CloneE7-PFT**	**CloneB6-BSD**	**CloneG1-BSD**
Pfseryl-tRNA	1.2	1.0	1.2	1.0
Pfdhodh	0.4	0.4	0.5	0.5
Pfpft-β-subunit	0.8	0.7	0.6	0.8
Pfpft-α-subunit	8.1	2.9	1.3	1.0

Table 4.1: *Copy number confirmation by qPCR.*

4.4 Future Directions

The primary concern in this project is the inability to accurately determine copy numbers of the inserted gene due to plasmids retention in the parasite genome. To address this problem, donor plasmids used in this experiment can be modified to carry a negative selectable marker, yeast cytosine deaminase and uridyl phosphoribosyl transferase (yfcu) as shown in Figure 4.9A. Cytosine deaminase converts the pro-drug 5-fluorocytosine into 5-fluorouracil. The toxic metabolites produced by cytosine deaminase inhibit RNA synthesis as well as the enzyme thymidylate synthase. In order to pursue a more efficient genetic manipulation of *P. falciparum* genome without plasmid retention, the inclusion of *yfcu* in the donor plasmid could be utilized. Following positive modification with the inserted gene at the desired locus, parasites can be treated with 5-fluorocytosine in order to isolate parasites without the donor plasmid (Figure 4.9B).

Using parasites without donor plasmid, qPCR analysis on Dd2-Gene17p-PFT would reflect two copies of *Pfpft-α-subunit* and one copy of each *Pfdhodh* and *Pfpft-β-subunit* gene. Through analysis of whole genome sequencing data from next-generation sequencing technology, we will be able to determine the copy numbers of each gene of interest. However, due to the length of the sequencing reads (∼150 bp), the exact location of the insertion of the gene may not be clear. With advanced Single Molecule, Real-Time (SMRT) sequencing technology, PacBio long-read sequencing of read lengths up to 30,000 bp can be achieved. This long-read sequencing enables us to perform *de novo* assembly of the genome and hence the ability to determine all inserted locations of the inserted *Pfpft-α-subunit*. However, the high-cost of PacBio long-read sequencing has to be taken into consideration before moving forward with this method.

Upon confirmation of the inserted *Pfpft-α-subunit* gene into the *Pfdhodh* region, a DSM1 selection experiment can be carried out to amplify the target gene. As observed in the previous experiment as shown in Figure 4.7, modified parasites established an accelerated rate of acquisition of resistance to DSM1 compound. Future selections with DSM1 on modified

parasites will be conducted with lower starting parasites populations (i.e. 10^6 or 10^5pRBCs) and/or higher selection pressure (i.e. 150 or 300 nM DSM1). This method would ensure the selection of DSM1-resistant parasites with the desired genetic background and has the best chance to result in duplication of *Pfdhodh* locus containing *Pfpfpt-αs-subunit*. After the gene duplication of the inserted *Pfpft-α-subunit* is confirmed, BMS-388891 selection experiment can be performed.

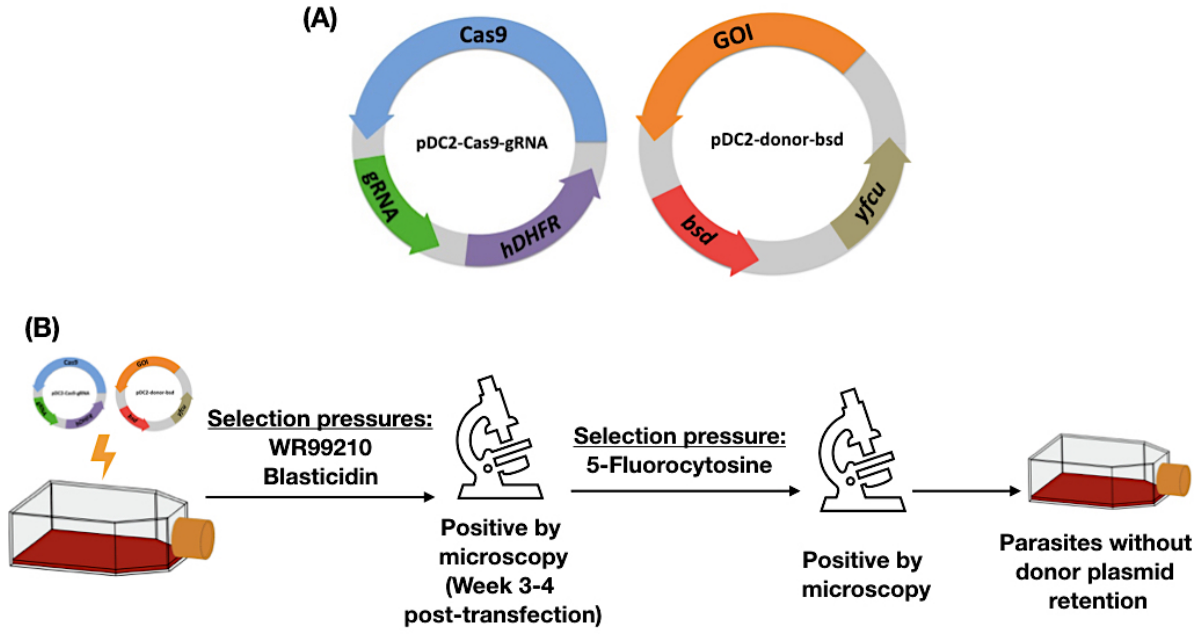

Figure 4.9: ***Modification on the donor plasmid and transfection scheme.*** *(A) pDC2-donor-bsd plasmid was modified to carry a negative selectable marker, yfcu. (B) Transfection scheme was modified to include a negative selection step with 5-fluorocytosine in order to remove parasites that carry the donor plasmid. Parasites isolated from this experiment would carry the desired modification without donor plasmid retention.*

4.5 Methods

4.5.1 Plasmid construction for gene knockout

The plasmid pDC2-gRNA-Cas9 was modified to include 20 nucleotides of the gRNA sequence targeting different genes of interest as shown in Table 4.2. gRNA constructs were designed using the CRISPR tool on the Geneious software. 100 μM of each pair of gRNA oligos (ordered from Eurofins Genomics) were cloned into the pDC2-gRNA-Cas9 plasmid as described in Section 2.4.1. The plasmid pDC2-donor-bsd was modified to carry homology arms of different gene of interests (PlasmoDB ID: PF3D7_0725000, PF3D7_0602900, PF3D7_0603000, PF3D7_0603100, PF3D7_0603600, and PF3D7_0603700) flanking the selectable marker Blasticidin S-deaminase (BSD), independently. For each gene of interest (GOI), 5' and 3' homology arms of length about 300 bp were amplified from the Dd2 clone using primers sets 5'-GOI-F/R or 3'-GOI-F/R while GOI-BSD-F/R primer sets were used to amplify BSD selectable marker from the pDC2-donor-bsd plasmid. These three PCR fragments were then assembled into a single piece that carries BamHI restriction site on the 5' end and SacI restriction site on the 3' end. The final assembled PCR construct was then digested with BamHI and SacI restriction enzymes and ligated into the double-digested pDC2-donor-bsd plasmid.

4.5.2 Plasmid construction for gene insertion

The plasmid pDC2-gRNA-Cas9 was modified to include a new gRNA sequence targeting the first 20 nucleotides of the Gene17 coding sequence. Two independent plasmids were modified: one for the insertion of *Pf*PFT-α-subunit, and the other for the insertion of Blasticidin S-Deaminase (BSD). 5'Gene17p-F and 5'Gene17p-PFT-R primers were used to amplify *Pfgene17* promoter (5' homology arm) from the Dd2 clone; Gene17p-PFT-F and Gene17p-PFT-R were used to amplify *Pfpft-α-subunit* from the Dd2 clone; while 3'Gene17p-PFT-F and 3'Gene17p-R were used to amplify the *Pfgene17* (3' homology arm) from the Dd2 clone. Similarly, 5'Gene17p-F and 5'Gene17p-BSD-R were used to amplify *Pfgene17*

promoter (5' homology arm) from the Dd2 clone; Gene17p-BSD-F and Gene17p-BSD-R were used to amplify the *bsd* gene from the pDC2-donor-BSD plasmid; while 3'Gene17p-BSD-F and 3'Gene17p-R were used to amplify the *Pfgene17* (3' homology arm) from the Dd2 clone. The three PCR fragments for two independent constructs were then independently assembled into a single piece that carries a HindIII restriction site on both the 5' and 3' end. The final two assembled PCR constructs were then independently digested with HindIII restriction enzymes and ligated into the HindIII-digested pDC2-donor-BSD plasmid.

4.5.3 Parasite cultures and transfection

Parasites cultures and transfection were done as described in Section 2.4.2 with the appropriate plasmid pairs and without the addition of the IPP. Parasite proliferation was monitored by Giemsa-stained blood samples taken at each media change, three times a week.

4.5.4 Analysis of modified clones

Parasite pellets from positive clones (Dd2ΔExonucleaseI, Dd2ΔGene15, Dd2ΔGene17, Dd2ΔGene22, Dd2-Gene17p-PFT-α-subunit, and Dd2-Gene17p-BSD) were lysed using 0.15% saponin solution. Genomic DNA was then extracted using Qiagen DNA Mini Kit according to the manufacturer's instructions. 50 ng of genomic DNA was used in the PCR reaction for targeted gene disruption and BSD-cassette/*Pfpft-α-subunit* integration verification of each independent clone. Different primers sets as shown in Table 4.4 and as discussed in the results section were used. After verification of the product size by gel electrophoresis, 10 μl of the PCR products were cleaned-up as described in Section 2.4.3 and sent for targeted gene sequencing using the same primer sets.

4.5.5 Gene expression confirmation

Parasite pellets from Dd2, Dd2-Gene17p-PFT-α-subunit, and Dd2-Gene17p-BSD were lysed using 0.15% saponin solution. Total RNA for each sample was extracted using Quick-RNA MiniPrep Plus Kit (Zymogen) according to the manufacturer's instructions with some modifications. 300 μl of RNA lysis buffer was added to the parasite pellet and transferred into the provided yellow column and centrifuged. The sample flow through was collected and 1/2 volume of 95-100% Ethanol was added to the same tube. The solution was transferred into the provided green column and centrifuged. The flow through was discarded and the column was washed with 400 μl of RNA wash buffer. A mixture of 5 μl of DNaseI and 75 μl of DNA digestion buffer was transferred to the column. The column was incubated at room temperature for an hour and then centrifuged to remove the buffer solution. The column was then washed with 400 μl of RNA prep buffer and twice with 700 μl of RNA wash buffer. The RNA was eluted with 50 μl of DNase/RNase free water. 1 μl of RNasin ribonuclease inhibitor was added to the eluted RNA to prevent digestion of RNA.

cDNA was synthesized from the total RNA collected using SuperScript III Reverse Transcriptase (Thermo Fisher Scientific). Briefly, 100 ng of random hexamers (Bioline USA), 60 ng of total RNA, 1 μl of 10 mM dNTP mix and water was heated to 65^{o}C for 5 minutes and incubated on ice for at least 1 minute. Next, 4 μl of 5X First-strand buffer, 1 μl of RNasin Ribonuclease inhibitor and 2 μ of SuperScript III reverse transcriptase was added and the tube was incubated at 25^{o}C for 5 minutes, 50^{o}C for 60 minutes and heat inactivated at 70^{o}C for 15 minutes. Finally, 1 μl of RNaseH was added and incubated at 37^{o}C for 20 minutes.

PCR analysis was performed on 2 μl of synthesized cDNA and/or 40 ng of total RNA isolated from different clones using the appropriate primer sets as shown in Table 4.5.

4.5.6 DSM1 selection experiment

Dd2 clone was serially diluted to 10 parasitized red blood cells (pRBCs) per flask in 9 independent flasks. Parasites were allowed to proliferate for about 10-14 days until each flask had about 10^7 pRBCs. Each flask was then split into two, with one set of flasks challenged with 150 nM of DSM1; while the other set of flasks was diluted to 10 pRBCs and treated with either DMSO or 150 nM DSM1. The 10 pRBCs, DMSO treated flasks act as positive control to gauge the minimum number of days required for each flask to be positive for parasites by microscopy. On the other hand, the 10 pRBCs, 150 nM DSM1 treated flasks act as negative control to make sure the concentration of the compound is lethal to parasites. The media was changed every other day while maintaining the initial drug concentration. Parasite proliferation was monitored by Giemsa-stained thin blood smear.

4.5.7 DSM1 sensitivity assay

Drug sensitivity assays were performed in 96-well plates containing parasite solutions of independent clones at 0.5% parasitemia and 0.5% hematocrit. A range of concentrations of DSM1 (from 10000 to 0.61 nM) were added to the parasites. To minimize the final concentration of DMSO in the parasite cultures, 200x DSM1 concentrations (in 100% DMSO) were first diluted 1:200 into RPMI (final 0.5% DMSO). Each concentration of interest was performed in triplicate and includes solvent-only controls. After incubating for about 72 hours, parasitized cells were stained using SYBR Green I for 20 minutes and counted by flow cytometry. Parasites proliferation in each well was expressed as a percentage of the solvent control. EC_{50} values were determined using GraphPad PRISM software.

4.5.8 Gene copy number determination

Genomic DNA isolated from different clones was quantified using Quant-iT PicoGreen dsDNA Reagent and Kits (Invitrogen). Aqueous working solution of the Quant-iT PicoGreen reagent

was prepared by making a 200-fold dilution of the concentrated DMSO solution in TE Buffer (10 mM Tris-HCl, 1 mM EDTA, pH 7.5). A standard DNA curve (range: 1 pg/ml - 1 ng/ml) was constructed using the DNA sample provided in the kit. The experimental DNA sample was diluted to a final volume of 100 μl with TE buffer and 100 μl of the 200X-diluted Quant-iT PicoGreen reagent was added to each well. After letting samples incubate at room temperature for 2-5 minutes, the sample fluorescence was measured with the micro-plate reader and standard fluorescein wavelengths (excitation - 480 nm, emission - 520 nm).

For quantitative PCR (qPCR), different primer sets as shown in Table 4.6 were used to quantify different genes. The qPCR protocol was 95^{o}C for 15 minutes, followed by 40 cycles of 95^{o}C for 15 seconds, 54^{o}C for 30 seconds and 60^{o}C for 30 seconds. For each experiment, the melt curve was performed at 65-95^{o}C with 0.5^{o}C increment every 5 seconds. The standard curve was carried out with the Dd2 parental clone (0 - 2000pg genomic DNA) with different primer sets. Relative copy number for each gene was determined with 2 pg and 200 pg of genomic DNA from each independent clones using Pfaffl method according to the equation $(\mathrm{E}_t arget)^{\Delta C_{t,target}(control-test)}$ / $(\mathrm{E}_r ef)^{\Delta C_{t,reference}(control-test)}$, where seryl-tRNA served as the reference gene [145]. Modified clones (Dd2-CloneD3-PFT, Dd2-CloneE7-PFT, Dd2-CloneB6-BSD and Dd2-CloneG1-BSD) served as the test, while the Dd2 parental clone served as the control.

Oligos	**Sequence**
Exonuclease I - Oligo 1	ATTGCCAGCATTCATAGATCCTCA
Exonuclease I - Oligo 2	AAACTGAGGATCTATGAATGCTGG
Gene 15 - Oligo 1	ATTGTGATAAACTTGTTAAAGATT
Gene 15 - Oligo 2	AAACAATCTTTAACAAGTTTATCA
Gene 16 - Oligo 1	ATTGAGATTAAGAGGGGGTAAAGG
Gene 16 - Oligo 2	AAACCCTTTACCCCCTCTTAATCT
Gene 17 - Oligo 1	ATTGGTGTATAATGGAATAAATGG
Gene 17 - Oligo 2	AAACCCATTTATTCCATTATACAC
Gene 17p - Oligo 1	ATTGACAATGAGTTCTTATAATAA
Gene17p - Oligo 2	AAACTTATTATAAGAACTCATTGT
Gene 22 - Oligo 1	ATTGGAAAACATATACGAATGCAA
Gene 22 - Oligo 2	AAACTTGCATTCGTATATGTTTTC
Gene 23 - Oligo 1	ATTGAGATGTCTTTCTGAATACAT
Gene 23 - Oligo 2	AAACAYGYAYYCAGAAAGACATCT

Table 4.2: *List of gRNA used in mutagenesis project.*

Primers	**Sequence**
5' ExoI - F	TTACTCGGATCCTAAAAATGATGACACACATAATAAA
5' ExoI - R	AAGCGAATTAGCTAAGCATGCATTTCTAGATATTCAAAA CATTC
ExoI-BSD - F	GAATGTTTTGAATATCTAGAAATGCATGCTTAGCTAATT CGCTT
ExoI-BSD - R	TTGAATATTATTATTTTGAGGATTTTCTCTGCGGTTTAA TAAATA
3' ExoI - F	TATTTATTAAACCGCAGAGAAAATCCTCAAAATAATAAT ATTCAA
3' ExoI - R	TGATAAGAGCTCAAATTATCTTGTGAATTACTGG
5' Gene15 - F	TTACTCGGATCCAATTTTAATGTAAATAAAGCAATTG
5' Gene15 - R	AAGCGAATTAGCTAAGCATGCTTTATCATTACATGTATT ATTATC
Gene15-BSD - F	GATAATAATACATGTAATGATAAAGCATGCTTAGCTAAT TCGCTT
Gene15-BSD - R	AACTGAATTACTAAATGAATACTTTCTCTGCGGTTTAAT AAATA
3' Gene15 - F	TATTTATTAAACCGCAGAGAAAGTATTCATTTAGTAATT CAGTT
3' Gene15 - R	TGATAAGAGCTCGTAAATTCCTTATAACATTCAAG
5' Gene16 - F	TTACTCGGATCCGTACAACTTGTTACAACAATA
5' Gene16 - R	AAGCGAATTAGCTAAGCATGCTTAATCTAAATAACAAAT AGATATC
Gene16-BSD - F	GATATCTATTTGTTATTTAGATTAAGCATGCTTAGCTAA TTCGCTT
Gene16-BSD - R	TTTATTTCTTAAATTGGCACCTTTCTCTGCGGTTTAATA AATA
3' Gene16 - F	TATTTATTAAACCGCAGAGAAAGGTGCCAATTTAAGAAA TAAA
3' Gene16 - R	TGATAAGAGCTCATATGTCGTGGATTCTTCATT
5' Gene17 - F	TTACTCGGATCCGCTCAATTTGAATTAAGAAATG

5' Gene17 - R	AAGCGAATTAGCTAAGCATGCTATACACATTTCCACATTGATT
Gene17-BSD - F	AATCAATGTGGAAATGTGTATAGCATGCTTAGCTAATTCGCTT
Gene17-BSD - R	CATATTATTTATATTGTCAATACTTTCTCTGCGGTTTAATAAATA
3' Gene17 - F	TATTTATTAAACCGCAGAGAAAGTATTGACAATATAAATAATATG
3' Gene17 - R	TGATAAGAGCTCCTTCATTATCTCTAATATTGTT
5' Gene17p - F	TTACTCAAGCTTGGGCTTGATTGAATTTTCA
5' Gene17p-PFT - R	GCATACAAGCATCGATTTTCCATTGTTTTCTTATTATTACTAC
Gene17p-PFT - F	GTAGTAATAATAAGAAAACAATGGAAAATCGATGCTTGTATGC
Gene17p-PFT - R	CGTAGTTATTGGACCTATTCATCATATTTTTAACCTTTTTTGAAC
3' Gene17p-PFT - F	GTTCAAAAAAGGTTAAAAATATGATGAATAGGTCCAATAACTACG
3' Gene17p-PFT - R	TGATACAAGCTTGGGTATCATTGTTATAATAATTTGG
5' Gene17p-BSD - R	CTTGGCATGCATTTATCACCATTGTTTTCTTATTATTACTAC
Gene17p-BSD - F	GTAGTAATAATAAGAAAACAATGGTGATAAATGCATGCCAAG
Gene17p-BSD - R	CGTAGTTATTGGACCTATTCATTAGCCCTCCCACACATA
3' Gene17p-BSD - F	TATGTGTGGGAGGGCTAATGAATAGGTCCAATAACTACG
5' Gene22 - F	TTACTCGGATCCAAAGAGCATAATATTATATTTACA
5' Gene22 - R	AAGCGAATTAGCTAAGCATGCGTTTTATTTACAACCATTTGG
Gene22-BSD - F	CCAAATGGTTGTAAATAAAACGCATGCTTAGCTAATTCGCTT
Gene22-BSD - R	CATAAACGTAAATATGAAAACATTCTCTGCGGTTTAATAAATAT

3' Gene22 - F	ATATTTATTAAACCGCAGAGAATGTTTTCATATTTACGTTTATG
3' Gene22 - R	TGATAAGAGCTCTCTTTGCTCCCTTTCTTTTAA
5' Gene23 - F	TTACTCGGATCCCCATGTCCTTATATCATAATCA
5' Gene23 - R	AAGCGAATTAGCTAAGCATGCTACTAAATGGGCGAAAAGTTG
Gene23-BSD - F	CAACTTTTCGCCCATTTAGTAGCATGCTTAGCTAATTCGCTT
Gene23-BSD - R	TGTTTAATATAAAATGAGATGTCTTTCTCTGCGGTTTAATAAATA
3' Gene23 - F	TATTTATTAAACCGCAGAGAAAGACATCTCATTTTATATTAAACA
3' Gene23 - R	TGATAAGAGCTCTCACCTTATGGAAACTTCAAAT

Table 4.3: *List of primers for plasmids constructions used in mutagenesis project.*

Primers	**Sequence**
ExoI - P1	GCTTAATGCCCATTAATGATCTTA
ExoI - P4	TTGTGTACTATTATGCATGTTATGA
Gene15 - P1	ACGATTATCTAATTCGTTTCATACT
Gene15 - P4	AAGGTACTTCAAAAGTGTCCA
Gene17 - P1	CCCAATATATATTAAATAAGAAAACAGC
Gene17 - P4	CATTATCGTCCTGAACAAAGTC
Gene22 - P1	AAATGGAAATGAATATAAAGATATGATG
Gene22 - P4	CTTTAGATTTGACAAGTTCCATTT
P2	GTGGATTCTTCTTGAGACAAAG
P3	TCAAAGCCATAGTGAAGGAC
Gene17p-PFT - P1	GCGAGAATATGAAGTAAGCATA
Gene17p-PFT - P2	TAGGCATTTAAAGCACTATCAG
Gene17p-PFT - P3	TATGACGATTTTAACGAACATGTG
Gene17p-PFT - P4	GTTCATTCCTTCGTTTTCGTTATA
Gene17p-BSD - P1	GCGAGAATATGAAGTAAGCATA
Gene17p-BSD - P2	TAGGCATTTAAAGCACTATCAG
Gene17p-BSD - P3	TTCACTGGTGTCAATGTATATCAT
Gene17p-BSD - P4	GTTCATTCCTTCGTTTTCGTTATA

Table 4.4: *List of primers used in confirmation of gene disruption/insertion.*

Primers	**Sequence**
HSP70 - F	TGCTGTCATTACCGTTCCAG
HSP70 - R	GATCTGCATGCTTCTTTACCATT
PFT - F	TCATGATTTAGCAAAAATGCAGAA
Gene17 - R	GTTAACCATCCCATAATTTCCA
BSD - F	ATGGTGATAAATGCATGCCAAG

Table 4.5: *List of primers used in gene expression confirmation.*

Primers	**Sequence**
seryl-tRNA - F	ACAATGGTAGCTGCACAAAGA
seryl-tRNA - R	TGTTCATGTATGGGCGCAAT
DHODH - F	ACCCATTATTGCATCAGGAGG
DHODH - R	ATTGACAAACTGAAGCACCTGC
PFT-B-subunit - F	ATTGAAATGTACAGATGGATCT
PFT-B-subunit - R	CATAGAACAAATAGATATAGCAC
PFT-A-subunit - F	GCATGGGTGTACAGAAGAAAATG
PFT-A-subunit - R	ATCTTCTATGGAACCAGCTCTG

Table 4.6: *List of primers used in copy number determination.*

Chapter 5

Conclusions and Future Directions

Malaria is a serious global disease in which the World Health Organization has estimated 200 million cases with 500,000 deaths per year. The most virulent species, *Plasmodium falciparum*, is responsible for the majority of clinical symptoms and deaths. Efforts to develop an effective vaccine have been unsuccessful but antimalarial drugs are able to prevent infections and cure disease. Although an array of treatments exists today, the emergence of resistance to antimalarial drugs is a continuing public health concern. Efforts to eradicate malaria hence require the advancement in discovery of essential genes that can potentially be new drug targets as well as deeper understanding of the resistance mechanism in blood-stage parasites.

Over the years, the Rathod lab has been involved in resistance studies and has developed a systematic approach to characterize mechanisms that drive genetic change when the parasite is exposed to challenges from its environment. The approach utilizes the meticulous selection experiment of resistant parasites in the *in vitro* culture system as well as detail analysis of whole genome sequences of resistant-mutants. Expanding the toolbox to include genome manipulation can further our understanding of the resistance mechanism as well as enable us to explore potential drug targets.

The CRISPR/Cas9 genome-editing tool has been widely used for genetic manipulation of various organisms. In the year 2014, the Pubmed search of "CRISPR human" has yield 1015 entries, "CRISPR mouse" yield 358 entries, "CRISPR drosophila" yield 67 entries, while "CRISPR Plasmodium" yield only 5 entries. Hence, the goal of this thesis project is

to introduce and complement the CRISPR/Cas9 technique to what the Rathod lab already does well in order to address the initiation of resistance acquisition and dissect drug-target relationships.

Optimization of the transfection protocol as shown in this work proved we could achieve 90% transfection efficiency. The initial success in transfection boosted our confidence in performing more complicated genome-manipulation experiments. As discussed in Chapter 2, the knockout of *Plasmodium falciparum* DNA gyrase A with the supplementation of IPP has confirmed the essentiality of this enzyme in the blood-stage parasites. Due to the difficulty in purifying the full-length *Pf*GyrA enzyme, the mode of action of the enzyme has yet to be tested and confirmed. The *Pf*ΔGyrA clone generated in these studies has for the first time provided evidence that this enzyme plays a crucial role in maintenance of the apicoplast genome. The loss of the apicoplast in the *Pf*ΔGyrA clone was confirmed through immunofluorescence assay as well as whole genome sequencing. Further characterization of the *Pf*ΔGyrA clone has led to the discovery that an antibacterial compound, Ciprofloxacin, might have an additional target in blood-stage parasites. In the future, dissection of the potential secondary target of the compound can lead to a better understanding of the mechanism of action of ciprofloxacin on blood-stage parasites. Also, utilizing the developed knockout and chemical rescue system will enable us to identify other essential apicoplast-targeted proteins that can serve as future drug targets.

In addition, we have successfully demonstrated the utilization of CRISPR/Cas9 tool in performing gene alteration and gene insertion in order to understand resistance mechanisms. In Chapter 3, we showed for the first time that a single-point mutation in the *Pfpft-β-subunit* gene is sufficient to confer *in vitro* resistance to BMS-388891 compound. In the future, mutations that have arisen during selection studies and found through whole genome sequences analysis can be confirmed with the genome manipulation experiments. These systematic steps allow a more precise association of a mutation to specific compound resistance.

Although the project as discussed in Chapter 4 is not complete, we showed here that

it is possible for insertion of an endogenous gene into a genome location that is prone to amplification. In the course of this work, we also showed that several genes near the *Pfdhodh* gene is not essential for the function of blood-stage parasites. Hence future work that require modification around that locus could be performed. Also, we proposed several modifications that could be performed in order to improve the genome manipulation experiment. Measures such as including a negative selectable marker in the donor plasmid would enable us to dissolve the issue of quantifying copy number of the inserted gene.

In conclusion, no scientific endeavor is ever truly complete. Here we have shown a few successful applications of CRISPR/Cas9 genome manipulation in *Plasmodium falciparum*. This work utilized mainly gene knockout, gene alteration and gene insertion techniques that led to a deeper understanding of drug targets as well as resistance mechanisms. It is in my hope that those who follow will use this work as a foundation to generate novel ideas that may contribute to better understanding of malaria parasites mutagenesis.

Bibliography

[1] CDC, *Malaria: Malaria Parasites* (2018).

[2] WHO, *World Malaria report 2017* (2017).

[3] N. J. White, *Antimalarial drug resistance: the pace quickens*, Journal of Antimicrobial Chemotherapy **30**, 571 (1992).

[4] T. E. Wellems and C. V. Plowe, *Chloroquine-resistant malaria.*, The Journal of infectious diseases **184**, 770 (2001), ISSN 0022-1899.

[5] W. H. Wernsdorfer, *Epidemiology of drug resistance in malaria*, Acta Tropica **56**, 143 (1994), ISSN 0001706X.

[6] R. W. Burgess and M. D. Young, *The development of pyrimethamine resistance by Plasmodium falciparum*, Bulletin of the World Health Organization **20**, 37 (1959), ISSN 0042-9686.

[7] N. J. White and F. Nosten, *Artemisinin-Based Combination Treatment of Falciparum Malaria*, The American Journal of Tropical Medicine and Hygiene **77**, 181 (2007), ISSN 0002-9637.

[8] J. T. Lin, J. J. Juliano, and C. Wongsrichanalai, *Drug-Resistant Malaria: The Era of ACT*, Current Infectious Disease Reports **12**, 165 (2010), ISSN 1534-3146.

[9] S. Vijaykadga, C. Rojanawatsirivej, S. Cholpol, D. Phoungmanee, A. Nakavej, and C. Wongsrichanalai, *In vivo sensitivity monitoring of mefloquine monotherapy and artesunate-mefloquine combinations for the treatment of uncomplicated falciparum malaria in Thailand in 2003*, Trop Med Int Health **11** (2006).

[10] R. Hutagalung, L. Paiphun, E. A. Ashley, R. McGready, A. Brockman, K. L. Thwai, P. Singhasivanon, T. Jelinek, N. J. White, and F. H. Nosten, *A randomized trial of artemether-lumefantrine versus mefloquine-artesunate for the treatment of uncomplicated multi-drug resistant Plasmodium falciparum on the western border of Thailand*, Malar J **4** (2005).

[11] J. M. Stohrer, S. Dittrich, V. Thongpaseuth, V. Vanisaveth, R. Phetsouvanh, S. Phompida, F. Monti, E. M. Christophel, N. Lindegardh, A. Annerberg, et al., *Therapeutic efficacy of artemether-lumefantrine and artesunate-mefloquine for treatment of uncomplicated Plasmodium falciparum malaria in Luang Namtha Province, Lao People's Democratic Republic*, Trop Med Int Health **9** (2004).

[12] A. P. Phyo, E. A. Ashley, T. J. C. Anderson, Z. Bozdech, V. I. Carrara, K. Sriprawat, S. Nair, M. M. White, J. Dziekan, C. Ling, et al., *Declining Efficacy of Artemisinin Combination Therapy Against P. Falciparum Malaria on the Thai-Myanmar Border (2003-2013): The Role of Parasite Genetic Factors*, Clinical infectious diseases : an official publication of the Infectious Diseases Society of America **63**, 784 (2016), ISSN 1537-6591.

[13] W. O. Rogers, R. Sem, T. Tero, P. Chim, P. Lim, S. Muth, D. Socheat, F. Ariey, and C. Wongsrichanalai, *Failure of artesunate-mefloquine combination therapy for uncomplicated Plasmodium falciparum malaria in southern Cambodia*, Malaria Journal **8**, 10 (2009), ISSN 1475-2875.

[14] M. B. Denis, R. Tsuyuoka, Y. Poravuth, T. S. Narann, S. Seila, C. Lim, S. Incardona, P. Lim, R. Sem, D. Socheat, et al., *Surveillance of the efficacy of artesunate and mefloquine combination for the treatment of uncomplicated falciparum malaria in Cambodia*, Trop Med Int Health **11** (2006).

[15] A. P. Alker, P. Lim, R. Sem, N. K. Shah, P. Yi, D. M. Bouth, R. Tsuyuoka, J. D. Maguire, T. Fandeur, F. Ariey, et al., *Pfmdr1 and in vivo resistance to artesunate-mefloquine in falciparum malaria on the Cambodian-Thai border*, Am J Trop Med Hyg **76** (2007).

[16] A. F. Cowman, J. Healer, D. Marapana, and K. Marsh, *Malaria: Biology and Disease.*, Cell **167**, 610 (2016), ISSN 1097-4172 (Electronic).

[17] R. T. Eastman, J. White, O. Hucke, K. Bauer, K. Yokoyama, L. Nallan, D. Chakrabarti, C. L. M. J. Verlinde, M. H. Gelb, P. K. Rathod, et al., *Resistance to a Protein Farnesyltransferase Inhibitor in Plasmodium falciparum*, Journal of Biological Chemistry **280**, 13554 (2005).

[18] R. T. Eastman, F. S. Buckner, K. Yokoyama, M. H. Gelb, and W. C. Van Voorhis, *Thematic review series: Lipid Posttranslational Modifications. Fighting parasitic disease by blocking protein farnesylation*, Journal of Lipid Research **47**, 233 (2006).

[19] J. L. Guler, D. L. Freeman, V. Ahyong, R. Patrapuvich, J. White, R. Gujjar, M. A. Phillips, J. DeRisi, and P. K. Rathod, *Asexual Populations of the Human Malaria Parasite, <italic>Plasmodium falciparum</italic>, Use a Two-Step Genomic Strategy to Acquire Accurate, Beneficial DNA Amplifications*, PLoS Pathog **9**, e1003375 (2013).

[20] E. Y. Klein, *Antimalarial drug resistance: a review of the biology and strategies to delay emergence and spread.*, International journal of antimicrobial agents **41**, 311 (2013), ISSN 1872-7913 (Electronic).

[21] T. Cavalier-Smith, *Kingdom protozoa and its 18 phyla.*, Microbiological Reviews **57**, 953 LP (1993).

[22] M. J. Gardner, N. Hall, E. Fung, O. White, M. Berriman, R. W. Hyman, J. M. Carlton, A. Pain, K. E. Nelson, S. Bowman, et al., *Genome sequence of the human malaria parasite Plasmodium falciparum*, Nature **419**, 498 (2002), ISSN 0028-0836.

[23] M. Obornik, J. Janouskovec, T. Chrudimsky, and J. Lukes, *Evolution of the apicoplast and its hosts: from heterotrophy to autotrophy and back again.*, International journal for parasitology **39**, 1 (2009), ISSN 1879-0135 (Electronic).

[24] J. Janouskovec, A. Horak, M. Obornik, J. Lukes, and P. J. Keeling, *A common red algal origin of the apicomplexan, dinoflagellate, and heterokont plastids.*, Proceedings of the National Academy of Sciences of the United States of America **107**, 10949 (2010), ISSN 1091-6490 (Electronic).

[25] B. J. Foth, S. A. Ralph, C. J. Tonkin, N. S. Struck, M. Fraunholz, D. S. Roos, A. F. Cowman, and G. I. McFadden, *Dissecting Apicoplast Targeting in the Malaria Parasite Plasmodium falciparum*, Science **299**, 705 (2003).

[26] J. Zuegge, S. Ralph, M. Schmuker, G. I. McFadden, and G. Schneider, *Deciphering apicoplast targeting signals feature extraction from nuclear-encoded precursors of Plasmodium falciparum apicoplast proteins*, Gene **280**, 19 (2001), ISSN 03781119.

[27] R. F. Waller, P. J. Keeling, R. G. K. Donald, B. Striepen, E. Handman, N. Lang-Unnasch, A. F. Cowman, G. S. Besra, D. S. Roos, and G. I. McFadden, *Nuclear-encoded proteins target to the plastid in Toxoplasma gondii and Plasmodium falciparum* , Proceedings of the National Academy of Sciences of the United States of America **95**, 12352 (1998), ISSN 0027-8424.

[28] S. A. Ralph, G. G. van Dooren, R. F. Waller, M. J. Crawford, M. J. Fraunholz, B. J. Foth, C. J. Tonkin, D. S. Roos, and G. I. McFadden, *Tropical infectious diseases: Metabolic maps and functions of the Plasmodium falciparum apicoplast*, Nat Rev Micro **2**, 203 (2004), ISSN 1740-1526.

[29] R. J. Wilson, P. W. Denny, P. R. Preiser, K. Rangachari, K. Roberts, A. Roy, A. Whyte, M. Strath, D. J. Moore, P. W. Moore, et al., *Complete gene map of the plastid-like DNA of the malaria parasite Plasmodium falciparum.*, Journal of molecular biology **261**, 155 (1996), ISSN 0022-2836 (Print).

[30] F. Seeber, *Biogenesis of ironsulphur clusters in amitochondriate and apicomplexan protists*, International Journal for Parasitology **32**, 1207 (2002), ISSN 0020-7519.

[31] R. F. Waller, P. J. Keeling, R. G. K. Donald, B. Striepen, E. Handman, N. Lang-Unnasch, A. F. Cowman, G. S. Besra, D. S. Roos, and G. I. McFadden, *Nuclear-encoded proteins target to the plastid in Toxoplasma gondii and Plasmodium falciparum *, Proceedings of the National Academy of Sciences **95**, 12352 LP (1998).

[32] V. A. Nagaraj, R. Arumugam, N. R. Chandra, D. Prasad, P. N. Rangarajan, and G. Padmanaban, *Localisation of Plasmodium falciparum uroporphyrinogen III decarboxylase of the heme-biosynthetic pathway in the apicoplast and characterisation of its catalytic properties*, International Journal for Parasitology **39**, 559 (2009), ISSN 0020-7519.

[33] S. Sato, B. Clough, L. Coates, and R. J. M. Wilson, *Enzymes for Heme Biosynthesis are Found in Both the Mitochondrion and Plastid of the Malaria Parasite Plasmodium falciparum*, Protist **155**, 117 (2004), ISSN 1434-4610.

[34] E. L. Dahl, J. L. Shock, B. R. Shenai, J. Gut, J. L. DeRisi, and P. J. Rosenthal, *Tetracyclines Specifically Target the Apicoplast of the Malaria Parasite Plasmodium falciparum*, Antimicrobial Agents and Chemotherapy **50**, 3124 LP (2006).

[35] E. L. Dahl and P. J. Rosenthal, *Apicoplast translation, transcription and genome replication: targets for antimalarial antibiotics.*, Trends in parasitology **24**, 279 (2008), ISSN 1471-4922 (Print).

[36] C. D. Goodman, V. Su, and G. I. McFadden, *The effects of anti-bacterials on the malaria parasite Plasmodium falciparum*, Mol Biochem Parasitol **152** (2007).

[37] C. D. Goodman and G. I. McFadden, *Targeting apicoplasts in malaria parasites.*, Expert opinion on therapeutic targets **17**, 167 (2013), ISSN 1744-7631.

[38] M. Yu, T. R. S. Kumar, L. J. Nkrumah, A. Coppi, S. Retzlaff, C. D. Li, B. J. Kelly, P. A. Moura, V. Lakshmanan, J. S. Freundlich, et al., *The Fatty Acid Biosynthesis Enzyme FabI Plays a Key Role in the Development of Liver-Stage Malarial Parasites*, Cell Host & Microbe **4**, 567 (2008), ISSN 1931-3128.

[39] A. M. Vaughan, M. T. O'Neill, A. S. Tarun, N. Camargo, T. M. Phuong, A. S. I. Aly, A. F. Cowman, and S. H. I. Kappe, *Type II fatty acid synthesis is essential only for malaria parasite late liver stage development*, Cellular Microbiology **11**, 506 (2009), ISSN 1462-5814.

[40] E. Yeh and J. L. DeRisi, *Chemical Rescue of Malaria Parasites Lacking an Apicoplast Defines Organelle Function in Blood-Stage <italic>Plasmodium falciparum</italic>*, PLoS Biol **9**, e1001138 (2011).

[41] Y. Wu, C. D. Sifri, H. H. Lei, X. Z. Su, and T. E. Wellems, *Transfection of Plasmodium falciparum within human red blood cells.*, Proceedings of the National Academy of Sciences of the United States of America **92**, 973 (1995), ISSN 0027-8424 (Print).

[42] K. W. Deitsch, C. L. Driskill, and T. E. Wellems, *Transformation of malaria parasites by the spontaneous uptake and expression of DNA from human erythrocytes*, Nucleic Acids Research **29**, 850 (2001).

[43] D. A. Fidock, T. Nomura, and T. E. Wellems, *Cycloguanil and Its Parent Compound Proguanil Demonstrate Distinct Activities against Plasmodium falciparumMalaria Parasites Transformed with Human Dihydrofolate Reductase*, Molecular Pharmacology **54**, 1140 (1998).

[44] C. B. Mamoun, I. Y. Gluzman, S. Goyard, S. M. Beverley, and D. E. Goldberg, *A set of independent selectable markers for transfection of the human malaria parasite Plasmodium falciparum*, Proceedings of the National Academy of Sciences of the United States of America **96**, 8716 (1999), ISSN 0027-8424.

[45] S. M. Ganesan, J. M. Morrisey, H. Ke, H. J. Painter, K. Laroiya, M. A. Phillips, P. K. Rathod, M. W. Mather, and A. B. Vaidya, *Yeast Dihydroorotate Dehydrogenase as a New Selectable Marker for Plasmodium falciparum Transfection*, Molecular and biochemical parasitology **177**, 29 (2011), ISSN 0166-6851.

[46] M. T. Duraisingh, T. Triglia, and A. F. Cowman, *Negative selection of Plasmodium falciparum reveals targeted gene deletion by double crossover recombination.*, International journal for parasitology **32**, 81 (2002), ISSN 0020-7519 (Print).

[47] J. A. M. Braks, B. Franke-Fayard, H. Kroeze, C. J. Janse, and A. P. Waters, *Development and application of a positivenegative selectable marker system for use in reverse genetics in Plasmodium*, Nucleic Acids Research **34**, e39 (2006), ISSN 0305-1048.

[48] T. F. De Koning-Ward, P. R. Gilson, and B. S. Crabb, *Advances in molecular genetic systems in malaria*, Nature Reviews Microbiology **13**, 373 (2015), ISSN 17401534.

[49] B. S. Crabb, B. M. Cooke, J. C. Reeder, R. F. Waller, S. R. Caruana, K. M. Davern, M. E. Wickham, G. V. Brown, R. L. Coppel, and A. F. Cowman, *Targeted Gene Disruption Shows That Knobs Enable Malaria-Infected Red Cells to Cytoadhere under Physiological Shear Stress*, Cell **89**, 287 (1997), ISSN 00928674.

[50] B. Balu, D. A. Shoue, M. J. Fraser Jr, and J. H. Adams, *High-efficiency transformation of Plasmodium falciparum by the lepidopteran transposable element piggyBac*, Proceedings of the National Academy of Sciences of the United States of America **102**, 16391 (2005), ISSN 0027-8424.

[51] M. Zhang, C. Wang, T. D. Otto, J. Oberstaller, X. Liao, S. R. Adapa, K. Udenze, I. F. Bronner, D. Casandra, M. Mayho, et al., *Uncovering the essential genes of the human malaria parasite Plasmodium falciparum by saturation mutagenesis.*, Science (New York, N.Y.) **360** (2018), ISSN 1095-9203 (Electronic).

[52] L. J. Nkrumah, R. A. Muhle, P. A. Moura, P. Ghosh, G. F. Hatfull, W. R. Jacobs, and D. A. Fidock, *Efficient site-specific integration in Plasmodium falciparum chromosomes mediated by mycobacteriophage Bxb1 integrase*, Nat Meth **3**, 615 (2006), ISSN 1548-7091.

[53] J. Straimer, M. C. S. Lee, A. H. Lee, B. Zeitler, A. E. Williams, J. R. Pearl, L. Zhang, E. J. Rebar, P. D. Gregory, M. Llinas, et al., *Site-specific genome editing in Plasmodium falciparum using engineered zinc-finger nucleases.*, Nature methods **9**, 993 (2012), ISSN 1548-7105 (Electronic).

[54] C. W. McNamara, M. C. Lee, C. S. Lim, S. H. Lim, J. Roland, O. Simon, B. K. Yeung, A. K. Chatterjee, S. L. McCormack, M. J. Manary, et al., *Targeting Plasmodium PI(4)K to eliminate malaria.*, Nature **504**, 248 (2013), ISSN 1476-4687 (Electronic).

[55] J. Straimer, N. F. Gnadig, B. Witkowski, C. Amaratunga, V. Duru, A. P. Ramadani, M. Dacheux, N. Khim, L. Zhang, S. Lam, et al., *Drug resistance. K13-propeller mutations confer artemisinin resistance in Plasmodium falciparum clinical isolates.*, Science (New York, N.Y.) **347**, 428 (2015), ISSN 1095-9203 (Electronic).

[56] L. A. Kirkman, E. A. Lawrence, and K. W. Deitsch, *Malaria parasites utilize both homologous recombination and alternative end joining pathways to maintain genome integrity.*, Nucleic acids research **42**, 370 (2014), ISSN 1362-4962 (Electronic).

[57] M. Singer, J. Marshall, K. Heiss, G. R. Mair, D. Grimm, A.-K. Mueller, and F. Frischknecht, *Zinc finger nuclease-based double-strand breaks attenuate malaria parasites and reveal rare microhomology-mediated end joining.*, Genome biology **16**, 249 (2015), ISSN 1474-760X (Electronic).

[58] C. L. Ramirez, J. E. Foley, D. A. Wright, F. Muller-Lerch, S. H. Rahman, T. I. Cornu, R. J. Winfrey, J. D. Sander, F. Fu, J. A. Townsend, et al., *Unexpected failure rates for modular assembly of engineered zinc fingers.* (2008).

[59] L. Cong, F. A. Ran, D. Cox, S. Lin, R. Barretto, N. Habib, P. D. Hsu, X. Wu, W. Jiang, L. A. Marraffini, et al., *Multiplex genome engineering using CRISPR/Cas systems.*, Science (New York, N.Y.) **339**, 819 (2013), ISSN 1095-9203 (Electronic).

[60] J. E. DiCarlo, J. E. Norville, P. Mali, X. Rios, J. Aach, and G. M. Church, *Genome engineering in Saccharomyces cerevisiae using CRISPR-Cas systems.*, Nucleic acids research **41**, 4336 (2013), ISSN 1362-4962 (Electronic).

[61] S. J. Gratz, A. M. Cummings, J. N. Nguyen, D. C. Hamm, L. K. Donohue, M. M. Harrison, J. Wildonger, and K. M. O'Connor-Giles, *Genome engineering of Drosophila with the CRISPR RNA-guided Cas9 nuclease.*, Genetics **194**, 1029 (2013), ISSN 1943-2631 (Electronic).

[62] W. Jiang, H. Zhou, H. Bi, M. Fromm, B. Yang, and D. P. Weeks, *Demonstration of CRISPR/Cas9/sgRNA-mediated targeted gene modification in Arabidopsis, tobacco, sorghum and rice.*, Nucleic acids research **41**, e188 (2013), ISSN 1362-4962 (Electronic).

[63] M. Ghorbal, M. Gorman, C. R. Macpherson, R. M. Martins, A. Scherf, and J.-J. Lopez-Rubio, *Genome editing in the human malaria parasite Plasmodium falciparum using the CRISPR-Cas9 system*, Nat Biotech **32**, 819 (2014), ISSN 1087-0156.

[64] N. Lander, Z.-H. Li, S. Niyogi, and R. Docampo, *CRISPR/Cas9-Induced Disruption of Paraflagellar Rod Protein 1 and 2 Genes in Trypanosoma cruzi Reveals Their Role in Flagellar Attachment.*, mBio **6**, e01012 (2015), ISSN 2150-7511 (Electronic).

[65] B. Shen, K. M. Brown, T. D. Lee, and L. D. Sibley, *Efficient gene disruption in diverse strains of Toxoplasma gondii using CRISPR/CAS9.*, mBio **5**, e01114 (2014), ISSN 2150-7511 (Electronic).

[66] L. Sollelis, M. Ghorbal, C. R. MacPherson, R. M. Martins, N. Kuk, L. Crobu, P. Bastien, A. Scherf, J.-J. Lopez-Rubio, and Y. Sterkers, *First efficient CRISPR-Cas9-mediated genome editing in Leishmania parasites.*, Cellular microbiology **17**, 1405 (2015), ISSN 1462-5822 (Electronic).

[67] P. Horvath and R. Barrangou, *CRISPR/Cas, the immune system of bacteria and archaea.*, Science (New York, N.Y.) **327**, 167 (2010), ISSN 1095-9203 (Electronic).

[68] D. Rath, L. Amlinger, A. Rath, and M. Lundgren, *The CRISPR-Cas immune system: biology, mechanisms and applications.*, Biochimie **117**, 119 (2015), ISSN 1638-6183 (Electronic).

[69] R. Sorek, C. M. Lawrence, and B. Wiedenheft, *CRISPR-mediated adaptive immune systems in bacteria and archaea.*, Annual review of biochemistry **82**, 237 (2013), ISSN 1545-4509 (Electronic).

[70] M. R. O/'Connell, B. L. Oakes, S. H. Sternberg, A. East-Seletsky, M. Kaplan, and J. A. Doudna, *Programmable RNA recognition and cleavage by CRISPR/Cas9*, Nature **516**, 263 (2014), ISSN 0028-0836.

[71] F. A. Ran, P. D. Hsu, J. Wright, V. Agarwala, D. A. Scott, and F. Zhang, *Genome engineering using the CRISPR-Cas9 system*, Nat. Protocols **8**, 2281 (2013), ISSN 1754-2189.

[72] X. Yang, *Applications of CRISPR-Cas9 mediated genome engineering*, Military Medical Research **2**, 11 (2015), ISSN 2095-7467.

[73] E. Deltcheva, K. Chylinski, C. M. Sharma, K. Gonzales, Y. Chao, Z. A. Pirzada, M. R. Eckert, J. Vogel, and E. Charpentier, *CRISPR RNA maturation by trans-encoded small RNA and host factor RNase III.*, Nature **471**, 602 (2011), ISSN 1476-4687 (Electronic).

[74] M. Jinek, K. Chylinski, I. Fonfara, M. Hauer, J. A. Doudna, and E. Charpentier, *A programmable dual-RNA-guided DNA endonuclease in adaptive bacterial immunity.*, Science (New York, N.Y.) **337**, 816 (2012), ISSN 1095-9203 (Electronic).

[75] F. Zhang, X. Guo, and Y. Wen, *CRISPR/Cas9 for genome editing: progress, implications and challenges*, Human Molecular Genetics **23**, R40 (2014), ISSN 0964-6906.

[76] J. C. Wagner, R. J. Platt, S. J. Goldfless, F. Zhang, and J. C. Niles, *Efficient CRISPR-Cas9-mediated genome editing in Plasmodium falciparum*, Nat Meth **11**, 915 (2014), ISSN 1548-7091.

[77] C. L. Ng, G. Siciliano, M. C. S. Lee, M. J. de Almeida, V. C. Corey, S. E. Bopp, L. Bertuccini, S. Wittlin, R. G. Kasdin, A. Le Bihan, et al., *CRISPR-Cas9-modified pfmdr1 protects Plasmodium falciparum asexual blood stages and gametocytes against a class of piperazine-containing compounds but potentiates artemisinin-based combination therapy partner drugs.*, Molecular microbiology **101**, 381 (2016), ISSN 1365-2958 (Electronic).

[78] J. Lu, Y. Tong, J. Pan, Y. Yang, Q. Liu, X. Tan, S. Zhao, L. Qin, and X. Chen, *A redesigned CRISPR/Cas9 system for marker-free genome editing in Plasmodium falciparum.*, Parasites & vectors **9** (2016), ISSN 1756-3305.

[79] E. Sonoiki, C. L. Ng, M. C. S. Lee, D. Guo, Y.-K. Zhang, Y. Zhou, M. R. K. Alley, V. Ahyong, L. M. Sanz, M. J. Lafuente-Monasterio, et al., *A potent antimalarial benzoxaborole targets a Plasmodium falciparum cleavage and polyadenylation specificity factor homologue*, Nature Communications **8**, 14574 (2017).

[80] E. D. Crawford, J. Quan, J. A. Horst, D. Ebert, W. Wu, and J. L. DeRisi, *Plasmid-free CRISPR/Cas9 genome editing in Plasmodium falciparum confirms mutations conferring resistance to the dihydroisoquinolone clinical candidate SJ733.*, PloS one **12**, e0178163 (2017), ISSN 1932-6203 (Electronic).

[81] G. Li, X. Zhang, C. Zhong, J. Mo, R. Quan, J. Yang, D. Liu, Z. Li, H. Yang, and Z. Wu, *Small molecules enhance CRISPR/Cas9-mediated homology-directed genome editing in primary cells*, Scientific Reports **7**, 8943 (2017), ISSN 2045-2322.

[82] J. S. Chen, E. Ma, L. B. Harrington, M. Da Costa, X. Tian, J. M. Palefsky, and J. A. Doudna, *CRISPR-Cas12a target binding unleashes indiscriminate single-stranded DNase activity*, Science pp. 1–7 (2018), ISSN 10959203.

[83] J. C. Wang, *DNA topoisomerases.*, Annual review of biochemistry **65**, 635 (1996), ISSN 0066-4154 (Print).

[84] L. A. Mitscher, *Bacterial topoisomerase inhibitors: quinolone and pyridone antibacterial agents.*, Chemical reviews **105**, 559 (2005), ISSN 0009-2665 (Print).

[85] Y. Pommier, E. Leo, H. Zhang, and C. Marchand, *DNA topoisomerases and their poisoning by anticancer and antibacterial drugs.*, Chemistry & biology **17**, 421 (2010), ISSN 1879-1301 (Electronic).

[86] C. Garcia-Estrada, C. F. Prada, C. Fernandez-Rubio, F. Rojo-Vazquez, and R. Balana-Fouce, *DNA topoisomerases in apicomplexan parasites: promising targets for drug discovery.*, Proceedings. Biological sciences **277**, 1777 (2010), ISSN 1471-2954 (Electronic).

[87] J. C. Wang, *Cellular roles of DNA topoisomerases: a molecular perspective.*, Nature reviews. Molecular cell biology **3**, 430 (2002), ISSN 1471-0072 (Print).

[88] E. Massé and M. Drolet, *Escherichia coli DNA topoisomerase I inhibits R-loop formation by relaxing transcription-induced negative supercoiling.*, The Journal of biological chemistry **274**, 16659 (1999), ISSN 0021-9258.

[89] J. W. Wallis, G. Chrebet, G. Brodsky, M. Rolfe, and R. Rothstein, *A hyper-recombination mutation in S. cerevisiae identifies a novel eukaryotic topoisomerase*, Cell **58**, 409 (1989), ISSN 0092-8674.

[90] H.-Y. Wu, S. Shyy, J. C. Wang, and L. F. Liu, *Transcription generates positively and negatively supercoiled domains in the template*, Cell **53**, 433 (1988), ISSN 0092-8674.

[91] J. C. Wang, P. R. Caron, and R. A. Kim, *The role of DNA topoisomerases in recombination and genome stability: A double-edged sword?*, Cell **62**, 403 (1990), ISSN 0092-8674.

[92] D. G. Mudeppa, S. Kumar, S. Kokkonda, J. White, and P. K. Rathod, *Topoisomerase II from Human Malaria Parasites: EXPRESSION, PURIFICATION, AND SELECTIVE INHIBITION*, The Journal of Biological Chemistry **290**, 20313 (2015), ISSN 0021-9258.

[93] S. Chalarapareddy, S. Chakrabarty, M. K. Bhattacharyya, and S. Bhattacharyya, *Radicicol-Mediated Inhibition of Topoisomerase VIB-VIA Activity of the*, Molecular Biology and Physiology **1**, 1 (2014).

[94] V. Weissig, T. S. Vetro-Widenhouse, and T. C. Rowe, *Topoisomerase II inhibitors induce cleavage of nuclear and 35-kb plastid DNAs in the malarial parasite Plasmodium falciparum.*, DNA and cell biology **16**, 1483 (1997), ISSN 1044-5498.

[95] M. Kalanon and G. McFadden, *Malaria, Plasmodium falciparum and its apicoplast*, Biochemical Society Transactions **38**, 775 LP (2010).

[96] M. A. Dar, A. Sharma, N. Mondal, and S. K. Dhar, *Molecular Cloning of Apicoplast-Targeted Plasmodium falciparum DNA Gyrase Genes: Unique Intrinsic ATPase Activity and ATP-Independent Dimerization of PfGyrB Subunit*, Eukaryotic Cell **6**, 398 (2007), ISSN 1535-9778.

[97] E. V. S. Raghu Ram, A. Kumar, S. Biswas, A. Kumar, S. Chaubey, M. I. Siddiqi, and S. Habib, *Nuclear gyrB encodes a functional subunit of the Plasmodium falciparum gyrase that is involved in apicoplast DNA replication.*, Molecular and biochemical parasitology **154**, 30 (2007), ISSN 0166-6851 (Print).

[98] S. Nagano, T.-Y. Lin, J. Edula, and J. Heddle, *Unique features of apicoplast DNA gyrases from Toxoplasma gondii and Plasmodium falciparum*, BMC Bioinformatics **15**, 416 (2014), ISSN 1471-2105.

[99] S. Nagano, E. Seki, T.-Y. Lin, M. Shirouzu, S. Yokoyama, and J. G. Heddle, *Investigating the Roles of the C-Terminal Domain of Plasmodium falciparum GyrA.*, PloS one **10**, e0142313 (2015), ISSN 1932-6203 (Electronic).

[100] S. C. Tang Girdwood, E. Nenortas, and T. A. Shapiro, *Targeting the gyrase of Plasmodium falciparum with topoisomerase poisons.*, Biochemical pharmacology **95**, 227 (2015), ISSN 1873-2968 (Electronic).

[101] M. C. Lee and D. A. Fidock, *CRISPR-mediated genome editing of Plasmodium falciparum malaria parasites.*, Genome medicine **6**, 63 (2014), ISSN 1756-994X.

[102] M. E. Fichera and D. S. Roos, *A plastid organelle as a drug target in apicomplexan parasites*, Nature **390**, 407 (1997), ISSN 0028-0836.

[103] E. L. Dahl and P. J. Rosenthal, *Multiple antibiotics exert delayed effects against the Plasmodium falciparum apicoplast*, Antimicrobial Agents and Chemotherapy **51**, 3485 (2007), ISSN 00664804.

[104] J. D. Bowman, E. F. Merino, C. F. Brooks, B. Striepen, P. R. Carlier, and M. B. Cassera, *Antiapicoplast and gametocytocidal screening to identify the mechanisms of action of compounds within the malaria box.*, Antimicrobial agents and chemotherapy **58**, 811 (2014), ISSN 1098-6596 (Electronic).

[105] T. Uddin, G. I. McFadden, and C. D. Goodman, *Validation of putative apicoplast-targeting drugs using a chemical supplementation assay in cultured human malaria parasites*, Antimicrobial Agents and Chemotherapy **62**, 1 (2018), ISSN 10986596.

[106] J. G. Doench, E. Hartenian, D. B. Graham, Z. Tothova, M. Hegde, I. Smith, M. Sullender, B. L. Ebert, R. J. Xavier, and D. E. Root, *Rational design of highly active sgRNAs for CRISPR-Cas9-mediated gene inactivation*, Nat Biotech **32**, 1262 (2014), ISSN 1087-0156.

[107] P. D. Hsu, D. A. Scott, J. A. Weinstein, F. A. Ran, S. Konermann, V. Agarwala, Y. Li, E. J. Fine, X. Wu, O. Shalem, et al., *DNA targeting specificity of RNA-guided Cas9 nucleases*, Nature Biotechnology **31**, 827 (2013).

[108] W. Trager and J. B. Jensen, *Human malaria parasites in continuous culture.*, Science (New York, N.Y.) **193**, 673 (1976), ISSN 0036-8075 (Print).

[109] A. A. Divo, T. G. Geary, N. L. Davis, and J. B. Jensen, *Nutritional requirements of Plasmodium falciparum in culture. I. Exogenously supplied dialyzable components necessary for continuous growth.*, The Journal of protozoology **32**, 59 (1985), ISSN 0022-3921 (Print).

[110] C. Lambros and J. P. Vanderberg, *Synchronization of Plasmodium falciparum erythrocytic stages in culture.*, The Journal of parasitology **65**, 418 (1979), ISSN 0022-3395 (Print).

[111] A. D. Bangham and R. W. Horne, *Action of Saponin on Biological Cell Membranes*, Nature **196**, 952 (1962), ISSN 1476-4687.

[112] P. Mirovsky, F. Gay, D. Bustos, D. Mazier, and M. Gentilini, *Cloning of a fresh isolate of Plasmodium falciparum and drug sensitivity of the clones*, Transactions of The Royal Society of Tropical Medicine and Hygiene **84**, 511 (1990), ISSN 0035-9203.

[113] C. J. Tonkin, G. G. Van Dooren, T. P. Spurck, N. S. Struck, R. T. Good, E. Handman, A. F. Cowman, and G. I. McFadden, *Localization of organellar proteins in Plasmodium falciparum using a novel set of transfection vectors and a new immunofluorescence fixation method*, Molecular and Biochemical Parasitology **137**, 13 (2004), ISSN 01666851.

[114] A. McKenna, M. Hanna, E. Banks, A. Sivachenko, K. Cibulskis, A. Kernytsky, K. Garimella, D. Altshuler, S. Gabriel, M. Daly, et al., *The Genome Analysis Toolkit: a MapReduce framework for analyzing next-generation DNA sequencing data.*, Genome research **20**, 1297 (2010), ISSN 1549-5469 (Electronic).

[115] G. A. Van der Auwera, M. O. Carneiro, C. Hartl, R. Poplin, G. Del Angel, A. Levy-Moonshine, T. Jordan, K. Shakir, D. Roazen, J. Thibault, et al., *From FastQ data to high confidence variant calls: the Genome Analysis Toolkit best practices pipeline.*, Current protocols in bioinformatics **43**, 11.10.1 (2013), ISSN 1934-340X (Electronic).

[116] V. J. Davisson, A. B. Woodside, T. R. Neal, K. E. Stremler, M. Muehlbacher, and C. D. Poulter, *Phosphorylation of isoprenoid alcohols*, The Journal of Organic Chemistry **51**, 4768 (1986), ISSN 0022-3263.

[117] W. Mckinney, *Data Structures for Statistical Computing in Python*, Proc. of the 9th Python in Science Conference pp. 51–56 (2010).

[118] J. D. Hunter, *Matplotlib: A 2D Graphics Environment*, Computing in Science & Engineering **9**, 90 (2007), ISSN 1521-9615 VO - 9.

[119] D. Chakrabarti, T. Azam, C. Delvecchio, L. Qiu, Y. I. Park, and C. M. Allen, *Protein prenyl transferase activities of Plasmodium falciparum*, Molecular and Biochemical Parasitology **94**, 175 (1998), ISSN 01666851.

[120] D. Chakrabarti, T. Da Silva, J. Barger, S. Paquette, H. Patel, S. Patterson, and C. M. Allen, *Protein farnesyltransferase and protein prenylation in Plasmodium falciparum.*, The Journal of biological chemistry **277**, 42066 (2002), ISSN 0021-9258 (Print).

[121] P. Haluska, G. K. Dy, and A. A. Adjei, *Farnesyl transferase inhibitors as anticancer agents.*, European journal of cancer (Oxford, England : 1990) **38**, 1685 (2002), ISSN 0959-8049 (Print).

[122] I. M. Bell, *Inhibitors of Farnesyltransferase: A Rational Approach to Cancer Chemotherapy?*, Journal of Medicinal Chemistry **47**, 1869 (2004), ISSN 0022-2623.

[123] S. M. Sebti and A. A. Adjei, *Farnesyltransferase inhibitors.*, Seminars in oncology **31**, 28 (2004), ISSN 0093-7754 (Print).

[124] F. Tamanoi, J. Kato-Stankiewicz, C. Jiang, I. Machado, and N. Thapar, *Farnesylated proteins and cell cycle progression.*, Journal of cellular biochemistry. Supplement **Suppl 37**, 64 (2001), ISSN 0733-1959 (Print).

[125] K. Zhu, A. D. Hamilton, and S. M. Sebti, *Farnesyltransferase inhibitors as anticancer agents: current status*, Current opinion in investigational drugs (London, England : 2000) **4**, 1428 (2003), ISSN 1472-4472.

[126] J. B. Gibbs, A. Oliff, and N. E. Kohl, *Farnesyltransferase inhibitors: Ras research yields a potential cancer therapeutic.*, Cell **77**, 175 (1994), ISSN 0092-8674 (Print).

[127] N. E. Kohl, M. W. Conner, J. B. Gibbs, S. L. Graham, G. D. Hartman, and A. Oliff, *Development of inhibitors of protein farnesylation as potential chemotherapeutic agents*, Journal of Cellular Biochemistry **59**, 145 (1995), ISSN 0730-2312.

[128] A. D. Cox and C. J. Der, *Farnesyltransferase inhibitors and cancer treatment: targeting simply Ras?*, Biochimica et biophysica acta **1333**, F51 (1997), ISSN 0006-3002 (Print).

[129] C. J. D. Bell and I. M, *Inhibitors of Farnesyltransferase and Geranylgeranyltransferase-I for Antitumor Therapy: Substrate-Based Design, Conformational Constraint and Biological Activity* (2003).

[130] S. M. Sebti and A. D. Hamilton, *Farnesyltransferase and geranylgeranyltransferase I inhibitors in cancer therapy: important mechanistic and bench to bedside issues*, Expert Opinion on Investigational Drugs **9**, 2767 (2000), ISSN 1354-3784.

[131] I. Marzo, P. Perez-Galan, P. Giraldo, N. Lopez-Royuela, M. Gomez-Benito, L. Larrad, P. Lasierra, D. Rubio-Felix, A. Anel, and J. Naval, *Farnesyltransferase inhibitor BMS-214662 induces apoptosis in B-cell chronic lymphocytic leukemia cells.*, Leukemia **18**, 1599 (2004), ISSN 0887-6924 (Print).

[132] S. M. Hahn, E. J. Bernhard, W. Regine, M. Mohiuddin, D. G. Haller, J. P. Stevenson, D. Smith, B. Pramanik, J. Tepper, T. F. DeLaney, et al., *A Phase I trial of the farnesyltransferase inhibitor L-778,123 and radiotherapy for locally advanced lung and head and neck cancer.*, Clinical cancer research : an official journal of the American Association for Cancer Research **8**, 1065 (2002), ISSN 1078-0432 (Print).

[133] A. G. Taveras, P. Kirschmeier, and C. M. Baum, *Sch-66336 (sarasar) and other benzocycloheptapyridyl farnesyl protein transferase inhibitors: discovery, biology and clinical observations.*, Current topics in medicinal chemistry **3**, 1103 (2003), ISSN 1568-0266 (Print).

[134] S. Rao, D. Cunningham, A. de Gramont, W. Scheithauer, M. Smakal, Y. Humblet, G. Kourteva, T. Iveson, T. Andre, J. Dostalova, et al., *Phase III double-blind placebo-controlled study of farnesyl transferase inhibitor R115777 in patients with refractory advanced colorectal cancer.*, Journal of clinical oncology : official journal of the American Society of Clinical Oncology **22**, 3950 (2004), ISSN 0732-183X (Print).

[135] J. V. Heymach, D. H. Johnson, F. R. Khuri, H. Safran, L. L. Schlabach, F. Yunus, R. F. r. DeVore, P. M. De Porre, H. M. Richards, X. Jia, et al., *Phase II study of the farnesyl transferase inhibitor R115777 in patients with sensitive relapse small-cell lung cancer.*, Annals of oncology : official journal of the European Society for Medical Oncology **15**, 1187 (2004), ISSN 0923-7534 (Print).

[136] V. Papadimitrakopoulou, S. Agelaki, H. T. Tran, M. Kies, R. Gagel, R. Zinner, E. Kim, G. Ayers, J. Wright, and F. Khuri, *Phase I Study of the Farnesyltransferase Inhibitor BMS-214662 Given Weekly in Patients with Solid Tumors*, Clinical Cancer Research **11**, 4151 LP (2005).

[137] L. Nallan, K. D. Bauer, P. Bendale, K. Rivas, K. Yokoyama, C. P. Horney, P. R. Pendyala, D. Floyd, L. J. Lombardo, D. K. Williams, et al., *Protein farnesyltransferase inhibitors exhibit potent antimalarial activity.*, Journal of medicinal chemistry **48**, 3704 (2005), ISSN 0022-2623 (Print).

[138] R. T. Eastman, J. White, O. Hucke, K. Yokoyama, C. L. M. J. Verlinde, M. A. Hast, L. S. Beese, M. H. Gelb, P. K. Rathod, and W. C. Van Voorhis, *Resistance mutations at the lipid substrate binding site of Plasmodium falciparum protein farnesyltransferase.*, Molecular and biochemical parasitology **152**, 66 (2007), ISSN 0166-6851.

[139] W. C. Van Voorhis, K. L. Rivas, P. Bendale, L. Nallan, C. Hornéy, L. K. Barrett, K. D. Bauer, B. P. Smart, S. Ankala, O. Hucke, et al., *Efficacy, Pharmacokinetics, and Metabolism of Tetrahydroquinoline Inhibitors of Plasmodium falciparum Protein Farnesyltransferase*, Antimicrobial Agents and Chemotherapy **51**, 3659 (2007), ISSN 0066-4804.

[140] J. Inselburg, D. J. Bzik, and T. Horii, *Pyrimethamine resistant Plasmodium falciparum: overproduction of dihydrofolate reductase by a gene duplication*, Molecular and Biochemical Parasitology **26**, 121 (1987), ISSN 01666851.

[141] M. Tanaka, H.-M. Gu, D. J. Bzik, W.-B. Li, and J. Inselburg, *Mutant dihydrofolate reductase-thymidylate synthase genes in pyrimethamine-resistant Plasmodium falciparum with polymorphic chromosome duplications*, Molecular and Biochemical Parasitology **42**, 83 (1990), ISSN 01666851.

[142] P. K. Rathod, T. McErlean, and P.-C. Lee, *Variations in frequencies of drug resistance in Plasmodium falciparum*, Proceedings of the National Academy of Sciences **94**, 9389 (1997).

[143] K. Ganesan, N. Ponmee, L. Jiang, J. W. Fowble, J. White, S. Kamchonwongpaisan, Y. Yuthavong, P. Wilairat, and P. K. Rathod, *A genetically hard-wired metabolic transcriptome in Plasmodium falciparum fails to mount protective responses to lethal antifolates.*, PLoS pathogens **4**, e1000214 (2008), ISSN 1553-7374 (Electronic).

[144] A. H. Lee and D. A. Fidock, *Evidence of a Mild Mutator Phenotype in Cambodian Plasmodium falciparum Malaria Parasites*, PLoS ONE **11**, e0154166 (2016), ISSN 1932-6203.

[145] M. W. Pfaffl, *A new mathematical model for relative quantification in real-time RT-PCR.*, Nucleic acids research **29**, e45 (2001), ISSN 1362-4962 (Electronic).